ROCK-MAGNETIC STUDY ON SHIELD BASALTS FROM GRAN CANARIA CONTAINING A RECORDED REVERSAL OF THE EARTH'S MAGNETIC FIELD

Ana Nap
July 2017
Bachelor thesis Utrecht University
Supervisors: Lennart de Groot & Annemarieke Béguin

ABSTRACT

The Earth's magnetic field is known to exhibit reversals in polarity. Such a reversal seems imminent to occur in the future, but little is known about the processes that govern such a reversal. We created a detailed record of a polarity reversal recorded in (Mid-Miocene) shield building lavas of Gran Canaria. In this part of the research we created a detailed record of the rock-magnetic properties of these lavas to assess their suitability as recorders of information on the ancient geomagnetic field. We used a Kappabridge (KLY-3) to obtain a magnetic susceptibility curve and a VSM (vibrating sample magnetometer) to determine if the samples are single domain (SD), pseudo-single domain (PSD) or MD (multi domain). With these techniques we determine the behaviour of samples when subjected to alternating temperatures (magnetic susceptibility) and strong magnetic fields (VSM). The results show that 80 of the samples are PSD and 17 are close to MD. We found that the samples have a higher abundance in magnetite than titanomagnetite and are in general characterized by high (< 500 ^{o}C) Curie temperatures. Correlating the rock-magnetic data to IZZI-Thellier measurements (Marijnissen, 2017) we found that most successful samples originate from the same susceptibility groups and agree with curves presented in de Groot et al. (2015). This implicates that in future measurements a higher success rate can be attained by measuring more flows that show the same magnetic susceptibility behaviour. Researching possible ways to minimize alteration could be to heat and cool the samples within an oxygen deprived environment (Lattard et al., 2012). This would possibly minimize high temperature oxidation making the samples more reliable during IZZI-Thellier measurements.

CONTENT

Abstract 2

1. Introduction 4

2. Geological Setting and sampling 5

3. Methods 7

3.1 Magnetic Susceptibility Measurements 7

3.2 VSM 8

3.2.1 Domain properties 9

3.2.2 Hys-Loop 10

3.2.3 DCD 10

3.2.4 Day plot 10

4. Results 11

4.1 Magnetic susceptibility measurements (Kly-3) 11

4.1.1 Group A-1 11

4.1.2 Group A-2 11

4.1.3 Group B-1 12

4.1.4 Group B-2 12

4.1.5 Group C-1 12

4.1.6 Group C-2 12

4.1.7 Group D-1 12

4.1.8 Group D-2 13

4.1.9 Group E 13

4.2 VSM 16

5. Discussion 18

5.1 Interpretation 18

5.1.2 Magnetic susceptibility measurements 18

5.1.2 VSM 21

5.1.3 Correlation with IZZI-Thellier measurements 21

5.1.4 Possibility of improvement in IZZI-Thelier measurements. 24

6. Conclusion 25

References 26

Appendices 28

Appendix A Details per sampled flow 28

Appendix B Kappabridge Analysis results 30

Appendix C Kappabridge –Graphs per sample 33

Appendix D VSM Data 67

1. INTRODUCTION

The polarity of the Earth's magnetic field can reverse, but still very little is known about the physical processes that govern such changes in polarity. The geologic record of the occurrence of these reversals is reliable up to 250 million years ago, the start of the Triassic. However, there is hardly information about the process that govern a polarity reversal. A polarity reversal of the Earth's magnetic field will happen in the future, some even believe that a reversal is imminent (Constable & Korte, 2006). It is therefore crucial to gather more data and research about these reversals to increase our knowledge on the process itself and to help understand the processes behind these reversals. A reversal is thought to take on average 1000-8000 years to be entirely completed (Merrill and McFadden, 1999). No detailed records are yet available that describe such a reversal in high resolution including pre- and post-reversal events.

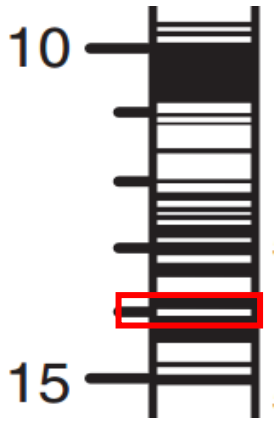

Figure 1: Record of reversals between 10 ma and 15 ma. The reversals focused on in this research is encircled in red. Source: https://www.geosociety.org/documents/gsa/timescale/timescl.pdf

Here we created a detailed record of a reversal captured in the shield lavas of Gran Canaria. Leonardt et al. (2002) discovered this reversal in the past and recorded data of these lavas. However, in the past 15 years the methods to measure paleo-directions, paleo-intensities and rock-magnetic data have improved significantly, so it is useful to repeat and add to this earlier research. The reversal recorded in these lavas is a reversal from reversed polarity to normal polarity corresponding to one recorded at 14.1 Ma (Leonardt et al., 2002). We also tried to capture the reversal from normal to reversed polarity at ~14.5 Ma (figure 1). These shield lavas erupted from ~14.5 Ma until 14.0 Ma continuously during the shield building phase of Gran Canaria (Carracedo, 2002). These continuous eruptions make these flows exceptionally suitable for a detailed record of this reversal because of the little time-lapse between data-points.

The overarching goal of the research project is to create a detailed record of a reversal including pre- and post-reversal events including paleo-directions (van Klaveren, 2017) and paleo-intensities (Marijnissen, 2017 and Tuinstra, 2017), supported by this rock magnetic study. In the rock-magnetic part of the research the main focus is the rock-magnetic properties of the lavas sampled, measured and studied. In Leonardt et al. (2002) very little rock-magnetic data was collected. For all lavas we assessed the magnetic susceptibility and their magnetic domain properties. This data can be used to support the paleo–intensity data in terms of behaviour of the magnetisation in the rocks when subjected to high temperatures and strong magnetic fields. We will assess the behaviour of the flows with Kappabridge measurements and with a vibrating sample magnetometer (VSM) the same way that has been done on younger lavas from Gran Canaria and Tenerife in de Groot et al. (2015).

These measurements will provide knowledge about magnetic domains within the samples and the possible alteration of minerals or the magnetic domain walls when subjected to high temperatures and strong magnetic fields. These alterations can cause samples to show different behaviour when heated or subjected to a large magnetic field. This could have consequences for paleo-intensity measurement. Which is why we eventually correlate this rock-magnetic data to the paleo-intensity data in Marijnissen (2017) of the same recorded reversal. We expect that the rock-magnetic studies can contribute to explaining why some data has very high quality and why some data has not. This can be done in terms of being able to tell if samples alter, how they alter and why they alter. Enabling us to tell why some lavas are likely to provide trustworthy magnetic paleo records and to possibly improve this in future research.

1. Geological Setting and sampling

Gran Canaria is part of the archipelago of the Canary Islands and located approximately 250 km of the Moroccan coast. The island has a circular shape with a 45 km diameter and a highest altitude of 1949 m above sea level. In contrast to Fuertaventura and Lanzarote towards the North-East, Gran Canaria appears to be built on Oceanic crust adjacent to the continental crust of Africa (Carracedo & Day, 2002). Gran Canaria is solely created by volcanic activity. McDougall & Schmincke (1976) distinguish three major subaerial magmatic phases that are separated by erosional intervals. The first phase contributed to the construction of a major shield volcano that is tholeiitic to alkali basaltic. This shield volcano surrounded most of the present area of the island. This volcano was covered by trachyte, rhyolite and trachyphonolite lava flows and welded ash flows that eventually resulted in a caldera collapse. The caldera that formed was about 15 km in diameter and got intruded by a trachyte cone swarm, syenite bodies and phonolite dikes. (McDougall & Schmincke, 1976).

Figure 2 Location of sampling on vector map of Gran Canaria.

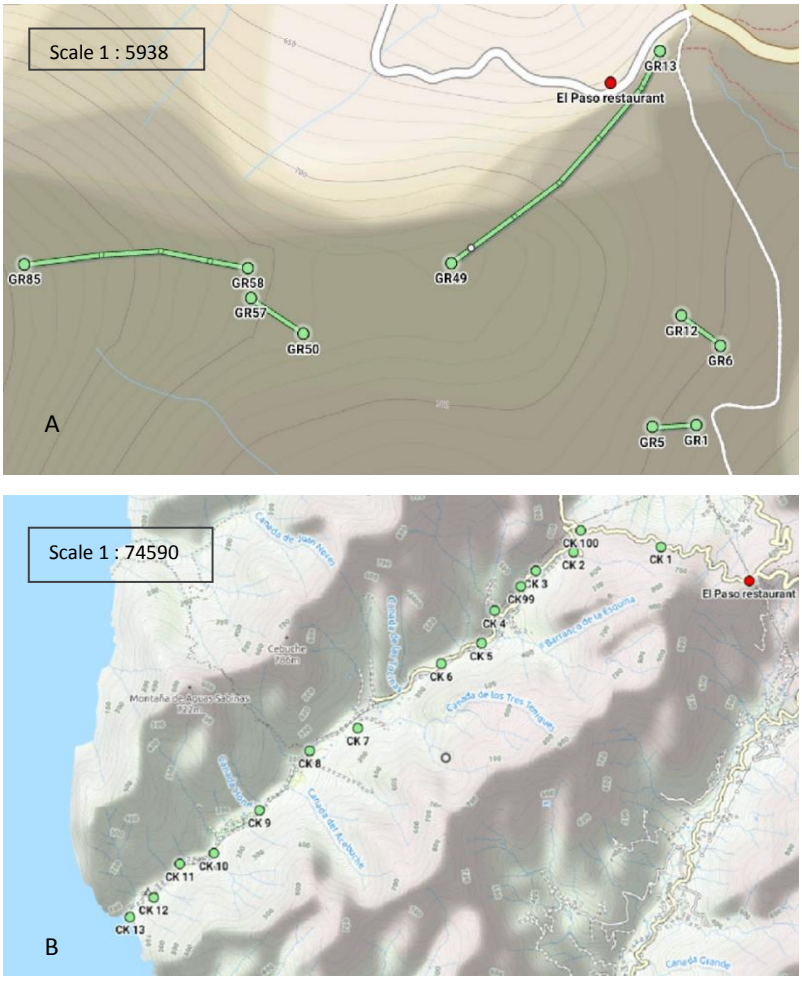

Figure 3 *Sampling routes. 3A displays section A (GR1-GR5 and GR6-GR12), section B (GR13-GR49) and section C (GR50-GR85). 3B displays section D (CK1-CK13 + CK99 and CK100).*

Due to erosion the shield building lavas are well exposed and have a clear succession. For this research we sampled lava flows that belong to the shield building phase that consists of tholeiitic basalts, as was done for the research of Leonardt et al. (2002). The main difference is that we did not follow the section across the road downward but started at 640 m in the sequence at the location of GR1 as section A (fig 3). The sections above the old El Paso restaurant, sections B and C, are mainly the same as described in Leonardt et al. (2002). We also extended the sequence downward until the sea with 15 flows with approximately 50 m elevation gaps as section D (figure 3). These should be within older shield building flows according to the geological map in Carracedo & Day (2002), then flows in the sequence presented in Leonardt et al. (2002).

We sampled the flows with a petrol-powered drill with a 2,5 cm diameter. We took 8-15 samples per flow and drilled samples, when possible, 1-2 meters apart to create a representative number of samples across each flow. Flows GR1-GR12 are part of section A, GR13-GR49 are part of section B, GR50-GR85 are part of section C and then section D constists of CK1-C13 including CK99 and CK100 (fig 4). We expect that between section A and section B there is a overlap between GR10-GR12 and GR13-GR15. Between section B and C the overlap is located at GR47-GR49 for section B and GR50-GR52 for section C. In appendix A a detailed record is displayed of each flow with its GPS location, number of samples, thickness and height.

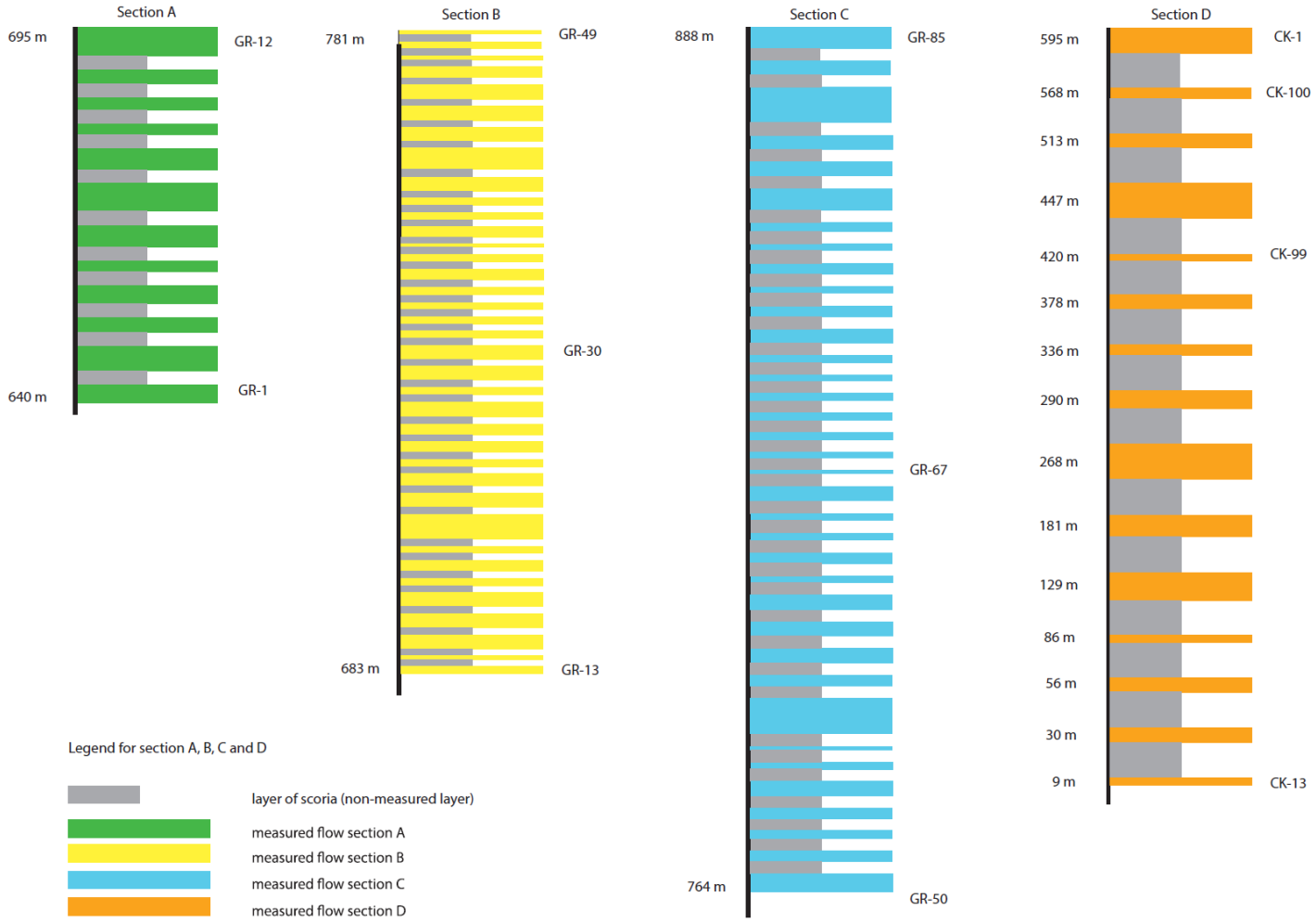

Figure 4 Logs of the different sections that were sampled. The coloured layers display the lava flows that were sampled. The grey layers in between indicate the layers of scoria that were present between each sampled lava layer. The thickness of each sampled layer is in scale. The thickness of the scoria layers has been evenly distributed in this log for we did not measure the thickness of these in the field.

2. METHODS

From each flow one or two samples are selected to assess their rock magnetic properties. One sample is used for susceptibility measurements in the Kappabridge and another sample is used for measurements with the Vibrating Sample Magnetometer (VSM).

3.1 MAGNETIC SUSCEPTIBILITY MEASUREMENTS

For the magnetic susceptibility measurements we crushed a sample until only small grains remained between 0.7 and 0.8 grams total. These were put within in a quartz glass sample holder in which a thermocouple was inserted as well; the sample holder was lowered into the Kappa-bridge**.** During the susceptibility measurements the sample is subjected to a low, external, magnetic field while being heated. The magnetic response (susceptibility) of the sample to this external field is measured as function of temperature. When inserted in the Kappabridge the induced magnetisation of the sample is measured.

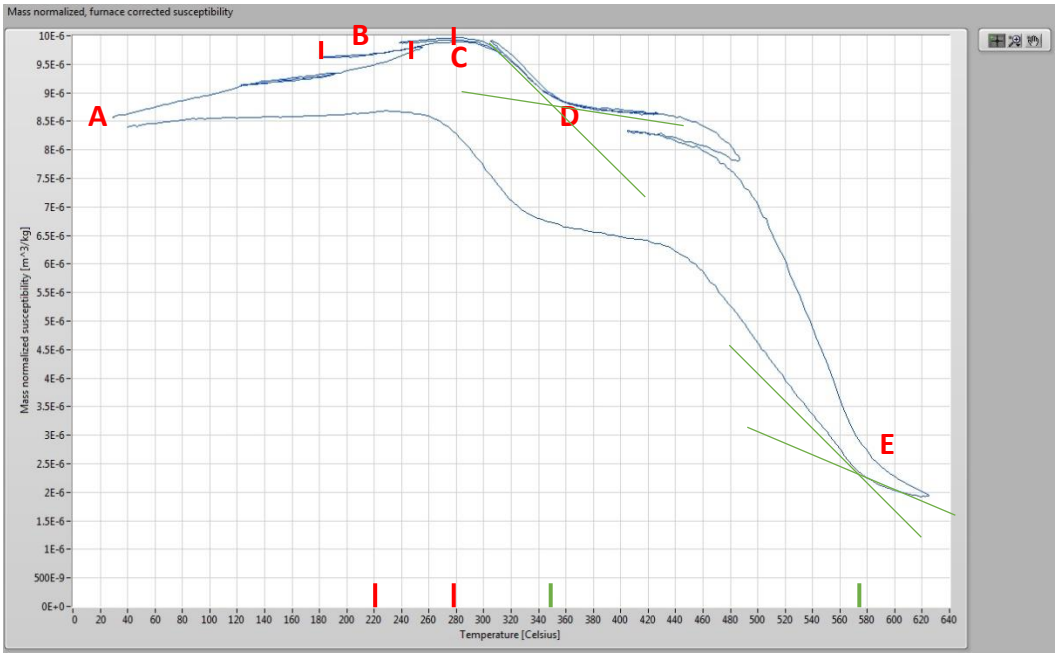

Figure 5 Example of Kappabridge measurments curve. A is the susceptibility at room temperature. B is the point of first alteration (defined by the red stripes) with corresponding temperature(left lower red stripe) and C is the Hopkinson peak (most right upper red stripe) with corresponding temperature (right lower red stripe). Curie temperatures can be obtained from the inflection points after the Hopkinson peak, point D and E, tangent lines in green with corresponding curie temperatures.

The induced magnetisation of the sample is the effect that the magnetisation of the sample has on the external constant field which is produced by a coil next to the sample holder. The Kappabridge measures the change that occurs in the external produced magnetic field when the sample is inserted. The temperature of the sample is increased in cycles with the following maximum temperatures: 180, 240, 300, 360, 420, 480, 620 ^{o}C. After reaching each maximum the sample is cooled down 40 ^{o}C to check the reversibility of the signal, as alterations in the signal may indicated permanent changes in the magnetic behaviour of the grains. The susceptibility is calculated by dividing the induced magnetisation of the sample which can change and the external magnetic field which is constant in our experiments. $Xd = \frac{M_I}{H}$ where Xd is the susceptibility, M_I is the induced magnetisation and H is the external magnetic field.

The results of the susceptibility measurements give information about the mineral content, Curie temperature and the behaviour of the magnetisation of the samples when heated and cooled.

Minerals and the magnetisation of a sample can change with temperature because minerals and magnetic domains (see VSM; domain properties) within the rock can alter with temperature and start to behave differently. Which in turn could clarify if and/or why the data from other experiments such as thermal demagnetization for the paleo-directions, and IZZI- and pseudo-Thellier measurements to obtain paleo-intensities are not clear or evident. The points in the resulting graph that are especially important for interpretation of these data are the following: the susceptibility at room temperature, the Hopkinson peak, the temperature of the first alteration and if possible the Curie temperature (fig 5).

The susceptibility at room temperature (fig 5A) is important in comparison with the rest of the graph to see if it increases, stays constant or directly decreases when the temperature is increased. The Hopkinson peak (fig 5B) relates to the Curie temperature of the magnetic minerals in a sample because after a certain temperature the magnetic minerals start to deteriorate significantly until there is no magnetisation left. The temperature at which this happens is distinctive per mineral content. Pure magnetite (Fe_3O_4) has a curie temperature of 580 ^oC but often the magnetic minerals are Titanomagnetite ($Fe_{3-x}Ti_xO_4$). The proportion between these minerals are displayed within the molecule formula, for example if there is sixty percent Titanomagnetite the formula would be: $Fe_{2.4}Ti_{0.6}O_4$ which is dubbed 'TM60'. The Curie temperature can be obtained from a susceptibility curve by drawing two tangent lines on either side of the first inflection point after the Hopkinson peak. The intersection of these two tangent lines can be correlated to a temperature which would be the Curie temperature. There can be more than one inflection point after the Hopkinson peak indicating more than one curie temperature which can be related to mineral compositions.

The first alteration point (fig 5C) is the point where the graph does not follow the same path back and forth when heating and cooling. Hence, the minerals in the sample are altered due to temperature and do not behave the same anymore when brought back to the same temperature. This temperature is important to know because it indicates permanent alteration in the samples. Above this temperature results of paleo-intensity experiments may not provide a trustworthy results. Combining all this information gives a clearer view on why flows can provide unreliable data.

3.2 VSM

The VSM (Vibrating Sample Magnetometer) measures high-field magnetic properties of the sample. The sample consists of a small piece of rock representative for its flow about 0.5 by 0.5 cm large. The sample is placed in between two strong electromagnets while the sample vibrates at a frequency of 75 Hz. The different experiments are done with the VSM: (1) a Hysteresis-Loop and (2) a DCD curve**.** The VSM measurements are used to determine the magnetic properties of the grains present sample. With the data obtained with these measurements the domain state of the grains can be assessed: single domain (SD), Multi Domain (MD) or Pseudo Single Domain (PSD). This can be done by measuring the magnetic behaviour of a sample when subjected to a large magnetic field. The theory of magnetic domains and the measurements is explained below. In short, results from the VSM may explain something about the potential of the rock to record an accurate paleo-direction and paleo-intensity at the time of deposit and crystallization. Further it provides information about the grains size of the magnetic minerals.

3.2.1 Domain properties

A magnetic grain is characterized to be Single Domain (SD), Multi Domain (MD) or Pseudo Single Domain (PSD). Single domain means a grain, often very small (10 - 1000 nm, depending on its shape), has one preferred magnetic direction, the so called easy axis, which is the favourable line for the magnetic field vector to align to (fig 7). So, a SD grain has one magnetic vector describing its magnetisation. When subjected to a large external magnetic field this magnetic vector will leave its easy axis and align towards the direction of the field that it is subjected to. When the field is removed the vector will position itself into the easy axis but with the vector pointing in the direction closest to the direction of the magnetic field it has been subjected to (fig 6).

In a MD (multi domain) grain there is not one easy axis and its external magnetization is a statistical sum of the magnetic moment of numerous magnetic 'domains' inside the grain that are separated by domain walls (fig 7). There are many vectors that each occupy a domain within the grain that all have a distinct direction, hence the multi domain. All the vectors will take directions along an easy axis that minimizes the needed energy and polar differences to stay put. This means that the vectors will position itself relative to each other in such a way that creates the smallest field lines and thus will cost the smallest energy; this is an optimization between the energy necessary to sustain the external field of the grain and the energy needed to overcome the potential that arises at domain walls.

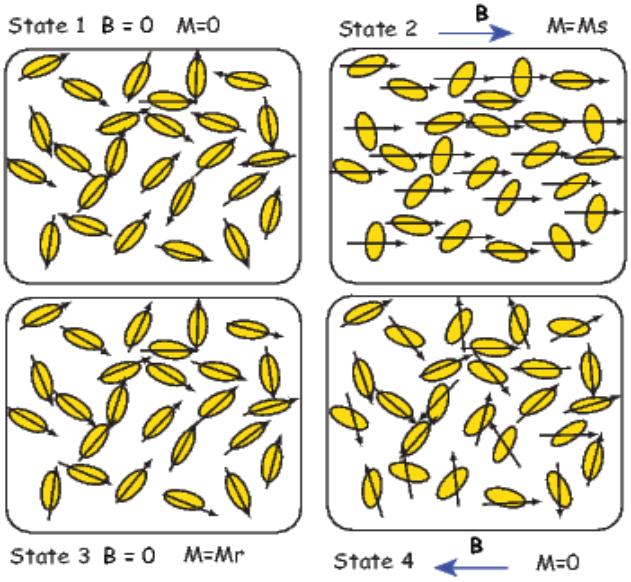

Figure 6: State 1 shows the original state of all the grains (SD) in a zero field (B=H=0) with no internal magnetisation (M=0) with all the vectors aligned along their easy axis. State 2 shows the state of the vectors when pulled at by a magnetic field B forcing them to leave their easy axis. State 3 shows the grains and their vectors in a zero field again but now with the vectors pointing towards the previously external magnetic field B aligned in their easy axis. State 3 shows the grains with zero internal magnetisation again because the external field B balances the vectors by pulling towards the opposite direction than before forcing some to leave the easy axis. Source : Tauxe (2010)

Between Multi domain and single domain there is pseudo single domain (PSD). This type of grain has more than one domain but the mean of all the vectors still gives a relatively clear direction in contrast to multi domain. It does however have smaller external field than expected based on its volume and the magnetisation of single domain grains**.** Because the remanence carrying grains grown inside a lava when it cools it is highly unlikely to find a mean of very small single domain grains in a sample, a combination of PSD and/or MD grains is much more likely to find.

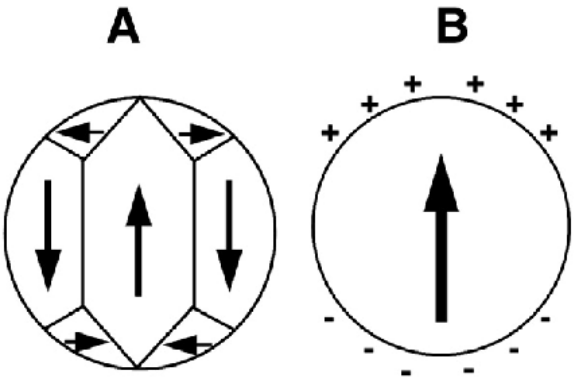

Figure 7: Showing a schematic multi domain grain with multiple vectors (A) and a schematic single domain grain with just one vector (B). Source: Austin et al (2014)

Determining if a sample has mostly SD, MD or PSD grains is useful to be able to tell how accurate paleo-directions and paleo-intensities are when measured. Because MD grains have many domains and thus many optimal positions for its vectors, the direction and quantity of the

magnetic field produced by such grains is often not representative for the actual field and intensity at the time of crystallization.

3.2.2 Hys-Loop

With the Hysteresis Loop (Hys-loop) measurement the sample is subjected to a constant magnetic field that goes from 1.5 T to -1.5 T and back to 1.5 T again. This is done in field steps, which are larger (0.1 T) when the field is higher but smaller (< 0.01 T) when it gets closer to the origin (fig 7). At each field step the magnetic field of the sample is measured. The intersection with the axes and the maximum/minimum value give information about the sample as shown in figure 8. The maximum at point 1 (fig 8) shows the magnetic saturation, Ms, point of the sample. This means that all the vectors are aligned towards the direction of the strong magnetic field it is subjected to, 1.5 T in our measurements, and that the magnetic field of the sample will not get any higher beyond this point even when it is subjected to larger magnetic forces in that direction. Then the magnetic field in the VSM is gradually reduced in field steps towards -1.5 T, so the opposite direction but identical strength. The point where it intersects the y-axis (figure 8 point 2) is called the remnant magnetisation, Mr. This is the magnetisation the sample still possesses when it is not subjected to an external field. So the magnetisation a sample can carry naturally. Further down the plot the signal crosses the x-axis in point 3, the Hc (Coercive magnetic field), this is the strength of field the sample has to be subjected to, to show no magnetisation, so the sample's remnant magnetization is nullified. Point 4, 5, 6 show the same value, theoretically, point 4 corresponding to – Ms, point 5 to –Mr and point 6 to – Hc.

3.2.3 DCD

The DCD measurement follows the same plot as the Hys from -1.5 T until – Hc (fig 8 point 5). The difference between Hys and DCD is that with the Hys-loop a constant magnetic field is applied but with DCD the field is removed while measuring, i.e. the field is applied in steps that increase in strength and removed while measuring. By doing this the plot will eventually intersect the x-axis (H) at a point that is called the Hcr (coercive remnant magnetic field, fig 8 point 7). Because the magnetic vectors of the domains will each time find a possible optimal position towards each other because the field returns to zero each time. The intersection with the axis will tell you how strong the field needs to be to align the vectors into a position that creates a zero magnetisation in the sample.

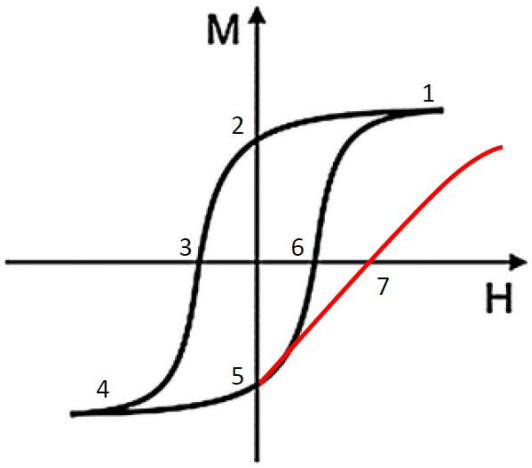

Figure 8: Simplified example of a hysterisis loop (black curve) and a simplified example of a DCD curve (red curve). Point 1=Ms, point 2=Mr, point 3= Hc, point 4=-Ms, point 5=-Mr, point 6=-Hc, point 7=Hcr.

3.2.4 Day plot

In Dunlop (2002) an improved way is presented to plot and combine the results of the Hys-loop and DCD measurements in a Day plot (Day, 1977). With a Day plot it is possible to distinguish what kind of grain domains are found in the samples. In this graph you plot the proportions of Mr/Ms on the y-axis and Hcr/Hc on the x-axis of a sample and these will most likely plot in certain segments that provide information if a sample is either single domain, multi domain or pseudo single domain.

3. Results

4.1 Magnetic susceptibility measurements (Kly-3)

The results of the magnetic susceptibility measurements show a variation in curves but homogeneity in temperature numbers. The magnetic susceptibility at room temperature of the samples varies from 1,60E-6 – 4,00E-5 (fig 9) and all except three retain 80 % of their room temperature susceptibility until 550 °C or higher. Only GR47-10, GR48-1 and GR49-4 lose 80% of their room temperature susceptibility before 500°C. 47 out of the 100 samples have a Hopkinson peak close to 300°C. The temperature of the first alteration lies at 150-160 °C for 32 samples and for 45 samples at 270-280°C. All the graphs are presented in appendix C and a table with all the results of the analysis are described appendix B. The samples are categorized into groups on the basis of two conditions: [1] The shape of the curve they show, [2] The temperature at which the first alteration occurs. For example: the curves of group A-1 and A-2 are similar but the first alteration temperature of A-1 is 275 °C or higher while group A-2 shows a first alteration temperature of 160 °C or lower. Only group B-1 and B-2 are separated for different reasons. Representative graphs of each group are shown in fig 9 and in table 2 is shown within which group each flow belongs.

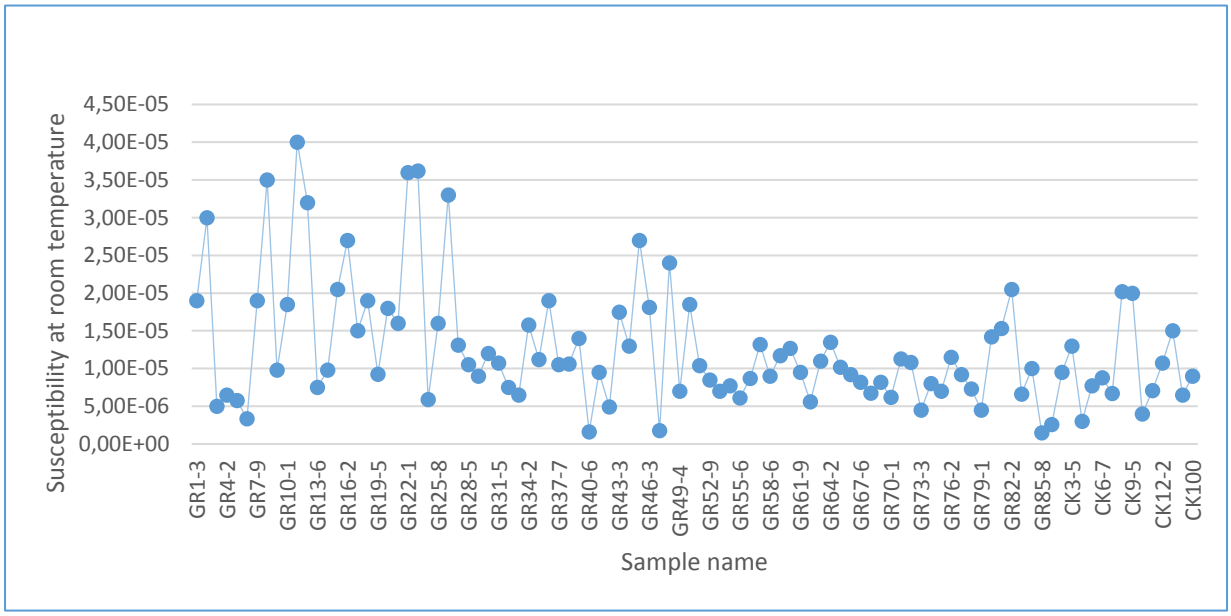

Figure 9 *Graph showing mass normalized magnetic susceptibility variation of the samples at room temperature (25°C). The samples are displayed in numerical order from low to higher flow number.*

3.1.1 Group A-1

Group A-1 consists of 18 samples. The samples of group A-1 (fig. 10.a) show a first alteration at 275 °C or higher and a Hopkinson peak between 300-445°C. Almost all samples show an increase in susceptibility at first and peak form alterations in the last three to one temperature cycles (420, 480, 620 °C), resulting in high peaks in the curves around these temperatures. These curves show an increase in susceptibility of sometimes a 100% of the susceptibility at room temperature, when cooling 40 °C after the peak temperature of that cycle. The susceptibility in some cases extends the Hopkinson peak.

3.1.2 Group A-2

The 13 samples in group A-2 (fig 10.b) show the same characteristics in their curve as group A-1 but have a first alteration temperature at 160 °C or lower. These samples show alteration from the first temperature cycle onwards. The Hopkinson peak temperatures vary more within this group: from 165 °C-480 °C.

3.1.3 GROUP B-1

Group B-1 (fig 10.c) consists of only three samples that all show almost directly decreasing susceptibility curves. Their first alteration temperature lies between 215-220 ^{o}C but overall the alterations are less than 2% of their susceptibility at room temperature. After the first alteration all three curves tend to follow mostly the same curve back and forth during heating and cooling. These curves together with group B-2 were the only ones from which the Curie temperature could be obtained (table 1).

3.1.4 GROUP B-2

Group B-2 (fig 10.d) shows the same shape of curve as group B-1 but they do not decrease at the same rate. There are only two samples in this group but they do not fit right with any other group as they do with each other. GR52-9 has a first alteration at 220^{o}C and GR75-8 has a first alteration at 275 ^{o}C. After the first alteration they both show little alteration at further temperature steps except for the last cycle.

Sample	**Group**	**First Curie temperature (^{o}C)**	**Second curie temperature(^{o}C)**
GR47-10	B-1	440	x
GR48-1	B-1	330	505
GR49-4	B-1	315	490
GR52-9	B-2	350	580
GR75-8	B-2	350	x

Table 1*: Displaying curie temperatures for samples from group B-1 and group B-2. The first curie temperature are obtained from the first inflection point after the Hopkinson peak and the second curie temperature from the second inflection point after the Hopkinson peak.*

3.1.5 GROUP C-1

Group C-1 (fig 10.e) all show a first alteration temperature of 270-275 ^{o}C and a Hopkinson peak temperature between 290-360 ^{o}C. These 17 samples all alter after the third temperature cycle often with almost 20% of their room temperature susceptibility. These curves does not follow the same path back and forth at all. After the first alteration the susceptibility decreases when cooling, increases slightly when heated and starts decreasing vast overall after the last temperature cycle.

3.1.6 GROUP C-2

Group C-2 (fig 10.f) consists of 10 samples and has a first alteration temperature of 160 ^{o}C. Further the Hopkinson peak temperatures vary more than in group C-1: 300 -540 ^{o}C.

3.1.7 GROUP D-1

The curves in group D-1 (fig 10.g) have a very characteristic curve. The 7 samples group D-1 also have a first alteration temperature around 275 ^{o}C. After this temperature the susceptibility of the samples decreases with up to 15 % of the room temperature susceptibility with each heating step and stays relatively level during the cooling steps. They still retain 80 % of their room temperature susceptibility until around 600 ^{o}C. Only CK4 is a bit of an exception in this group. It could also have been categorized in A-1, because it shows a peak at the last temperature step suddenly increasing in susceptibility when cooling.

3.1.8 GROUP D-2

Group D-2 (fig 10.h) consists of 10 samples. These again have a first alteration temperature of 160 ^{o}C but start the same vast decrease and large (up to 15%) alterations in susceptibility at the same point the samples in group D-1 show, so after 275 ^{o}C.

3.1.9 GROUP E

Group E (fig 10.i) does not have two separate groups. All 20 samples have a first alteration temperature between 275-450^{o}C and a Hopkinson peak between 300-500 ^{o}C. The curves are very similar and show relatively no large alterations, some samples show larger alterations but not until the last temperature cycles.

Sample	Group	Sample	Group	Sample	Group	Sample	Group
GR1-3	Group D-2	GR26-6	Group C-1	GR51-3	Group A-1	GR76-2	Group C-2
GR2-2	Group E	GR27-4	Group D-1	GR52-9	Group B-2	GR77-5	Group A-2
GR3-5	Group D-1	GR28-5	Group A-2	GR53-8	Group C-1	GR78-9	Group E
GR4-2	Group D-2	GR29-9	Group D-2	GR54-8	Group C-1	GR79-1	Group E
GR5-9	Group D-2	GR30-3	Group A-1	GR55-6	Group A-2	GR80-9	Group E
GR6-10	Group C-1	GR31-5	Group D-1	GR56-6	Group E	GR81-1	Groep C-1
GR7-9	Groep C-2	GR32-1	Group A-1	GR57-8	Group E	GR82-2	Group E
GR8-3	Group C-1	GR33-3	Group D-2	GR58-6	Group A-1	GR83-3	Group E
GR9-9	Group C-1	GR34-2	Group D-2	GR59-3	GroupA-1	GR84-7	Group C-2
GR10-1	Group C-1	GR35-5	Group A-1	GR60-2	Group C-1	GR85-8	Group E
GR11-8	Group A-2	GR36-4	Group C-1	GR61-9	Group E	CK1-6	Group D-2
GR12-4	Group E	GR37-7	Group A-2	GR62-7	Group C-2	CK2-4	Group D-1
GR13-6	Group D-2	GR38-10	Group A-1	GR63-4	Group A-2	CK3-5	Group A-2
GR14-1	Group D-2	GR39-11	Group A-1	GR64-2	Group A-1	CK4-2	Group D-1
GR15-4	Group C-1	GR40-6	Group D-2	GR65-8	Group A-1	CK5-1	Group A-2
GR16-2	Group C-1	GR41-8	Group C-2	GR66-4	Group A-2	CK6-7	Group E
GR17-10	Group A-1	GR42-9	Group C-1	GR67-6	Group C-1	CK7-1	Group A-2
GR18-8	Group A-1	GR43-3	Group A-1	GR68-8	Group A-1	CK8-9	Group E
GR19-5	Group D-1	GR44-7B	Group E	GR69-3	Group A-1	CK9-5	Group E
GR20-3	Group D-1	GR45-2	Group C-1	GR70-1	Group A-1	CK10-6	Group A-1
GR21	Groep C-2	GR46-3	Group A-2	GR71-1	Group C-2	CK11-2	Group E
GR22-1	Group C-1	GR47-10	Group B-1	GR72	Group E	CK12-2	Group E
GR23-1	GroupA-1	GR48-1	Group B-1	GR73-3	Group E	CK13-3	Group C-2
GR24-3	Group C-1	GR49-4	Group B-1	GR74-6	Group A-2	CK99-6	Group D-2
GR25-8	Groep C-2	GR50-1	Group A-2	GR75-8	Group B-2	CK100	Group C-2

Table 2: Displaying all flows with their corresponding group from the susceptibility measurements.

Figure 10: Examples of susceptibility curves per group. Orange = Hopkinson peak with corresponding temperature. Green= First alteration with corresponding temperature.

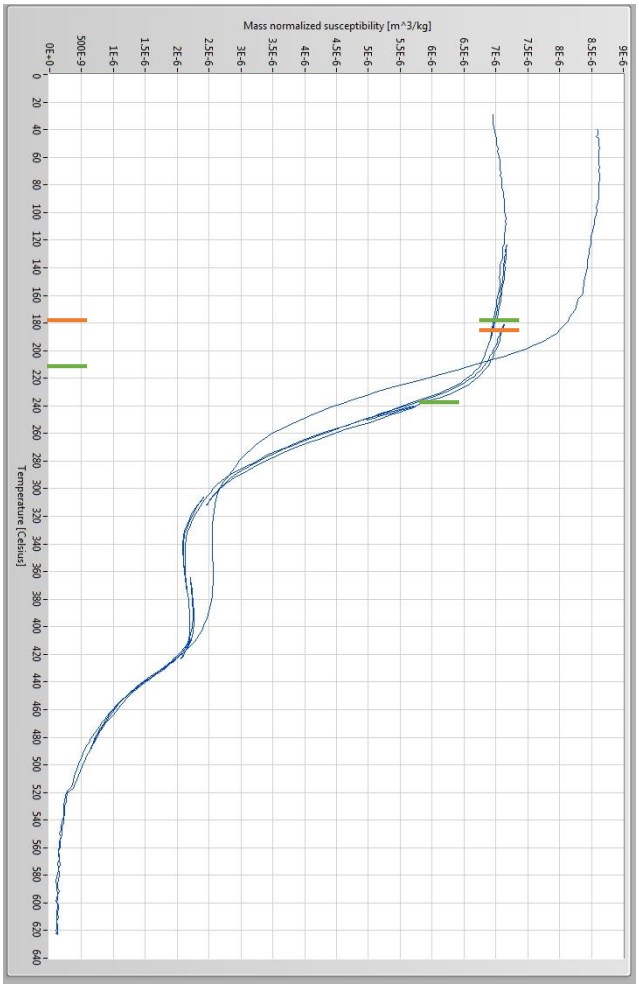

Figure 10.c: group B -1 sample GR49-4

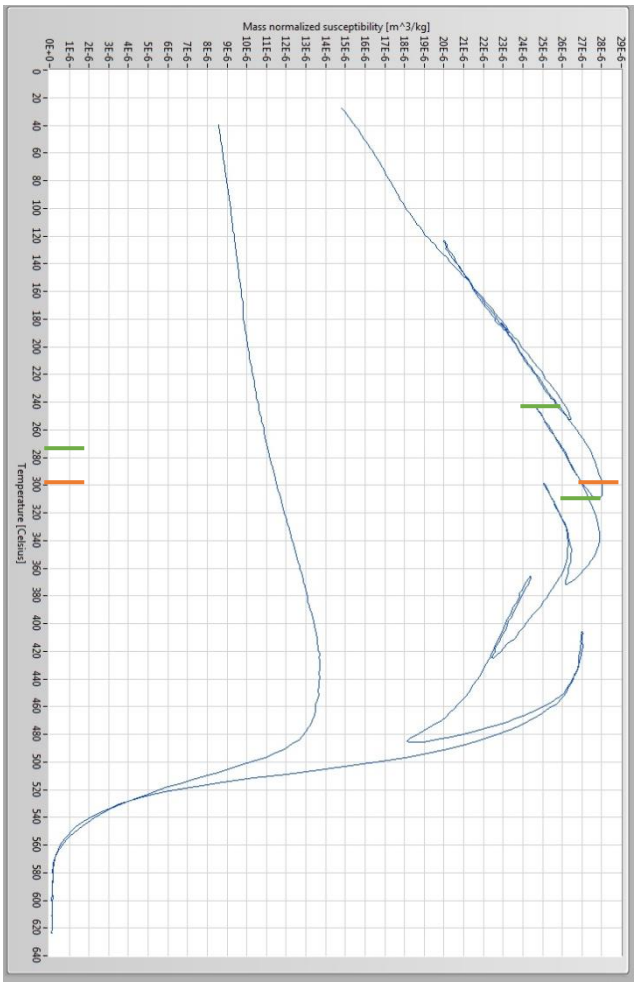

Figure 10.a: group A-1 sample GR17-10.

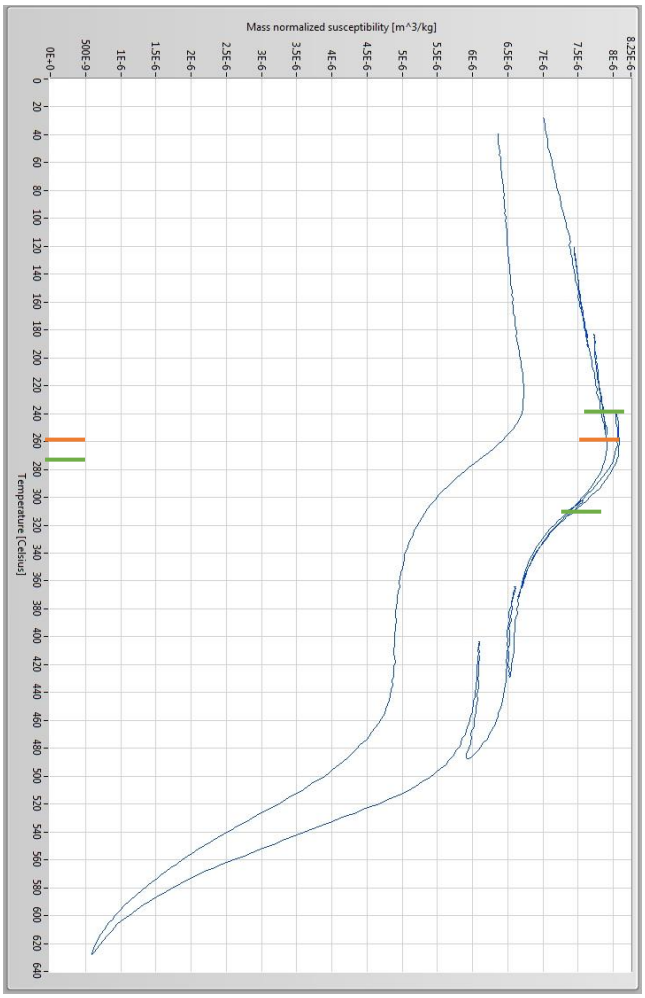

Figure 10.d: group B-2 sample GR75-8..

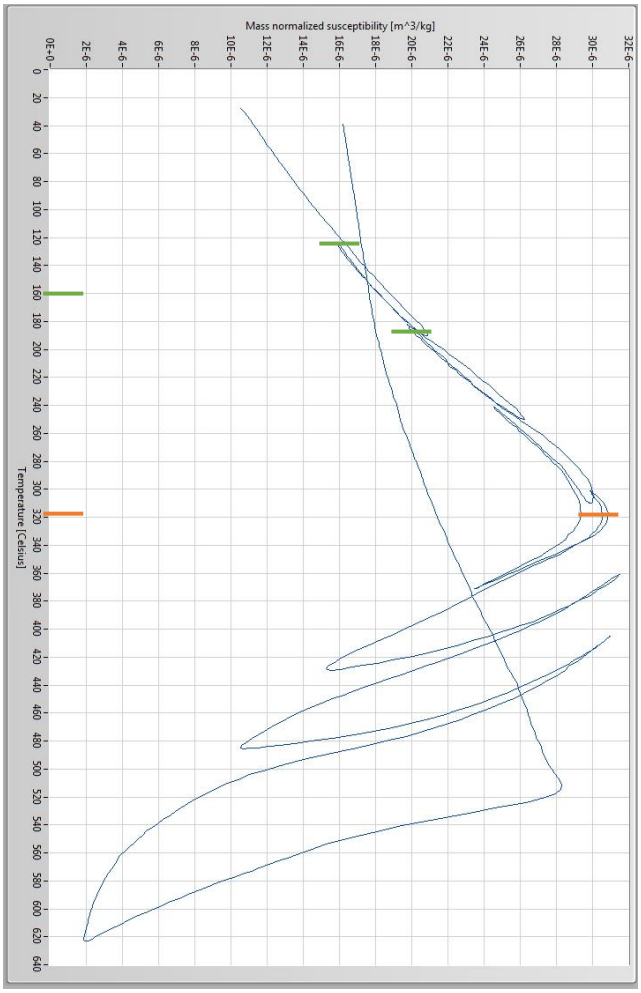

Figure 10.b: group A-2 sample GR28-5.

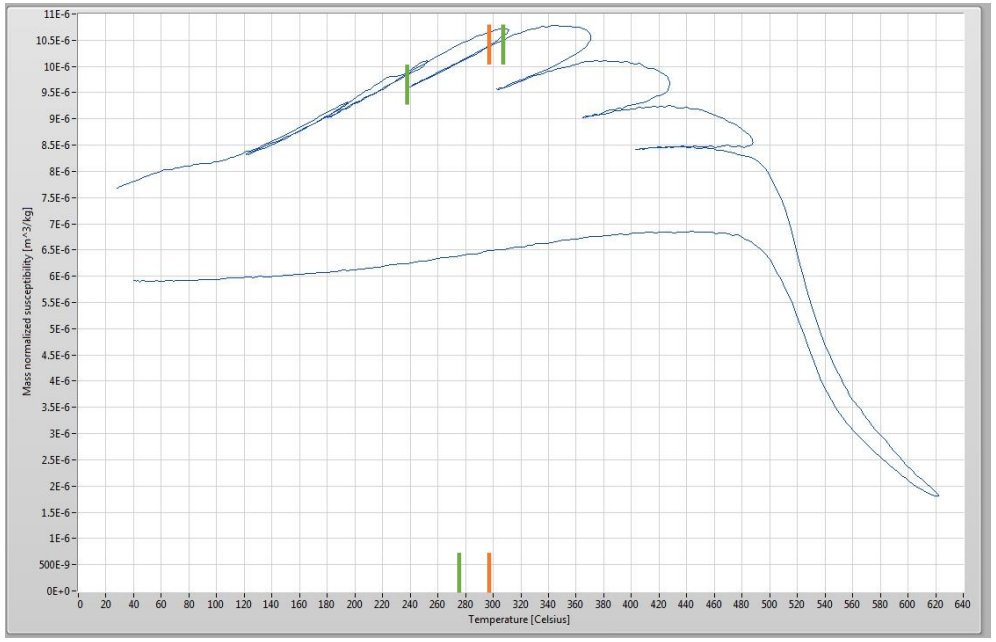

Figure 10.e: group C-1 sample GR54-8.

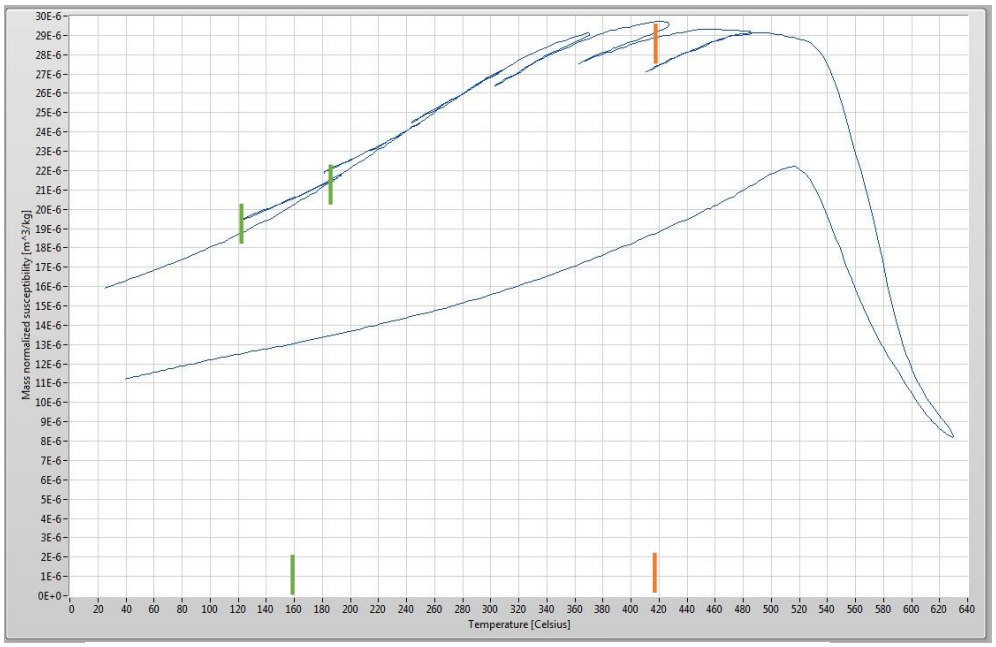

Figure 10.f: group C-2 sample GR25-8.

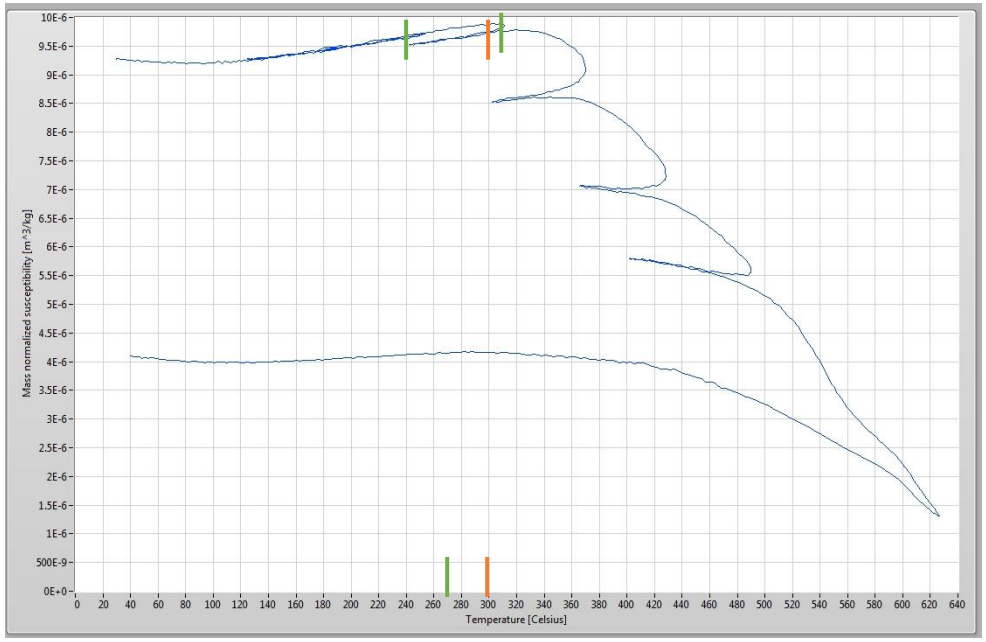

Figure 10.g: group D-1 sample GR19-5.

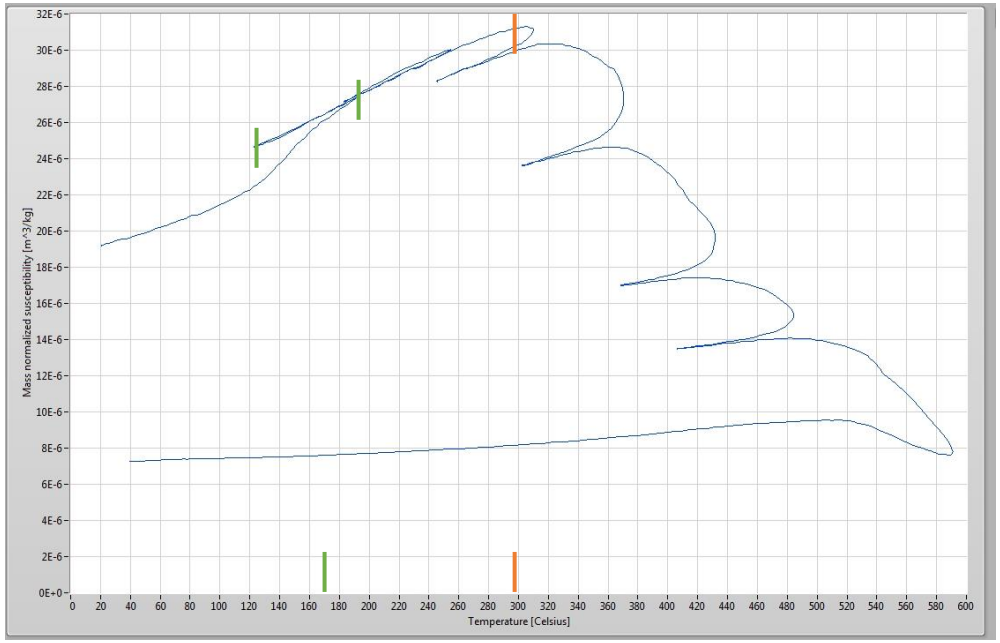

Figure 10.h: group D-2 sample GR1-3.

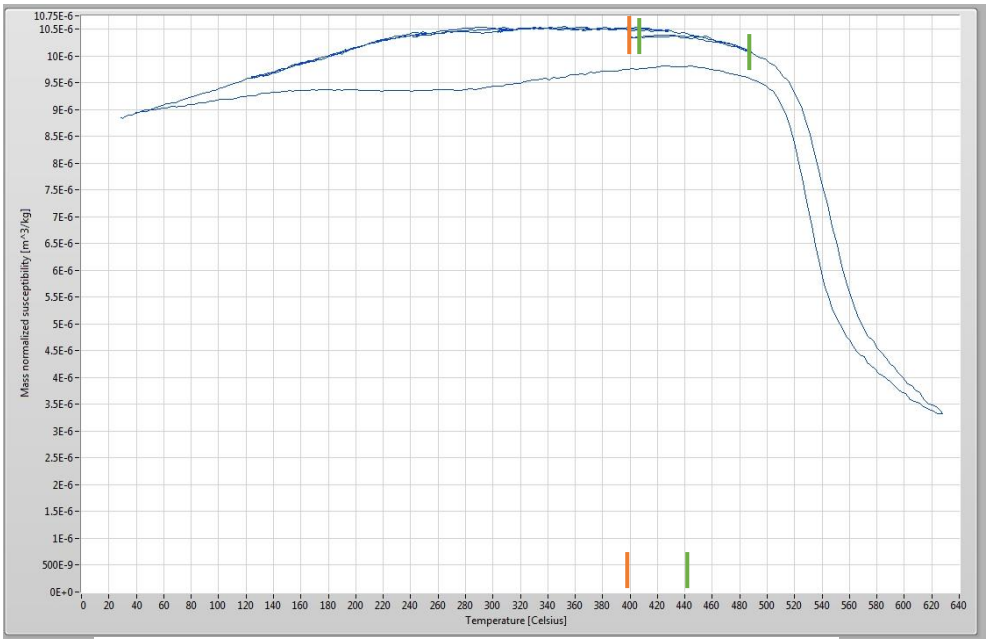

Figure 10.i: group E sample CK6-7.

4.2 VSM

A table with all the results of the VSM measurements is displayed in appendix D. In this table the points discussed within the method are shown. During measurements some DCD loops did not show an intersection with the x-axis in the eventual result (axis that displays the measured magnetisation within the sample). The measurements that showed this are shaded red within the table in appendix D. For these measurements a linear continuation was calculated from the last three measured points. From this calculated linear equation the point where the curve should have intersected with the axis was obtained, giving the value of Hcr for that sample. The results of the proportions between Mr/Ms and Hcr/Hc are plotted in fig. 12. The results are subdivided within the same groups as the results from the susceptibility measurements making potential correlation possible later on. 80 samples plot within the PSD (pseudo-single domain) area but 17 samples plot within the segment above the MD (multi domain) area (fig. 11). The segment limitations that indicate whether a sample plots within MD, PSD or SD segments, are taken from de Groot et al. (2015). Only for GR11, GR80 and GR81 there is no available data because the saved data-files showed errors causing the data to be unusable.

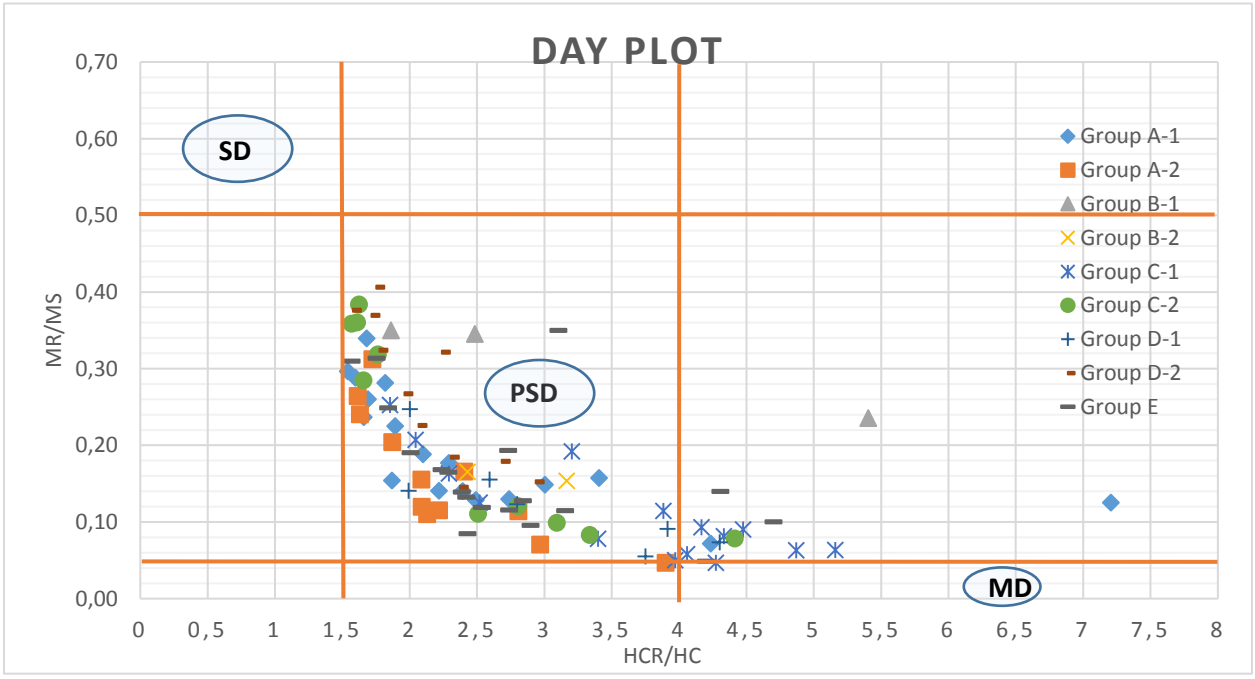

Figure 11 Day plot (Day et al., 1977) showing the results of the VSM measurements of each sample in Mr/Ms and Hcr/Hc proportions. Limitations for the segments of the SD, PSD and MD grains are taken from de Groot et al. (2015) .Most samples plot within the PSD segment af few above the MD and none in the SD segment.

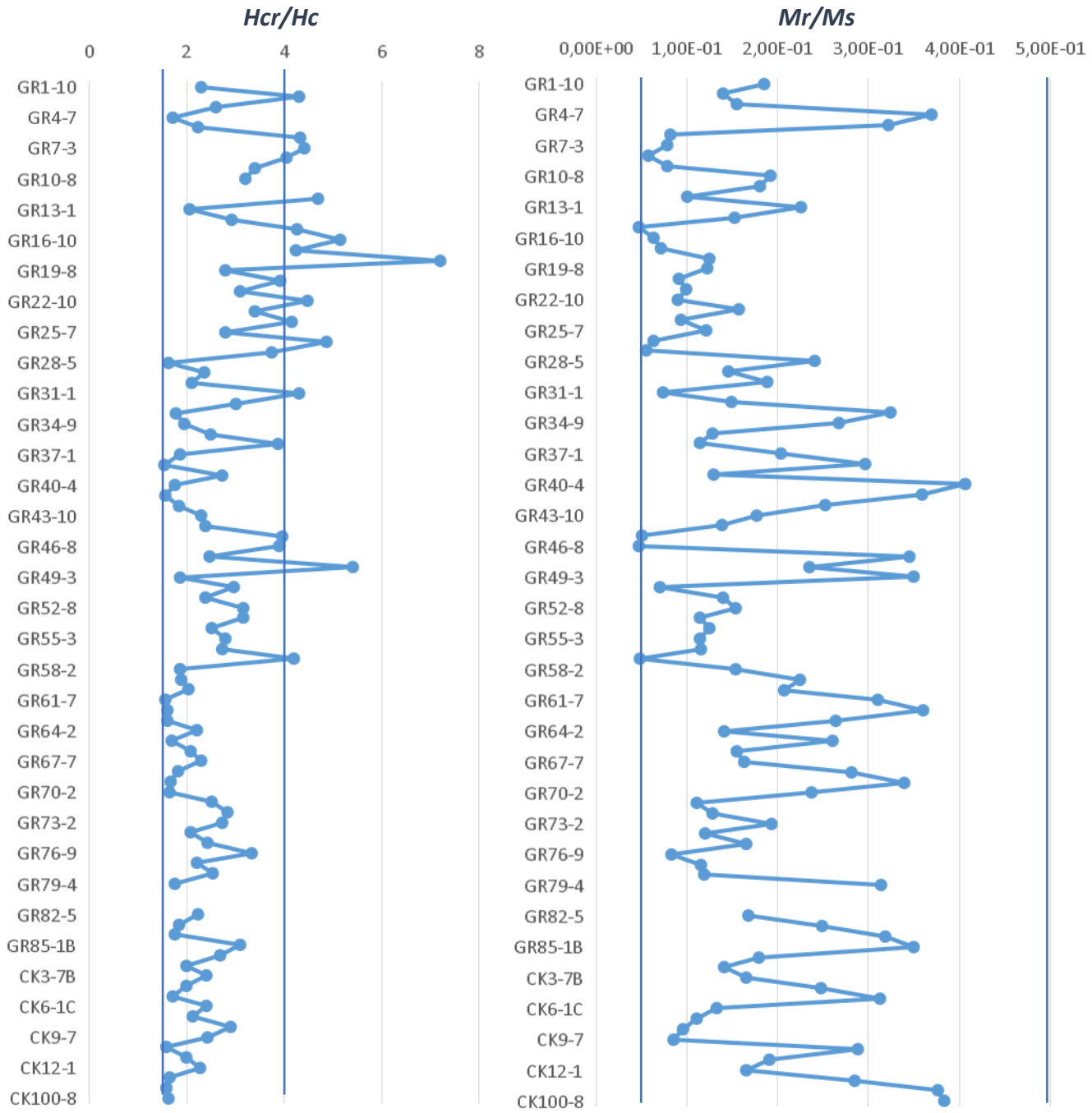

Figure 11: Displaying the proportions of Hcr/Hc and Mr/Ms per sample. The straight vertical lines represent the segment boundaries that are also used in the Day plot in figure 10.

4. Discussion

The overall goal of this research was to construct a detailed record of a magnetic polarity reversal captured in the shield building lavas of Gran Canaria. In this part of the research we constructed a detailed overview of the rock magnetic properties, the susceptibility and domain properties, on the basis of one hand selected sample per flow to assess the suitability of the lavas to record and store information of the Earth's magnetic field acquired at the time of cooling.

5.1 Interpretation

5.1.2 Magnetic susceptibility measurements

The susceptibility measurements are categorized into 9 groups (see Results; magnetic susceptibility). The shape of the curves show large variations but the temperatures (first alteration and Hopkinson peak) vary little. The resemblance in the temperatures of first alteration can partly be attributed to the fact that the measurements are done in cycles and that the temperature of first alteration always lies within one of these cycles (temperature intervals). Still it is clear that in 32 samples alteration already occurs in the first cycle (< 160 ^{o}C) and for another 45 samples in the third temperature cycle (~275 ^{o}C). This suggests that the samples are already altered around 160 ^{o}C in 32 cases and around 275 ^{o}C in 45 cases.

Almost 50 % of the samples shows a Hopkinson peak at 300 ^{o}C suggesting that the maximum magnetic susceptibility is reached and that less minerals alter after this point. Only in group A some alteration curves extend the Hopkinson peak when cooling. Normally the Curie temperature can be closely approximated by these graphs but as no inflection point is visible in most curves this was eventually only done for group B. The samples in group B almost all show two inflection points and therefor two Curie temperatures are acquired. The first Curie temperature is around 350 ^{o}C for most and a second one, possibly for three samples, around 500 ^{o}C. Because the inflection point is not visible in the other 95 samples, it would suggest that the Curie temperature is rather high, above 500 ^{o}C. The Curie temperatures in group B suggest two minerals with a distinct Curie temperature to be present. The first Curie temperature indicates the presence of x=0.2-0.4 $Fe_{3-x}Ti_xO_4$ (titanomagnetite) and the second is closer to that of pure magnetite (Dunlop & Özdemir, 1997). The other samples that do not show an inflection point would also suggest an abundance in magnetite or maybe even hematite, corresponding to a higher Curie temperature (fig 14). In Tauxe (2010), however, it is suggested that the inflection point might not always be an indication of the Curie temperature but that the Hopkinson peak represents unblocking and that the inflection point just indicates the alteration of minerals. Whether the Curie temperatures are actually this high can be checked partly with the Zijderveld diagrams during thermal magnetisation (van Klaveren, 2017), because these samples should unblock at higher temperatures. Further it would be helpful to measure the Curie temperature from each flow with a Curie balance for comparison.

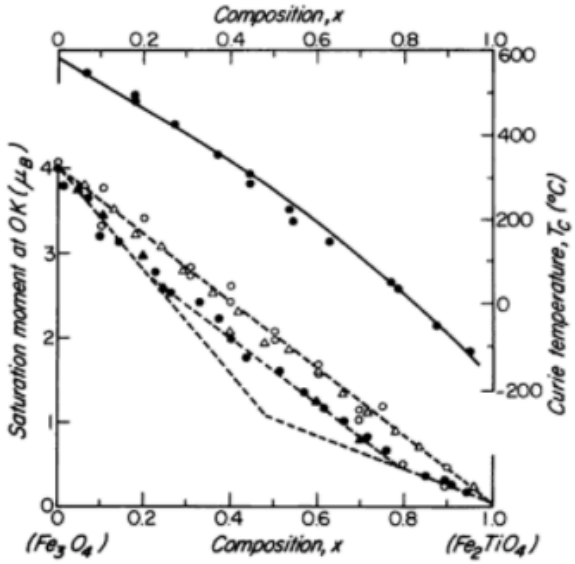

Figure 14: Figure from Dunlop & Özdemir (1997) displaying (top curve) the curie temperature ranging from pure magnetite to titanomagnetite.

The first alteration indicates the first temperature at which the sample alters in some way causing it not to show the same behaviour anymore at the same temperature. Three different causes can attribute to these alterations: [1] The alteration of the magnetic minerals (Larson et al., 1969; Petersen et al., 1979; Lattard et al., 2012) [2] The alteration of the domain walls. (Sherbakov, 1993) [3] Unmixing of magnetic minerals (Heslop & Dillon, 2007). Our samples show possibly all of these kind of alterations but it is difficult to exactly tell by only the susceptibility curves which kind of alteration has taken place in each sample. All of these possible alterations are assessed below.

[1] The alteration of minerals is known to happen with temperature. Mainly high temperature oxidation attributes to this (fig 15). Through oxidation titanomagnetite will oxidise into ilmenite and magnetite. Magnetite can alter to hematite during high temperature oxidation processes (Larson et al. 1969). In microscopic research they found that with increasing temperature ilmenite and sometimes hematite lamellae will form within titanomagnetite or magnetite crystals (Larson et al., 1969; Lattard et al., 2012). Because of these alterations the magnetic properties of the crystals change. Magnetite has other properties than titanomagnetite and the ilmenite lamellae that form, construct natural barriers within the crystal that alter the size of the magnetic grains, probably altering the domain walls. Hematite is also a ferromagnetic mineral but shows less strong magnetisation. Larson et al. (1969) concluded that when these lamellae form the crystals show more stable magnetic behaviour. Because they now resemble SD grains more than MD grains due to the natural barriers formed by the lamellae. If these kind of alterations happen during the measurements with the Kappabridge it will show in the susceptibility curves. The alteration of titanomagnetite towards magnetite will show in an increase in susceptibility due to higher abundance of magnetic minerals. But alteration of magnetite to hematite will earlier show a decrease in susceptibility because this mineral shows less strong magnetic behaviour. Altogether these alterations are permanent and will change the magnetic properties of the samples, causing them to be less reliable when measuring paleo-intensities. Larson et al. (1969) did show that the directions recorded within the magnetic crystals are saved, only the intensity of the magnetisation changes.

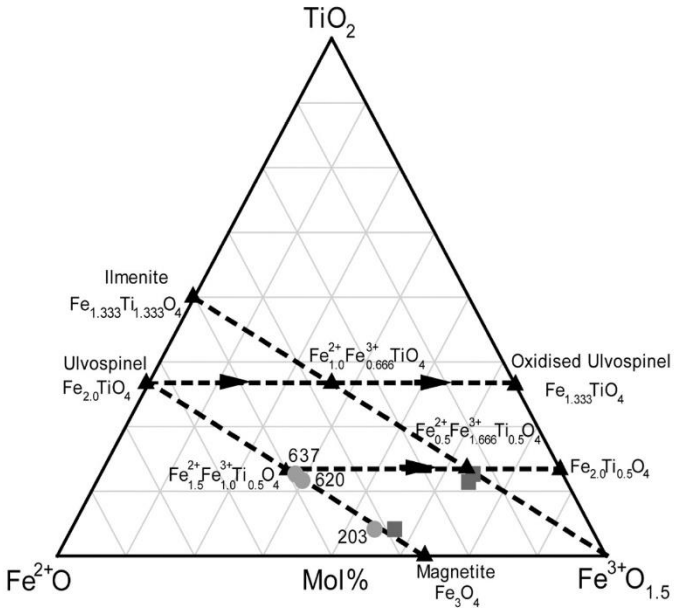

Figure 15 : Triangle plot showing the endmembers of the spinel-family and the possible oxidation and unmixing routes. Source: http://ammin.geoscienceworld.org/content/gsammin/91/5-6/880/F9.large.jpg

[2] Sherbakov (1993) researched the behaviour of domain walls within MD grains when heated and cooled. He showed that during cooling domain wall reorganization takes place within samples. These domain wall reorganization causes the magnetisation of a sample to decrease during cooling. This could be visible within the susceptibility diagrams as a decrease in susceptibility because the grains apparently reorganize in such a way that it decreases the magnetisation of the minerals. A decrease in susceptibility during alterations is clearly visible within the curves of group C and D.

[3] The mineral series that includes titanomagnetite and magnetite are prone to unmixing. The unmixing is partly dependent on the cooling rate of the basalt thus the time the minerals get to form different end-members (Heslop & Dillon, 2007). The faster the cooling rate the lesser the mineral

endmembers that form. The possible minerals that can form include titanomagnetite, magnetite and ilmenite (fig 15). Ongoing unmixing can occur when a rock is heated again which also can cause alteration to show in the susceptibility curves. The alteration that will occur within the susceptibility curves is dependent on the kind of unmixing that has taken place. If the unmixing happened from a ferromagnetic mineral to a mineral without such magnetic properties it will show a decrease in susceptibility (hence lower abundance of magnetic minerals) and vice versa.

When comparing the susceptibility curves obtained in this research and that of de Groot et al. (2015) two main differences stand out. [1] In this research most samples do not show a decay in susceptibility until temperatures above 300 ^{o}C and the samples in de Groot et al. (2015) often start decreasing already before reaching 200 ^{o}C. [2] The lavas used for this research are much older (~14 Ma). The ones used in de Groot et al. (2015) date back to ~4000 BC-1909 AD. There are also two similarities found between the curves from de Groot et al. (2015) and this research: [1] The curves from group B show similarities with the curves from de Groot et al. (2015) that were successful with intensity measurements. [2] The curves from group E also show the same type of curve as a group from de Groot et al. (2015) but they were viewed to be less successful with intensity measurements in de Groot et al. (2015) while some were successful with our measurements (fig 16).

The age difference between the lavas used in de Groot et al. (2015) and the lavas used in this research could account for the difference in Curie temperatures. According to Petersen et al. (1979) older lavas tend to have higher quantities of magnetite compared to younger ones due to the conversion of titanomagnetite to magnetite under the influence of low-temperature oxidation which is connected to weathering of the lavas. The research of Petersen et al. (1976) was performed on oceanic basalts that are weathered in different conditions than our lavas, but some of these processes are likely to have had an influence on the rocks used in our research as well. In Petersen et al. (1979) he concludes that low temperature oxidation is combined by Fe-migration out of the crystal changing the initial Fe/Ti ratio. They observe that due to this low temperature oxidation the saturation magnetisation of these rocks first decreases. Then, when a certain degree of low temperature oxidation is reached, the magnetisation starts increasing again. Peteresen et al. (1979) concludes this variation is caused by first Fe migrating from octahedral sites within the crystal lattice and then from tetrahedral sites. Further they observe an increase of the Curie temperatures that rises almost linear with age of the basalts. The older the rock the higher the Curie temperature, which agrees with the observation we make when comparing to our data to that of de Groot et al. (2015).

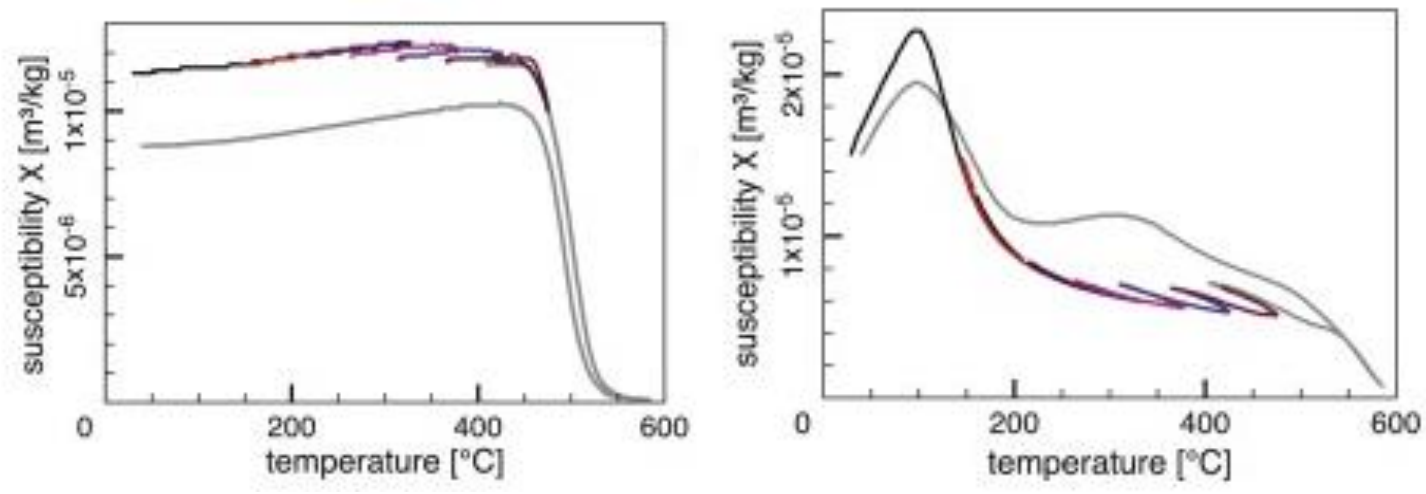

Figure 16: Two curves presented in de Groot et al. (2015). On the left the curve that shows great similarities with the curves in this research categorized in group E. In the Groot et al. (2015) they expected it to be hard to obtain a reliable paleo-intensity from these curves. On the right is the representative curve for a successful group from de Groot et al. (2015) that resembles the curves we obtained for group B, especially group B-1.

5.1.2 VSM

The VSM results show clearly that the 80 flows are within the PSD area (as expected) and that 17 samples plot outside the PSD segment but above the MD segment. The only visible differentiation is that more than half of the C-1 group samples plot above the MD segment but it is difficult to obtain a clear explanation on why this would be the case when comparing magnetic susceptibility data and VSM measurements. Most theories in other measurement techniques (e.g. IZZI-Thellier; pseudo-Thellier; thermal demag) work with the assumption of SD grains but also work with PSD grains because they are assumed to behave in a similar way on macroscopic level. That so many samples plot within the PSD segment is therefore good for the reliability of other measurements done within the other theses (Marijnissen (2017), Tuinstra (2017), van Klaveren (2017)).

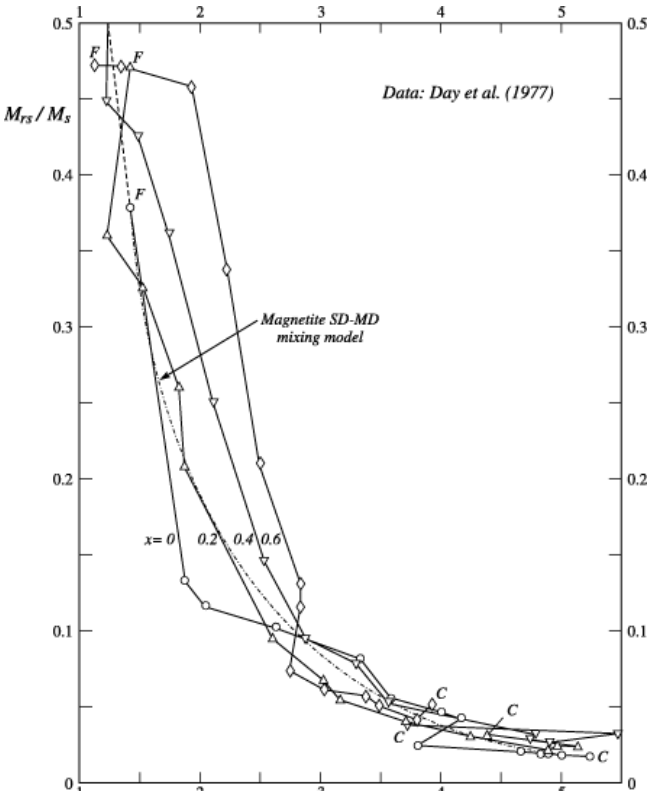

Figure 17: Plot obtained from Dunlop et al. (2002) showing the mixing curves of x=0-0.6 $Fe_{3-x}Ti_xO_4$.

PSD grains suggest a mean grain size that is between SD an MD sized. In Dunlop et al. (2002) different mixing curves of SD and MD grains are presented consistent with TM60 or pure magnetite (fig 17). Comparing these mixing curves with the plotted points of our results it shows that is most consistent with the magnetite mixing curve and much less with the TM60 one. This is in agreement with the suspected high Curie temperatures also matching magnetite rather than titanomagnetite. Day et al. (1977) states that the critical size for singe domain behaviour in magnetite is 0.1 µm and for TM60 1-2 µm. The grains size that causes the onset of MD behaviour shows a broader transition of 10-20µm in magnetite. Microscopic research of the samples is needed to see if they are consistent with these grain sizes. In the results no consistent pattern can be found connecting the groups of the susceptibility measurements with the VSM results.

5.1.3 Correlation with IZZI-Thellier measurements

Marijnissen (2017) presents IZZI-Thellier measurements for the same lavas as were studied here. Because of the generally low success rate of the IZZI experiments it is important to assess whether any correlation can be made with the rock magnetic data, especially with the susceptibility behaviour of the samples.

With IZZI measurements the samples experience varying temperatures and are assumed to show the same behaviour over the whole range. To ensure this, a pTRM check is incorporated and a flow is generally only successful if this pTRM check shows that a sample at an (repeated) lower temperature still acquires the same pTRM as at that temperature when it was measured initially, suggesting constant behaviour of the sample.

All but one successful IZZI sample originate from either group B, C or E. It is worth noticing that four out of the twelve flows originate from group B. This group only consists of five flows in total and four of those are successful with IZZI measurements. These flows in general show little alteration along their whole curve and a steady decay in susceptibility. As mentioned before, they show much similarity with the susceptibility curves presented in de Groot et al. (2015) that were successful with intensity

measurements. These samples often show that they have a steadier fit in the Zijderveld diagrams and the Arai plot. This makes it is possible to take in account more temperature steps when determining the intensity within the Arai plot (fig 15), causing these flows to be suitable for successful IZZI-Thellier measurements.

Sample	Susceptibility group	VSM
GR24	Group C-1	MD
GR42	Group C-1	PSD
GR47	Group B-1	PSD
GR49	Group B-1	PSD
GR52	Group B-2	PSD
GR53	Group C-1	PSD
GR67	Group C-1	PSD
GR75	Group B2	PSD
GR84	Group C-2	PSD
GR85	Group E	PSD
CK3	Group A-2	PSD
CK6	Group E	PSD

Table 3: Displaying the flows that were succesful with IZZI-Thellier, their corresponding group from the magnetic susceptibiltiy measurements and their domain properties.

Two successful flows that originate from group E are also flows that show little alteration in their susceptibility curves making them suitable for IZZI measurements. With 19 flows IZZI-Thellier measurements were done for 7 samples per flow. From the remainder of the flows only two samples have been measured yet and measuring more is still a possibility (Marijnissen, 2017). I would expect that more successful flows will originate from group E in further measurements. However their decay in susceptibility does not start until temperatures around 500^{o}C. The late onset of the decay implies high Curie temperatures, this often provides only higher temperatures as option to fit a line in the Arai plots (fig 18). This leads to less temperature steps that can be used, which is not always in favour of the quality of the result. Because alteration is relatively small in these samples the results are more likely to still be reliable because no large alteration have yet taken place at these temperatures.

The sample selected for susceptibility measurements will not always represent an entire flow. From each flow, just one sample is measured for magnetic susceptibility and for the VSM. From each flow there is a minimum of 8 samples that are measured in other experiments. It is therefore possible that a sample measured for magnetic susceptibility or VSM does not represent all other samples taken from the same flow. I expect this possibly to be the case for CK3 and GR84. These flows show rather large alterations from the first temperature step onward making them in theory unfit for successful IZZI-Thellier measurements. However apparently, they do provide successful IZZI-Thellier measurements suggesting that the samples measured for VSM and susceptibility do not represent the rest of the flow.

The four flows that have curves corresponding to group C-1 are in theory not ideally suitable for IZZI-Thellier measurements. They alter significantly from 275 °C onward. Looking at the Arai plots from Marijnissen (2017) often the line plotted to determine the intensity originates from rather high temperatures (fig 18). It could be that the measured samples for magnetic susceptibility do not represent the flow they were taken from. However because 1/3 of the samples that were successful originate from this group, the theory that they do not represent their flow is less likely. Because these flows show alteration at temperatures from above 275 °C it remains the question if the obtained intensities are reliable.

Looking at the success of the flows and groups they originate from I would recommend measuring more samples with IZZI that have magnetic susceptibility curves that are similar to that of group B or group E. These show little alteration making the measurements far more likely to be successful and trustworthy. Especially the samples in group B that show a relative faster decay and have similarities with curves that were successful in other researches. The faster decay and little alteration make these samples the most suitable for successful IZZI-Thellier measurements.

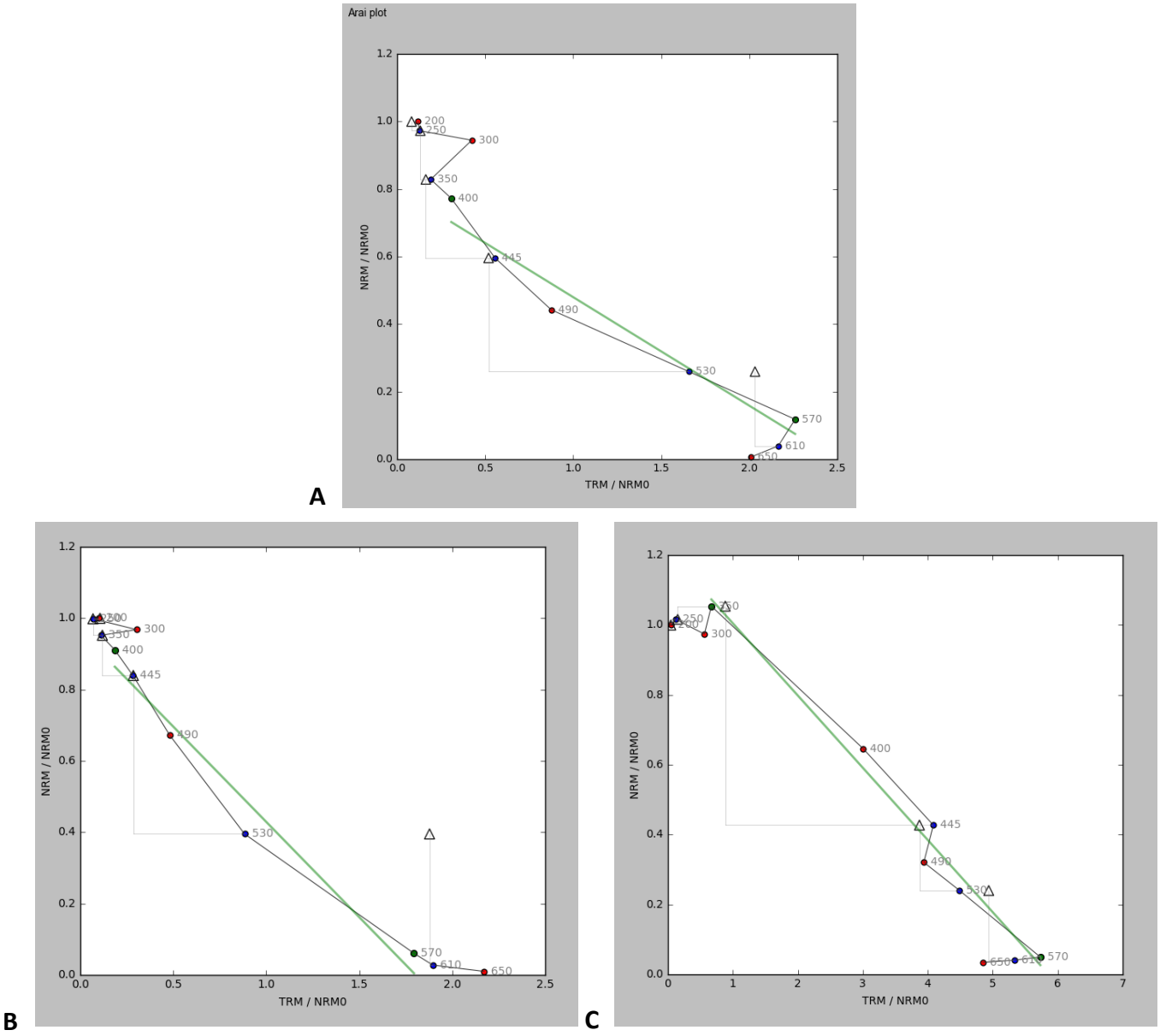

Figure 18 *: Arai plots that show the temperature steps used to obtain the paleo-intensities. On the y-axis you have NRM (natural remenant magnetisation) and the x-axis shows TRM (pTRM; (partial) thermal remenant magnetisation) A: shows sample GR42-2 originating from group C-1. B: shows CK6-5 originating from group E. C: shows GR49-2 originating from group B-1.*

5.1.4 Possibility of improvement in IZZI-Thellier measurements.

Many of our samples how large alterations with temperature when looking at the magnetic susceptibility curves. IZZI-Thellier measurements can be unsuccessful due to alteration within the samples. Part of the alteration that happens cannot be prevented but high temperature oxidation might be possible to minimize. Lattard et al. (2012) researched the effects of high temperature oxidation on synthetic samples of titanomagnetite and magnetite. They found that when a sample is heated to high temperatures (< 440 ^{o}C) and then exposed to air it will already show significant alteration within minutes. The minerals on the surface of the sample will alter until possibly a 100 μm deep layer. They showed that the alteration of the minerals in this surface layer already causes change in the magnetisation intensity measured. When measuring with IZZI-Thellier these alterations could cause a change in the amount of pTRM a sample can store. When the pTRM that a sample can store changes, intensity measurements done with the IZZI-Thellier method are not reliable anymore (more on IZZI-Thellier and pTRM gain in Marijnissen et al., 2017). A possible solution according to Lattard et al. (2012) for the occurrence of high temperature oxidation is to heat and cool the samples within an oxygen deprived environment minimizing the high temperature oxidation and there for the alteration in a sample. So finding a method to heat and cool the samples without them being in contact with oxygen might prove valuable.

5. CONCLUSION

Here we assessed the suitability of 100 Mid-Miocene flows from the island of Gran Canaria to record and store the primary magnetic signal they acquired because of the Earth's magnetic field at the time of cooling. The results presented here corroborate the data obtained in Tuinstra (2017), van Klaveren (2017) and Marijnissen (2017) with rock magnetic data. The rock-magnetic measurements were overall successful and provided useful data to support the other theses, especially that of Marijnissen (2017) that presents the IZZI-Thellier data of paleo-intensity. Both VSM and magnetic susceptibility measurements indicate that the samples have a higher abundance in magnetite than titanomagnetite. 80 samples plotted within the PSD segment making other data (e.g. pseudo-Thellier; IZZI-Thellier; thermal demag) more reliable because these theories assume SD or PSD grains. We found from the correlation of magnetic susceptibility measurements and IZZI-Thellier (Marijnissen, 2017) that the most successful flows with IZZI-Thellier measurements originated form group B and group E (DEFINE GROUPS HERE). Especially group B which also showed great similarities with successful samples from de Groot et al. (2015) was very successful in the IZZI-Thellier experiments. One third of the successful samples originated from group C-1 but these are expected to be less reliable due to early onset of thermal alteration revealed by the susceptibility experiments. For future measurements it is advisable to measure more samples that originate from group B and E to attain a higher success rate. A possible solution for alteration in the samples, which is caused by high temperature oxidation, could be to heat and cool the samples in an oxygen deprived environment, minimizing high temperature oxidation of the magnetic minerals.

REFERENCES

Austin, J., Geuna, S., Clark, D., & Hillan, D. (2014). Remanence, self-demagnetization and their ramifications for magnetic modelling of iron oxide copper-gold deposits: An example from Candelaria, Chile. *Journal of Applied Geophysics*, *109*(January 2015), 242–255. https://doi.org/10.1016/j.jappgeo.2014.08.002

Carracedo, J. C., & Day, S. (2002). *Canary Islands*. Terra Publishing.

CONSTABLE, C., & KORTE, M. (2006). Is Earth's magnetic field reversing? *Earth and Planetary Science Letters*, *246*(1–2), 1–16. https://doi.org/10.1016/j.epsl.2006.03.038

Day, R., Fuller, M. D., & Schmidt, V. A. (1976). Magnetic hysteresis properties of synthetic titanomagnetites. *Journal of Geophysical Research*, *81*(5), 873–880. https://doi.org/10.1029/JB081i005p00873

de Groot, L. V., Béguin, A., Kosters, M. E., van Rijsingen, E. M., Struijk, E. L. M., Biggin, A. J., … Dekkers, M. J. (2015). *High paleointensities for the Canary Islands constrain the Levant geomagnetic high*. *Earth and Planetary Science Letters* (Vol. 419). https://doi.org/10.1016/j.epsl.2015.03.020

Dunlop, D. J. (2002). Theory and application of the Day plot (M_{rs}/M_s versus H_{cr}/H_c) 1. Theoretical curves and tests using titanomagnetite data. *Journal of Geophysical Research*, *107*(B3), 2056. https://doi.org/10.1029/2001JB000486

Dunlop, D. J., & Özdemir, O. (1997). *Rock magnetism : fundamentals and frontiers*. Cambridge University Press.

Heslop, D., & Dillon, M. (2007). Unmixing magnetic remanence curves without a priori knowledge. *Geophysical Journal International*, *170*(2), 556. https://doi.org/10.1111/j.1365-246X.2007.03432.x

Larson, E., Ozima, M., Ozima, M., Nagata, T., & Strangway, D. (1969). Stability of Remanent Magnetization of Igneous Rocks. *Geophysical Journal International*, *17*(3), 263. https://doi.org/10.1111/j.1365-246X.1969.tb00237.x

Lattard, D., Sauerzapf, U., & Kontny, A. (2012). Rapid surficial oxidation of synthetic Fe-Ti oxides at high temperature: Observations and consequences for magnetic measurements. *Geochemistry, Geophysics, Geosystems*, *13*(8). https://doi.org/10.1029/2012GC004152

Leonhardt, R., & Soffel, H. C. (2002). A reversal of the Earth's magnetic field recorded in mid-Miocene lava flows of Gran Canaria: Paleointensities. *Journal of Geophysical Research: Solid Earth*, *107*(B11), EPM 5-1-EPM 5-11. https://doi.org/10.1029/2001JB000949

Leonhardt, R., Matzka, J., Hufenbecher, F., Soffel, H. C., & Heider, F. (2002). A reversal of the Earth's magnetic field recorded in mid-Miocene lava flows of Gran Canaria: Paleodirections. *Journal of Geophysical Research: Solid Earth*, *107*(B1), EPM 7-1-EPM 7-12. https://doi.org/10.1029/2001JB000322

McDougall, I., & Schmincke, H.-U. (1976). Geochronology of Gran Canaria, Canary Islands: Age of shield building volcanism and other magmatic phases. *Bulletin Volcanologique*, *40*(1), 57–77. https://doi.org/10.1007/BF02599829

Merrill, R. T., & McFadden, P. L. (1999). Geomagnetic polarity transitions. *Reviews of Geophysics*, *37*(2), 201–226. https://doi.org/10.1029/1998RG900004

Petersen, N., Eisenach, P., & Bleil, U. (1979). Low temperature alteration of the magnetic minerals in ocean floor basalts (pp. 169–209). American Geophysical Union. https://doi.org/10.1029/ME002p0169

Shcherbakov, V. P., McClelland, E., & Shcherbakova, V. V. (1993). A model of multidomain thermoremanent magnetization incorporating temperature-variable domain structure. *Journal of Geophysical Research: Solid Earth*, *98*(B4), 6201–6216. https://doi.org/10.1029/92JB02572

Tauxe, L. (2010). *Essentials of paleomagnetism*. Berkeley: University of California Press.

APPENDICES

APPENDIX A DETAILS PER SAMPLED FLOW

APPENDIX A.1

Flow number	Section	Coordinates		Height (m ±4m)	Thickness (m)	# samples	unorientated samples	details
GR-1	A	28R 425126	UTM 3090180	640	2,5	10	0	
GR-2	A	28R 425127	UTM 3090155	645	3,5	8	3	
GR-3	A	28R 425112	UTM 3090171	651	2	18	3	variation in thickness
GR-4	A	28R 425107	UTM 3090171	655	2,5	8	3	flow gets thinner toward the north
GR-5	A	28R 425107	UTM 3090160	660	1,5	10	0	
GR-6	A	28R 425170	UTM 3090319	665	3	12	2	
GR-7	A	28R 425163	UTM 3090311	672	4	9	1	
GR-8	A	28R 425153	UTM 3090312	677	3	11	2	GR8-9 could be another flow
GR-9	A	28R 425143	UTM 3090246	681	1,5	9	0	coordinates incorrect. Took average of upper and lower flow
GR-10	A	28R 425155	UTM 3090180	685	1,7	9	1	
GR-11	A	28R 425157	UTM 3090333	689	2	8	3	
GR-12	A	28R 425143	UTM 3090331	695	4	9	0	
GR-13	B	28R 0425091	UTM 3090547	683	1	9	0	
GR-14	B	28R 0425076	UTM 3090537	686	0,5	10	2	
GR-15	B	28R 0425085	UTM 3090525	688	2	10	0	flow contains lose blocks
GR-16	B	28R 0425051	UTM 3090498	691	2	10	3	
GR-17	B	28R 0425085	UTM 3090525	694	2	10	3	
GR-18	B	28R 0425032	UTM 3090517	696	1	9	5	
GR-19	B	28R 042543	UTM 3090498	699	1,5	11	1	flow is very porous
GR-20	B	28R 0425034	UTM 3090503	701	1	7	2	flow is very porous
GR-21	B	28R 0425026	UTM 3090501	706	3,5	11	6	GR-21 and GR-22 could be the same flow, measured seperatly
GR-22	B	28R 0425016	UTM 3090501	709	2	10	0	
GR-23	B	28R 0425014	UTM 3090597	712	1,7	9	2	
GR-24	B	28R 425012	UTM 3090500	714	1	10	3	
GR-25	B	28R 0425006	UTM 3090485	717	1,5	9	5	
GR-26	B	28R 0425003	UTM 3090482	720	1,5	10	3	
GR-27	B	28R 0424994	UTM 3090476	723	2	10	2	
GR-28	B	28R 0424985	UTM 3090475	725	1	10	0	
GR-29	B	28R 0424981	UTM 3090469	728	2	9	3	
GR-30	B	28R 0424983	UTM 3090474	731	2	10	3	
GR-31	B	28R 0424980	UTM 3090469	733	1	9	2	
GR-32	B	28R 0424977	UTM 3090463	735	1	10	1	
GR-33	B	28R 0424983	UTM 3090474	737	1	10	4	flow is very lose, soft and crumbling
GR-34	B	28R 0424964	UTM 3090462	739	1	9	4	flow is very lose, soft and crumbling
GR-35	B	28R 0424965	UTM 3090459	742	1,5	9	3	
GR-36	B	28R 0424959	UTM 3090462	744	1	8	1	
GR-37	B	28R 0424959	UTM 3090459	746	0,4	11	0	
GR-38	B	28R 0424958	UTM 3090458	749	1,5	11	2	
GR-39	B	28R 0424958	UTM 3090449	751	1	13	0	
GR-40	B	28R 0424955	UTM 3090449	753	1	11	0	
GR-41	B	28R 0424955	UTM 3090442	756	2	9	2	
GR-42	B	28R 0424954	UTM 3090441	760	3	11	0	
GR-43	B	28R 0424950	UTM 3090435	763	2	8	0	
GR-44	B	28R 0424984	UTM 3090432	766	2	10	2	
GR-45	B	28R 0424941	UTM 3090433	769	2	11	1	
GR-46	B	28R 0424940	UTM 3090434	772	1,5	10	4	flow looks more like a blob than a whole layer
GR-47	B	28R 0424927	UTM 3090439	775	0,5	11	0	flow looks more like a blob than a whole layer
GR-48	B	28R 0424917	UTM 3090423	777	1	11	1	
GR-49	B	28R 0424912	UTM 3090421	781	0,5	10	1	first top
GR-50	C	28R 0424702	UTM 3090331	764	2,5	8	0	

APPENDIX A.2

Flow number	Section	Coordinates		Height (m ±4m)	Thickness (m)	# samples	unorientated samples	details
GR-51	C	28R 0424693	UTM 3090334	768	1,5	8	0	
GR-52	C	28R 0424679	UTM 3090353	771	1,2	11	2	flow is very crumbling
GR-53	C	28R 0424680702	UTM 3090350	775	1,5	8	2	
GR-54	C	28R 0424679	UTM 3090361	779	2	8	3	
GR-55	C	28R 0424675	UTM 3090376	782	1	9	0	
GR-56	C	28R 0424670	UTM 3090379	785	0,5	8	0	
GR-57	C	28R 0424669	UTM 3090373	792	5	8	0	
GR-58	C	28R 0424572	UTM 3090400	796	1,5	6	5	
GR-59	C	28R 0424564	UTM 3090393	800	2	8	0	
GR-60	C	28R 0424561	UTM 3090393	804	2	8	0	
GR-61	C	28R 0424543	UTM 3090393	808	2	9	2	flow is very porous
GR-62	C	28R 0424551	UTM 3090399	811	1	9	0	
GR-63	C	28R 0424543	UTM 3090403	815	1,5	8	2	flow is very soft
GR-64	C	28R 0424542	UTM 3090396	818	1	7	0	
GR-65	C	28R 0424542	UTM 3090401	821	1	8	0	
GR-66	C	28R 0424540	UTM 3090397	825	2	8	0	
GR-67	C	28R 0424543	UTM 3090400	828	0,5	8	0	
GR-68	C	28R 424535	UTM 3090401	831	0,8	8	0	
GR-69	C	28R 0424528	UTM 3090400	834	1	9	1	
GR-70	C	28R 0424531	UTM 3090404	837	1	8	1	
GR-71	C	28R 0424526	UTM 3090406	840	1	8	2	
GR-72	C	28R 0424514	UTM 3090395	843	0,8	8	0	
GR-73	C	28R 0424511	UTM 3090389	846	1	8	5	
GR-74	C	28R 0424500	UTM 3090385	850	2	8	2	
GR-75	C	28R 0424501	UTM 3090390	853	1,5	8	0	
GR-76	C	28R 0424508	UTM 3090405	856	1	10	2	
GR-77	C	28R 0424502	UTM 3090407	859	1,5	8	4	
GR-78	C	28R 0424501	UTM 3090409	862	1	9	0	
GR-79	C	28R 0424502	UTM 3090412	864	1,2	9	0	
GR-80	C	28R 0424503	UTM 3090414	868	3	9	4	
GR-81	C	28R 0424486	UTM 3090408	872	2	9	1	
GR-82	C	28R 0424480	UTM 3090412	876	2	8	2	
GR-83	C	28R 0424463	UTM 3090401	879	5	8	4	
GR-84	C	28R 0424451	UTM 3090404	885	2	8	1	
GR-85	C	28R 0424455	UTM 3090414	888	3	8	2	
CK-1	CK	28R 424140	UTM 3090890	595	3,5	8	0	
CK-2	CK	28R 0423202	UTM 3090864	568	2	8	6	CK-100 between CK-1 en CK-2
CK-3	CK	28R 0422786	UTM 3090656	513	5	8	3	CK-99 between CK-3 en CK-4
CK-4	CK	28R 0422386	UTM 3090245	447	2	8	0	
CK-5	CK	28R 0422250	UTM 3090931	420	1,5	7	5	
CK-6	CK	28R 0421780	UTM 3089694	378	2,5	8	4	
CK-7	CK	28R 0421495	UTM 3089551	336	5	8	10	
CK-8	CK	28R 0420404	UTM 3038790	290	3	9	1	
CK-9	CK	28R 0419879	UTM 3088220	268	4	8	0	
CK-10	CK	28R 0419401	UTM 3087825	181	1	8	2	
CK-11	CK	28R 0419042	UTM 3087650	129	2	8	0	
CK-12	CK	28R 0418756	UTM 3087304	86	2	9	0	
CK-13	CK	28R 0418543	UTM 3087084	56	1	8	0	
CK-99	CK	28R 0422666	UTM 3090481	30	1	8	3	
CK-100	CK	28R 0423292	UTM 3091087	9	1,5	8	0	

APPENDIX B

TABLE KAPPABRIDGE (KLY 3) RESULTS ANALASYS

Sample	Susceptibility at room T (25°C)	T(°C) of first alteration	T(°C) at Hopkinson peak	Susceptibility at Hopkinson peak	Group
GR1-3	1,90E-05	160	302	3,10E-05	Group D-2
GR2-2	3,00E-05	215	500	4,60E-05	Group E
GR3-5	5,00E-06	275	30	5,00E-06	Group D-1
GR4-2	6,50E-06	155	300	9,60E-06	Group D-2
GR5-9	5,75E-06	160	310	7,50E-06	Group D-2
GR6-10	3,35E-06	275	360	5,30E-06	Group C-1
GR7-9	1,90E-05	160	300	2,70E-05	Groep C-2
GR8-3	3,50E-05	275	300	4,50E-05	Group C-1
GR9-9	9,80E-06	275	340	1,60E-05	Group C-1
GR10-1	1,85E-05	270	340	2,38E-05	Group C-1
GR11-8	4,00E-05	155	350	4,40E-05	Group A-2
GR12-4	3,20E-05	270	300	4,42E-05	Group E
GR13-6	7,50E-06	150	285	1,23E-05	Group D-2
GR14-1	9,80E-06	160	280	1,23E-05	Group D-2
GR15-4	2,05E-05	275	300	2,75E-05	Group C-1
GR16-2	2,70E-05	275	300	3,20E-05	Group C-1
GR17-10	1,50E-05	275	300	2,80E-05	Group A-1
GR18-8	1,90E-05	275	350	2,70E-05	Group A-1
GR19-5	9,25E-06	270	300	9,75E-06	Group D-1
GR20-3	1,80E-05	275	300	2,00E-05	Group D-1
GR21-8	1,60E-05	150	305	2,80E-05	Groep C-2
GR22-1	3,60E-05	270	290	4,60E-05	Group C-1
GR23-1	3,62E-05	445	350	4,02E-05	GroupA-1
GR24-3	5,90E-06	275	340	7,70E-06	Group C-1
GR25-8	1,60E-05	155	420	2,95E-05	Groep C-2
GR26-6	3,30E-05	275	300	3,90E-05	Group C-1
GR27-4	1,31E-05	280	300	1,63E-05	Group D-1
GR28-5	1,05E-05	160	320	3,05E-05	Group A-2
GR29-9	9,00E-06	155	300	1,62E-05	Group D-2
GR30-3	1,20E-05	275	305	1,70E-05	Group A-1
GR31-5	1,08E-05	275	300	1,30E-05	Group D-1
GR32-1	7,50E-06	275	300	1,25E-05	Group A-1
GR33-3	6,50E-06	155	305	1,06E-05	Group D-2
GR34-2	1,58E-05	160	295	2,42E-05	Group D-2
GR35-5	1,12E-05	275	300	2,08E-05	Group A-1
GR36-4	1,90E-05	275	310	2,70E-05	Group C-1
GR37-7	1,05E-05	160	300	2,45E-05	Group A-2
GR38-10	1,06E-05	280	320	1,68E-05	Group A-1
GR39-11	1,40E-05	280	340	2,78E-05	Group A-1
GR40-6	1,60E-06	160	310	2,15E-05	Group D-2
GR41-8	9,50E-06	160	360	1,93E-05	Group C-2

Sample	Susceptibility at room T (25°C)	T(°C) of first alteration	T(°C) at Hopkinson peak	Susceptibility at Hopkinson peak	Group
GR42-9	4,90E-06	275	420	7,50E-06	Group C-1
GR43-3	1,75E-05	275	340	2,91E-05	Group A-1
GR44-7B	1,30E-05	275	500	1,84E-05	Group E
GR45-2	2,70E-05	275	365	4,40E-05	Group C-1
GR46-3	1,81E-05	160	460	2,58E-05	Group A-2
GR47-10	1,80E-06	215	370	2,10E-05	Group B-1
GR48-1	2,40E-05	220	140	2,57E-05	Group B-1
GR49-4	7,00E-06	215	180	7,20E-06	Group B-1
GR50-1	1,85E-05	160	480	3,05E-05	Group A-2
GR51-3	1,04E-05	275	300	1,50E-05	Group A-1
GR52-9	8,50E-06	220	280	9,90E-06	Group B-2
GR53-8	7,00E-06	275	355	1,11E-05	Group C-1
GR54-8	7,70E-06	270	340	1,08E-05	Group C-1
GR55-6	6,10E-06	160	305	1,21E-05	Group A-2
GR56-6	8,70E-06	315	480	1,36E-05	Group E
GR57-8	1,32E-05	400	420	2,00E-05	Group E
GR58-6	9,00E-06	340	300	1,58E-05	Group A-1
GR59-3	1,17E-05	275	305	2,18E-05	GroupA-1
GR60-2	1,27E-05	275	300	1,55E-05	Group C-1
GR61-9	9,50E-06	335	480	1,34E-05	Group E
GR62-7	5,60E-06	160	365	9,70E-06	Group C-2
GR63-4	1,10E-05	150	165	2,33E-05	Group A-2
GR64-2	1,35E-05	275	300	2,31E-05	Group A-1
GR65-8	1,02E-05	275	300	3,20E-05	Group A-1
GR66-4	9,20E-06	155	300	2,10E-05	Group A-2
GR67-6	8,20E-06	275	310	1,05E-05	Group C-1
GR68-8	6,75E-06	400	420	8,30E-06	Group A-1
GR69-3	8,20E-06	335	480	1,70E-05	Group A-1
GR70-1	6,20E-06	335	300	1,36E-05	Group A-1
GR71-1	1,13E-05	160	360	1,63E-05	Group C-2
GR72-7	1,08E-05	275	360	1,65E-05	Group E
GR73-3	4,50E-06	395	300	5,10E-06	Group E
GR74-6	8,00E-06	160	380	1,62E-05	Group A-2
GR75-8	7,00E-06	275	260	8,00E-06	Group B-2
GR76-2	1,15E-05	155	310	1,32E-05	Group C-2
GR77-5	9,20E-06	160	220	1,40E-05	Group A-2
GR78-9	7,30E-06	275	295	9,50E-06	Group E
GR79-1	4,50E-06	455	500	7,60E-06	Group E
GR80-9	1,42E-05	275	360	1,95E-05	Group E
GR81-1	1,53E-05	275	300	2,40E-05	Groep C-1
GR82-2	2,05E-05	275	420	4,10E-05	Group E
GR83-3	6,60E-06	395	410	8,50E-06	Group E
GR84-7	1,00E-05	160	305	1,52E-05	Group C-2
GR85-8	1,50E-06	400	490	2,15E-06	Group E
CK1-6	2,60E-06	160	260	3,90E-06	Group D-2
CK2-4	9,50E-06	275	300	1,24E-05	Group D-1

Sample	Susceptibility at room T (25°C)	T(°C) of first alteration	T(°C) at Hopkinson peak	Susceptibility at Hopkinson peak	Group
CK3-5	1,30E-05	160	305	3,10E-05	Group A-2
CK4-2	3,00E-06	275	300	5,00E-06	Group D-1
CK5-1	7,70E-06	160	290	1,55E-05	Group A-2
CK6-7	8,80E-06	440	400	1,05E-05	Group E
CK7-1	6,70E-06	160	340	1,50E-05	Group A-2
CK8-9	2,02E-05	395	420	2,78E-05	Group E
CK9-5	2,00E-05	275	490	3,40E-05	Group E
CK10-6	4,00E-06	275	230	9,70E-06	Group A-1
CK11-2	7,10E-06	450	420	9,80E-06	Group E
CK12-2	1,08E-05	450	420	1,43E-05	Group E
CK13-3	1,50E-05	160	540	2,60E-05	Group C-2
CK99-6	6,50E-06	160	360	1,33E-05	Group D-2
CK100	9,00E-06	160	300	1,35E-05	Group C-2

APPENDIX C KAPPABRIDGE –GRAPHS PER SAMPLE

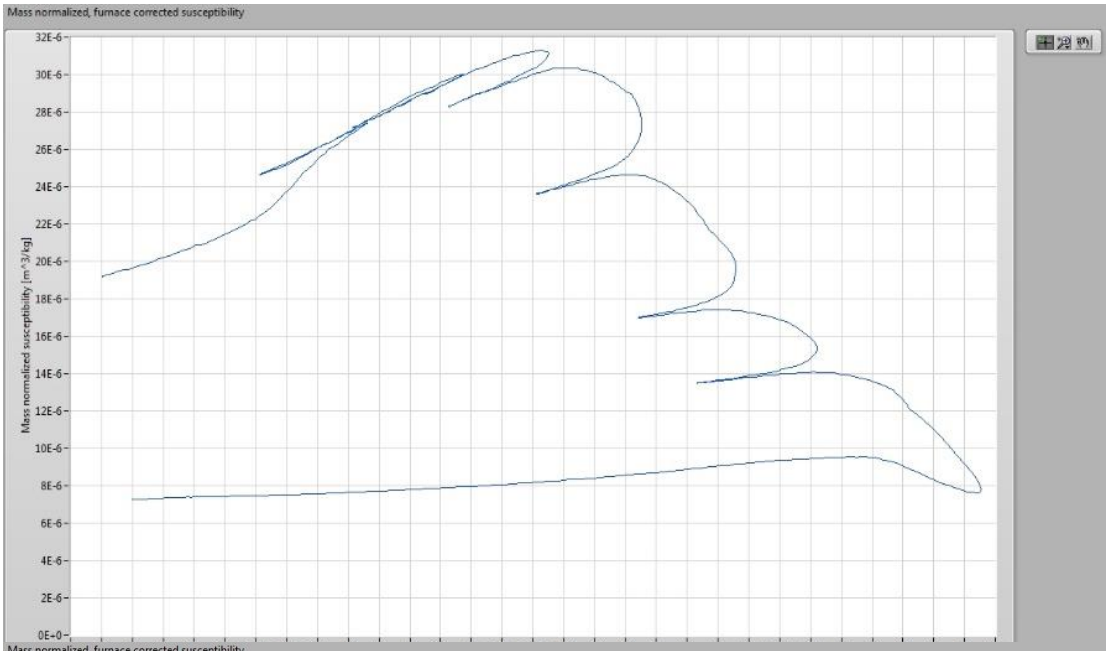

GR1

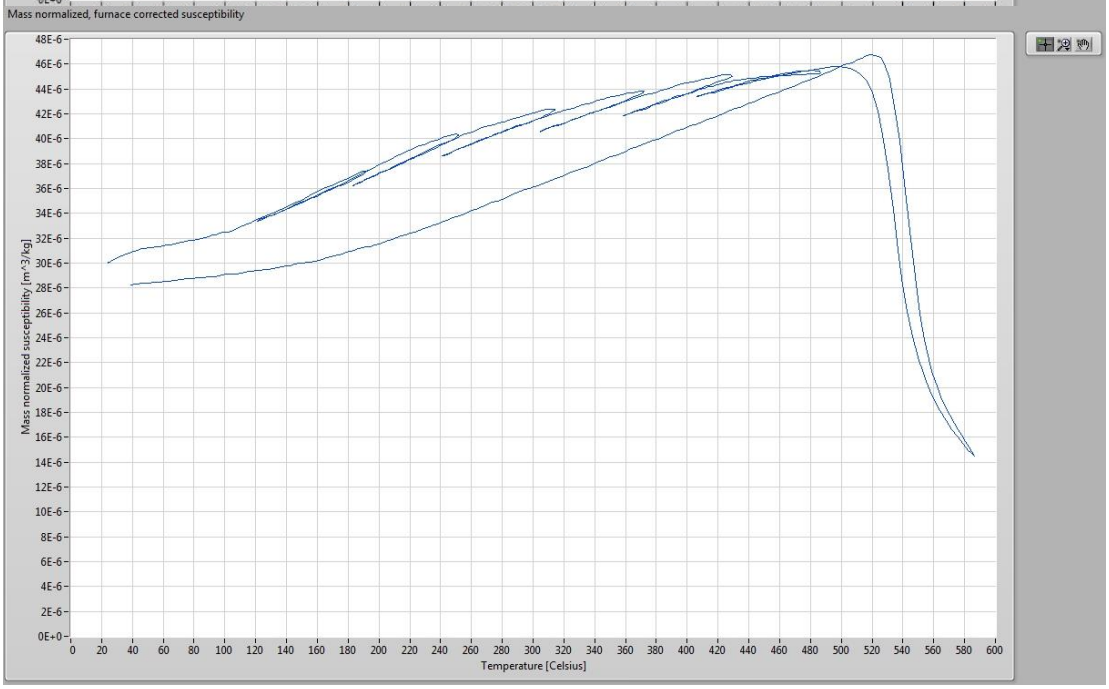

GR2-2

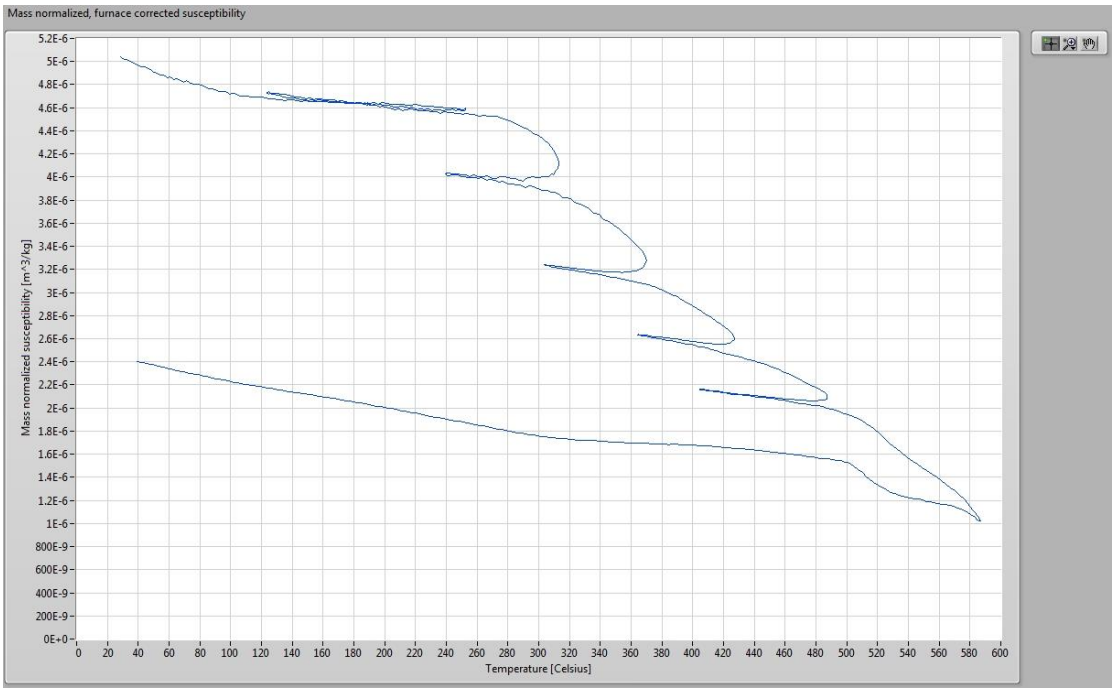

GR3-5

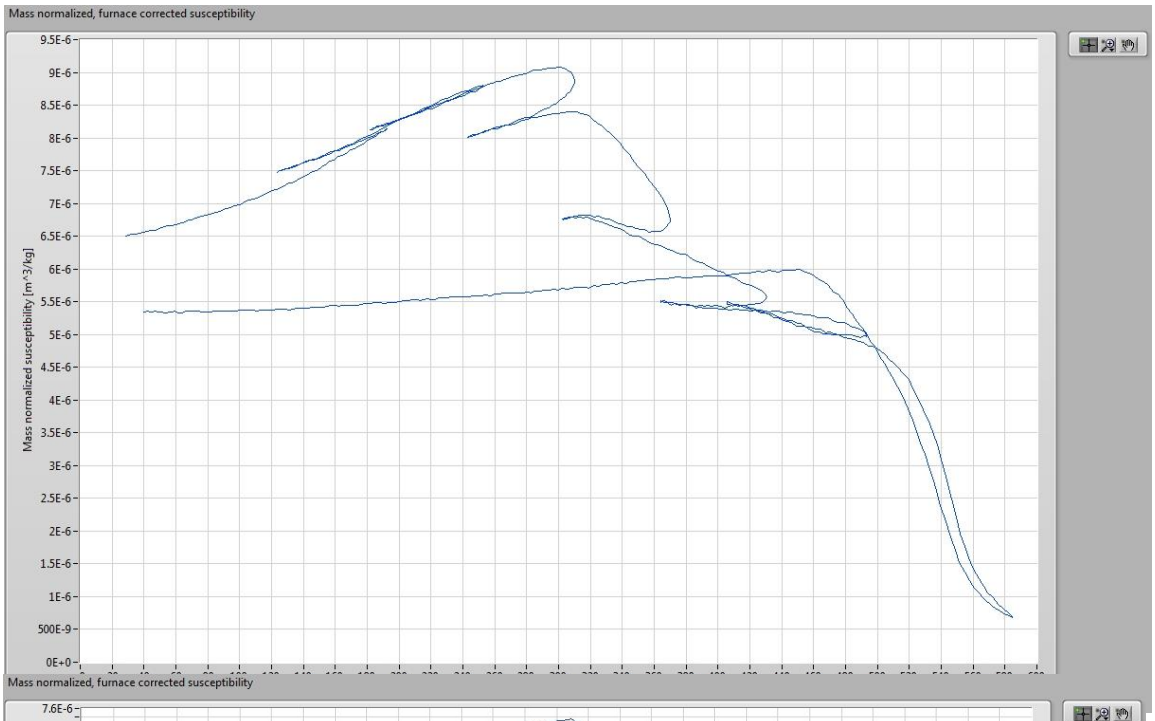

GR4-2

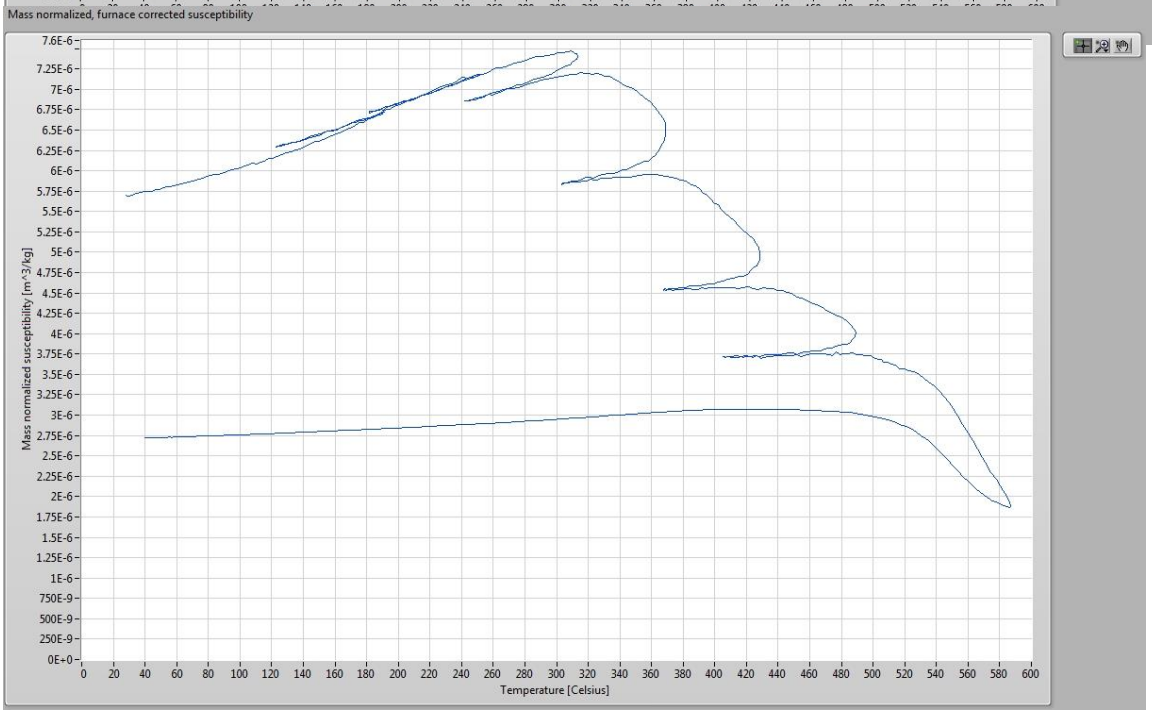

GR5-9

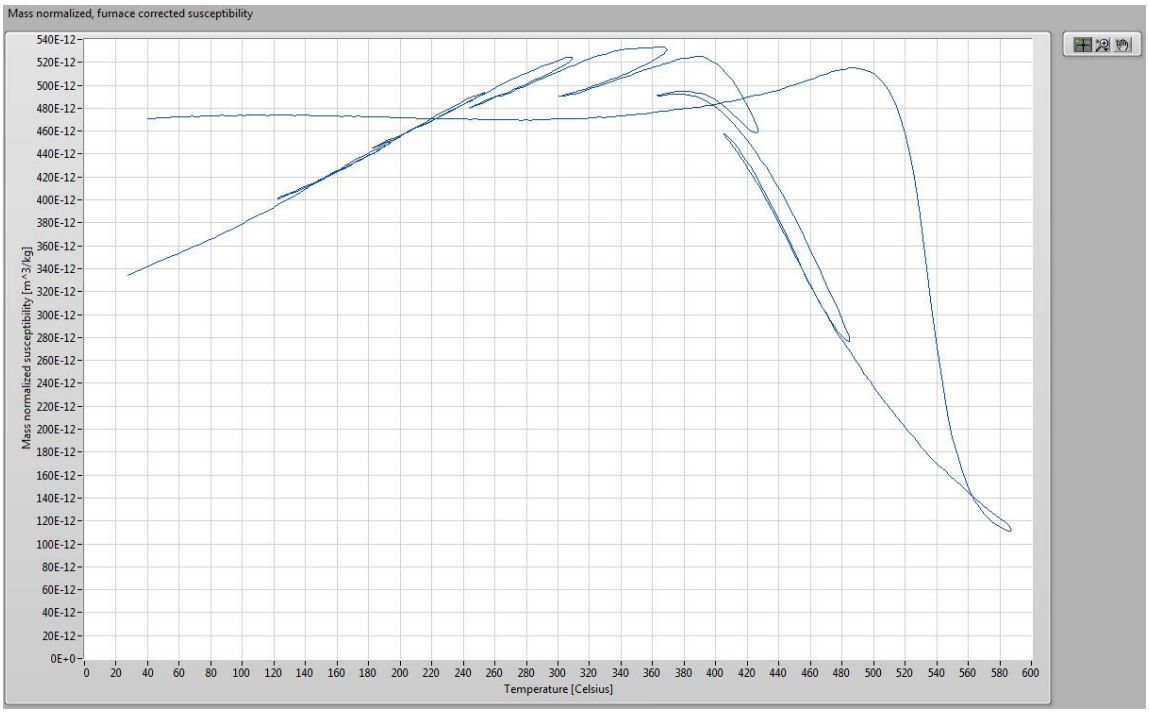

GR6-10

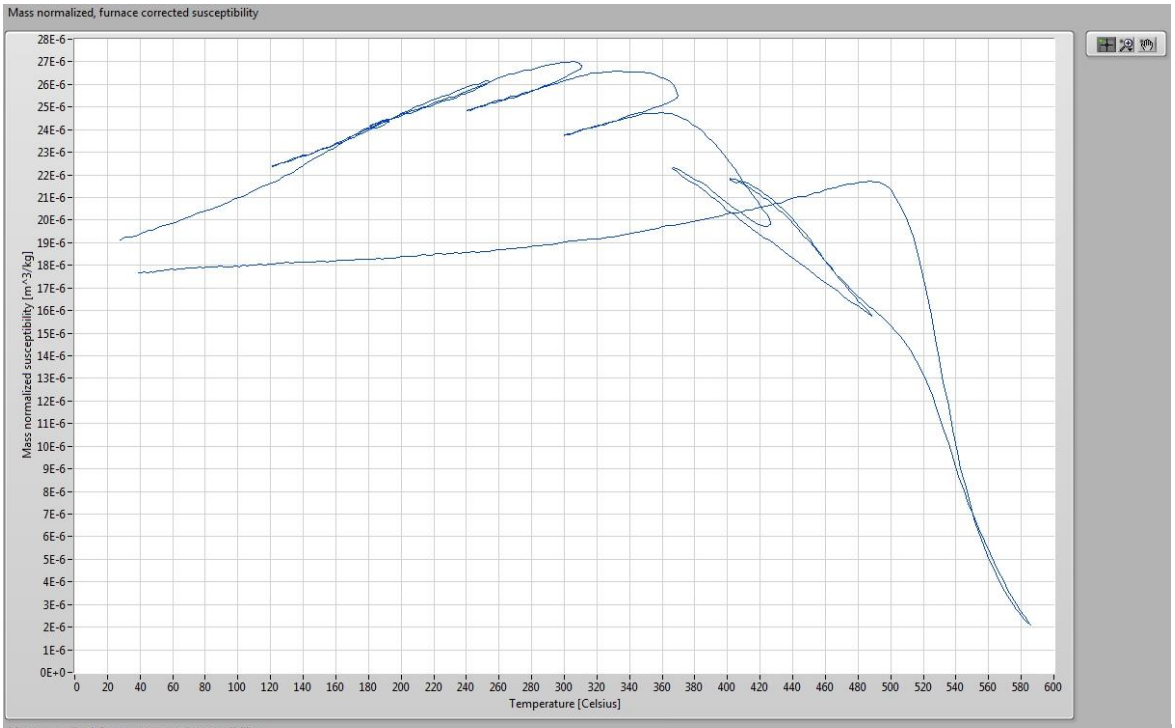

GR7-9

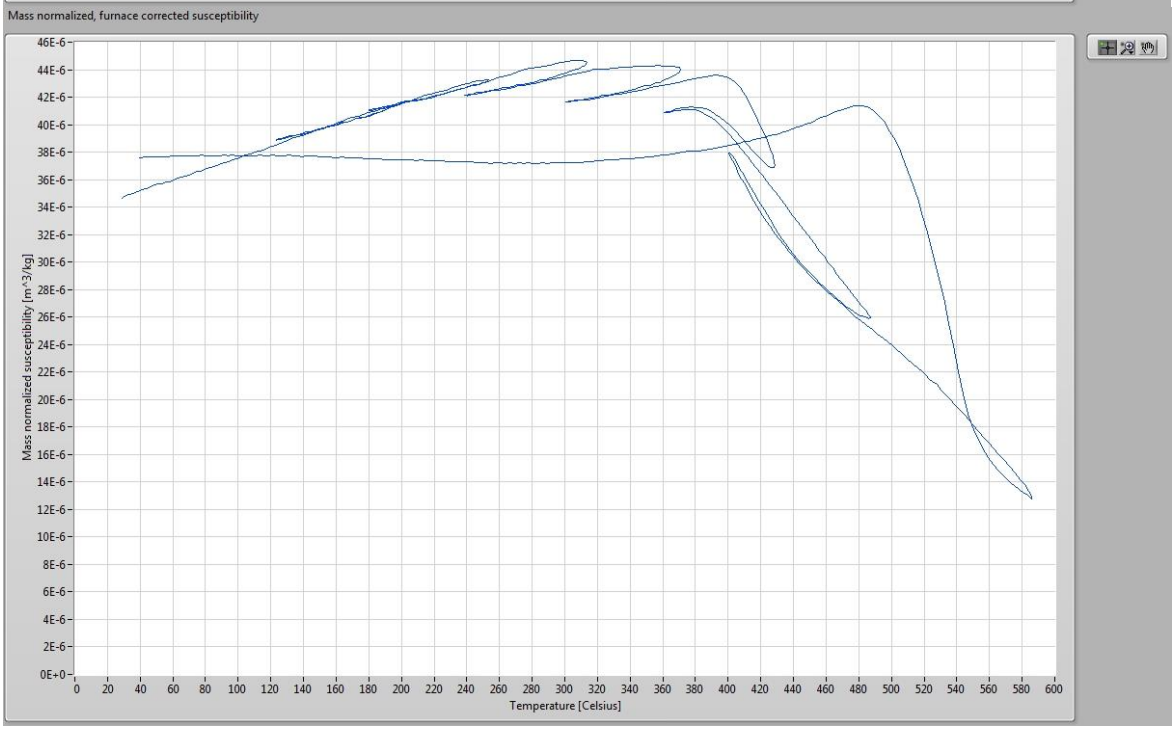

GR8-3

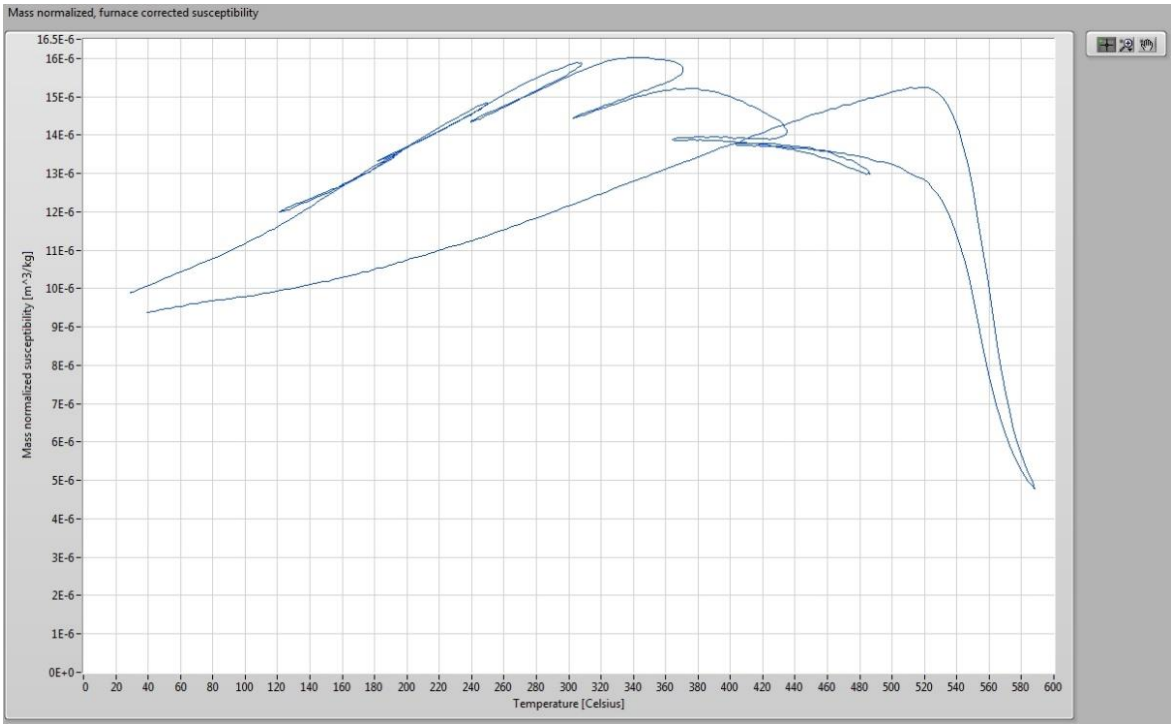

GR9-9

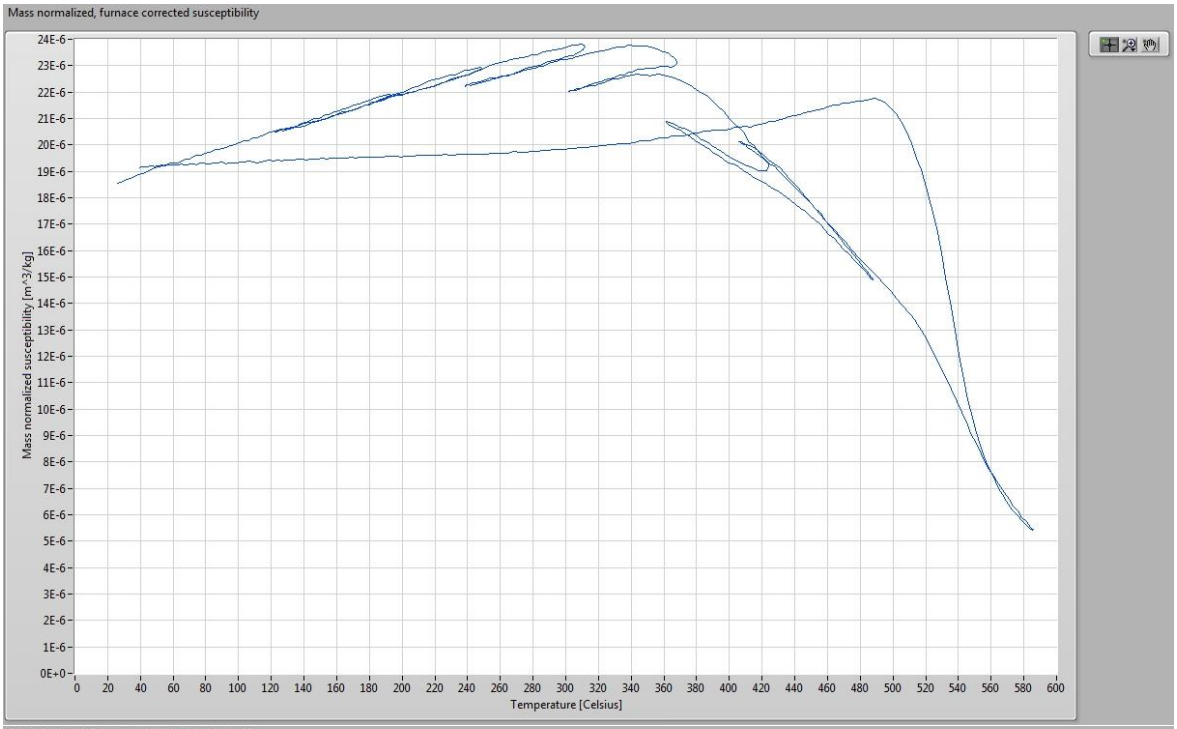

GR10-1

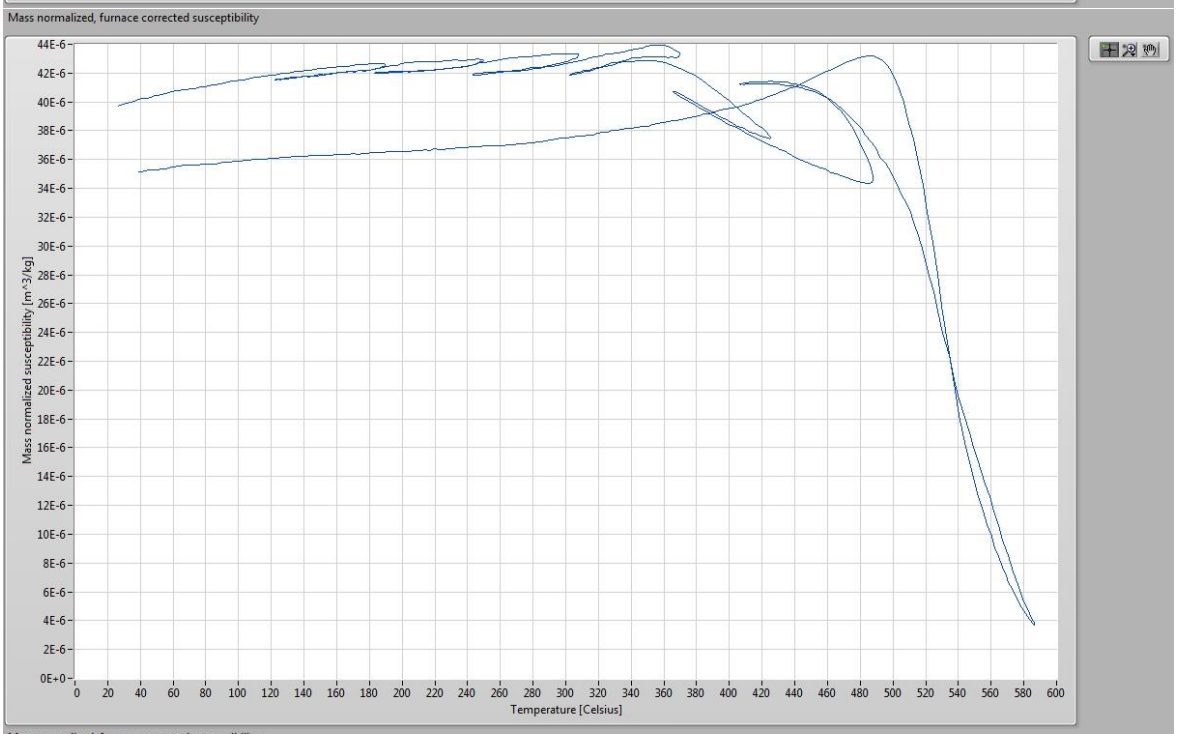

GR11-8

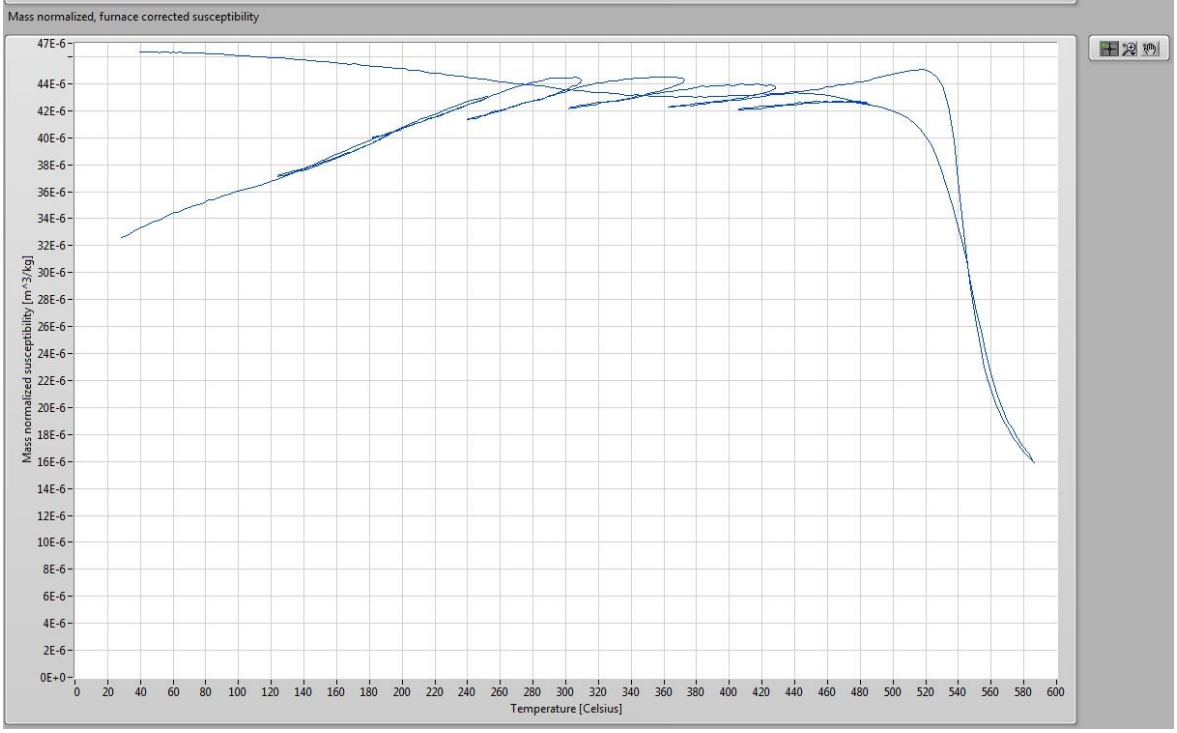

GR12-4

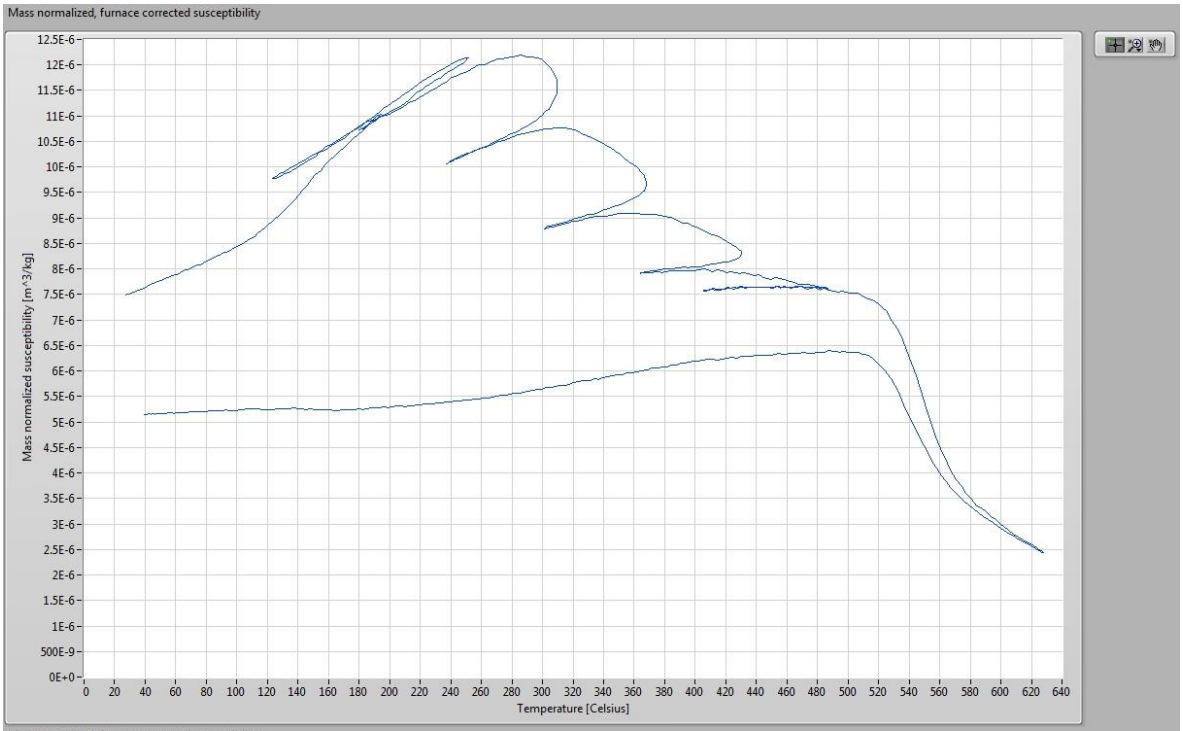

GR13-6

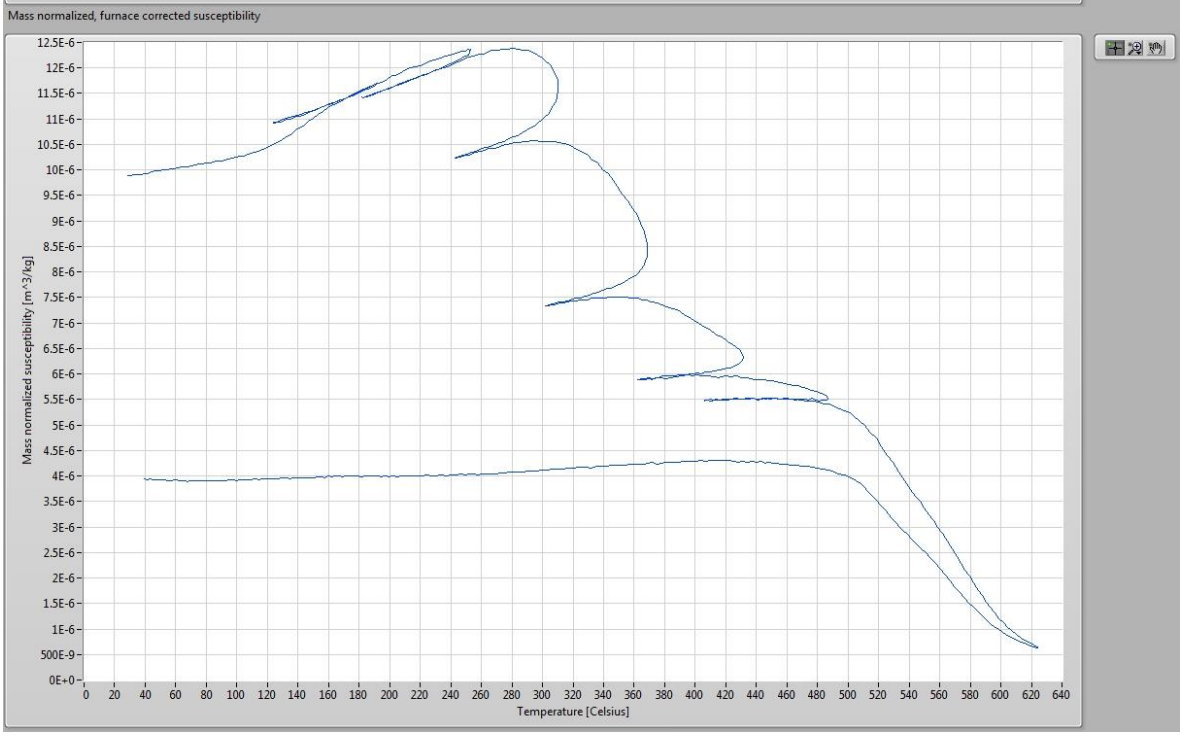

GR14-1

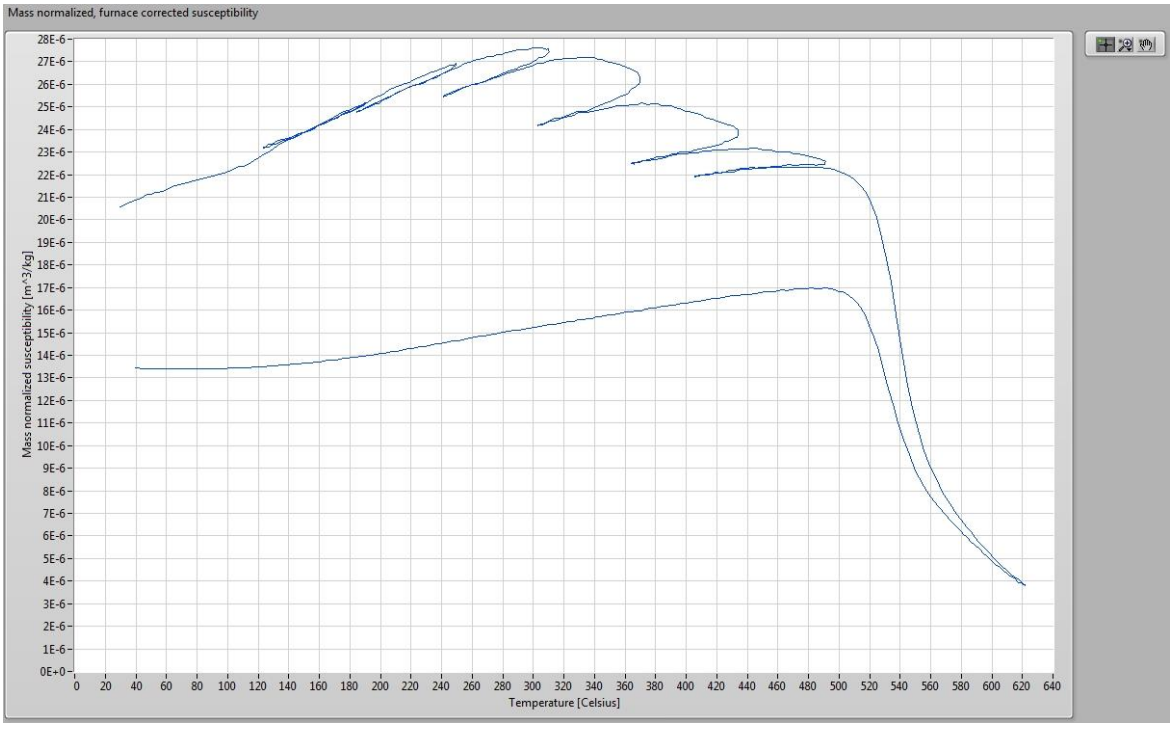

GR15-4

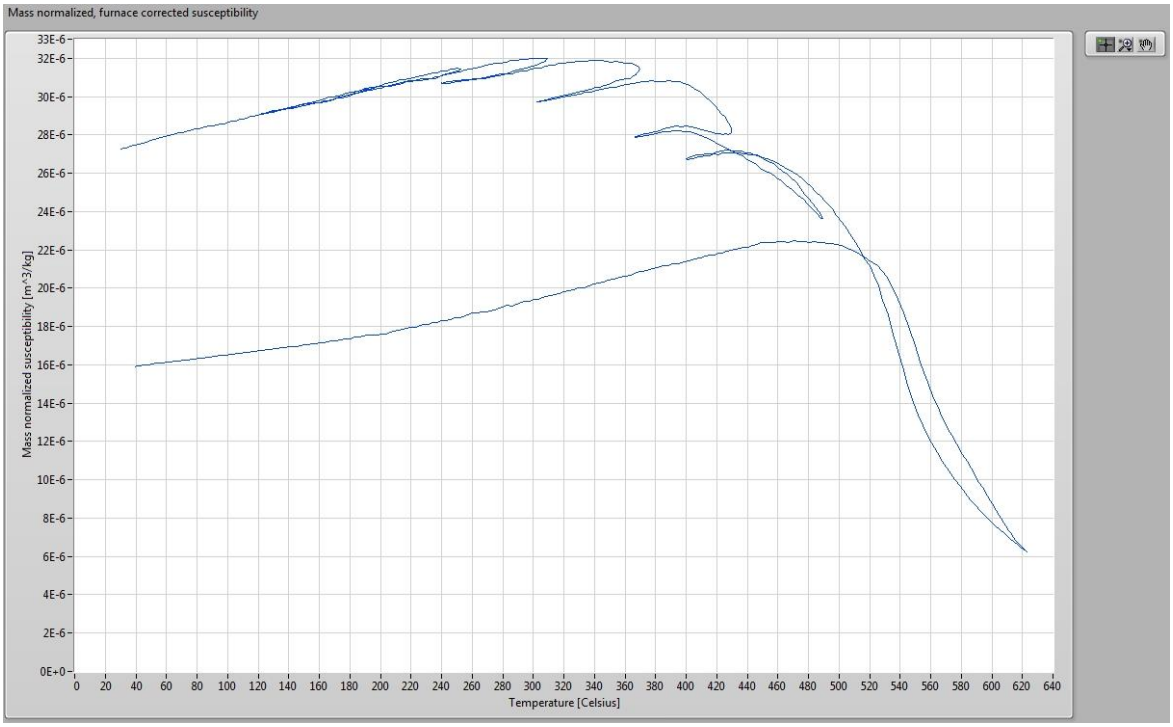

GR16-2

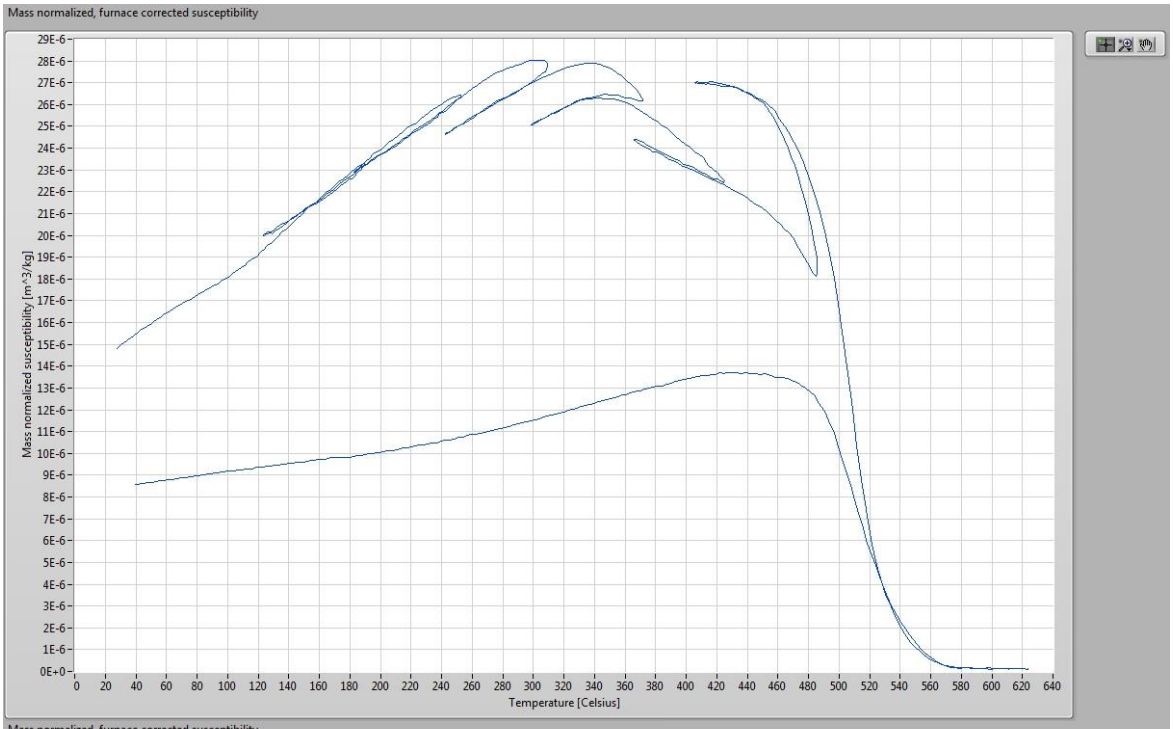

GR17-10

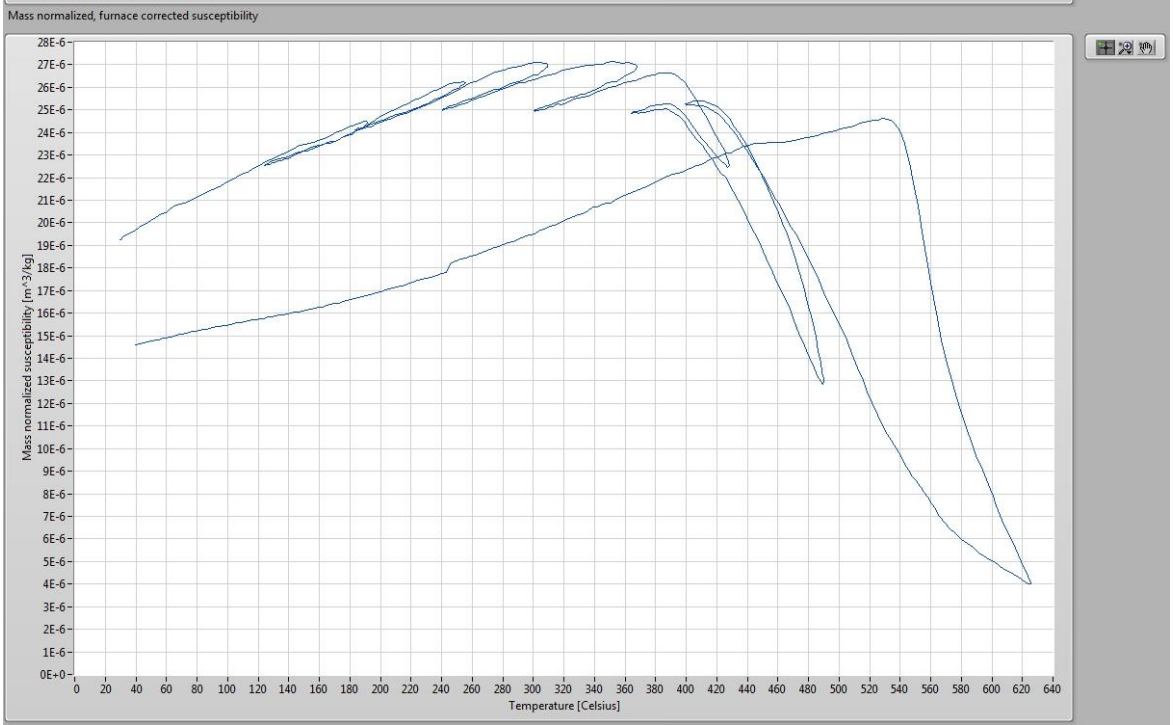

GR18-8

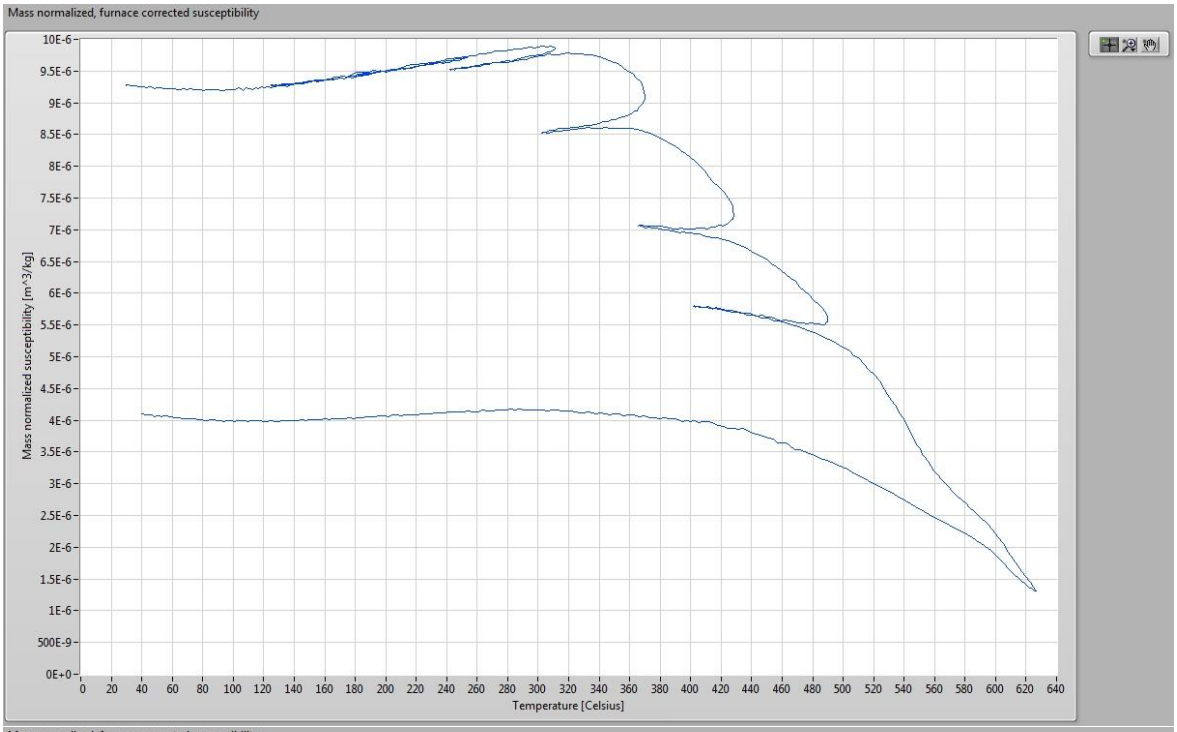

GR19-5

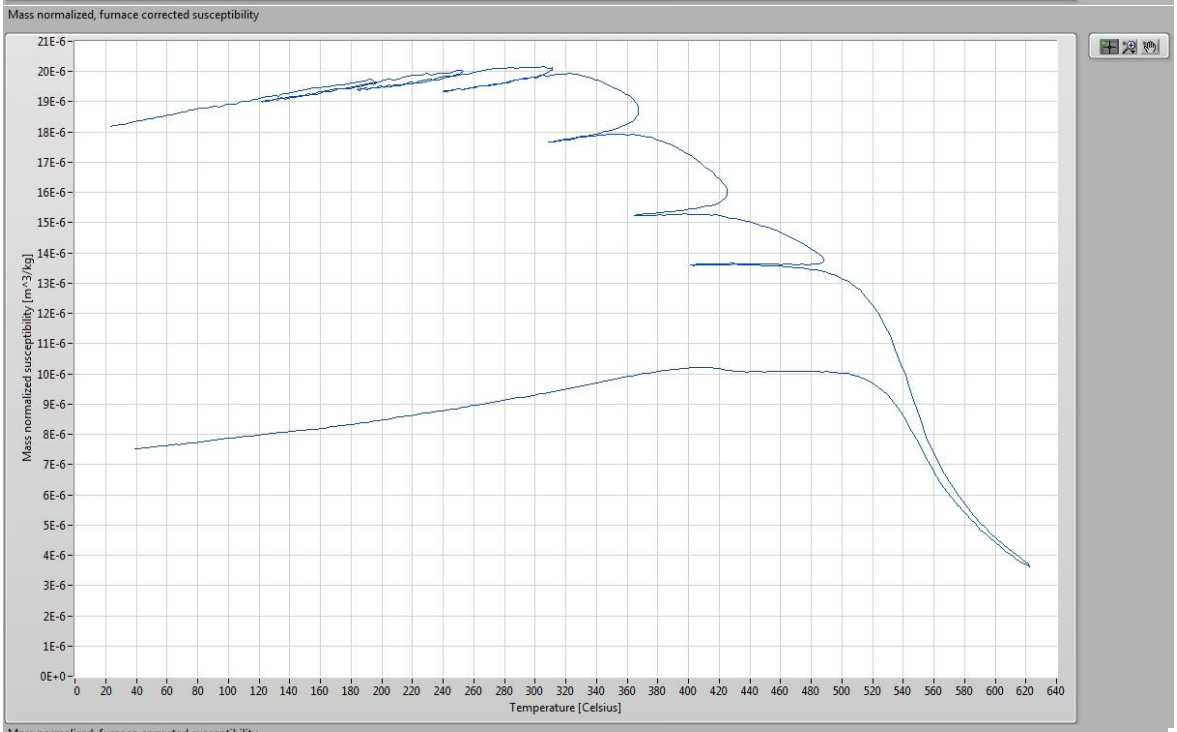

GR20-3

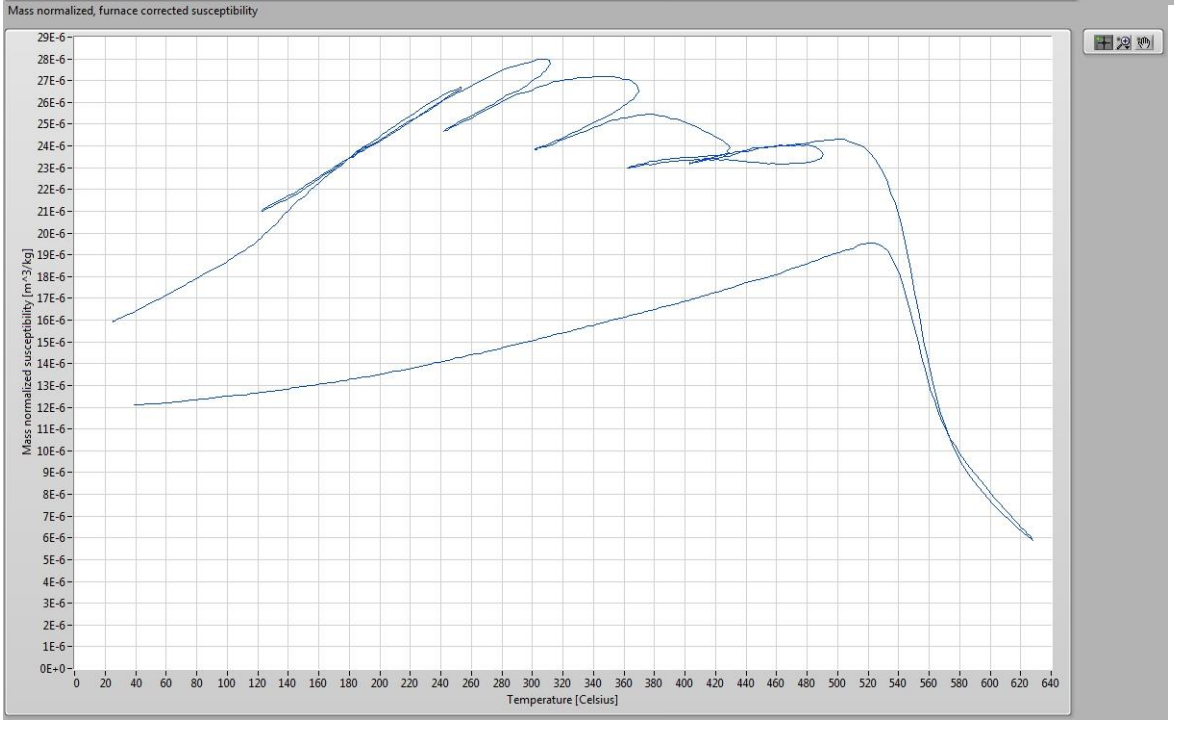

GR21-8

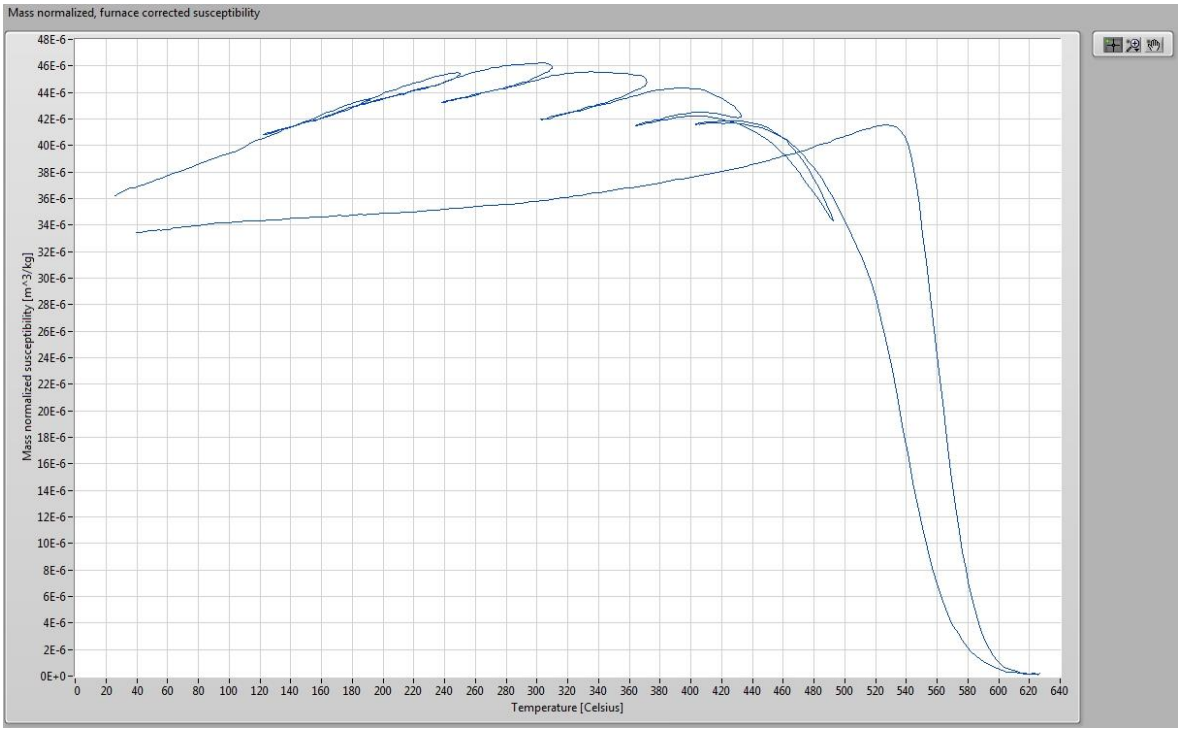

GR22-1

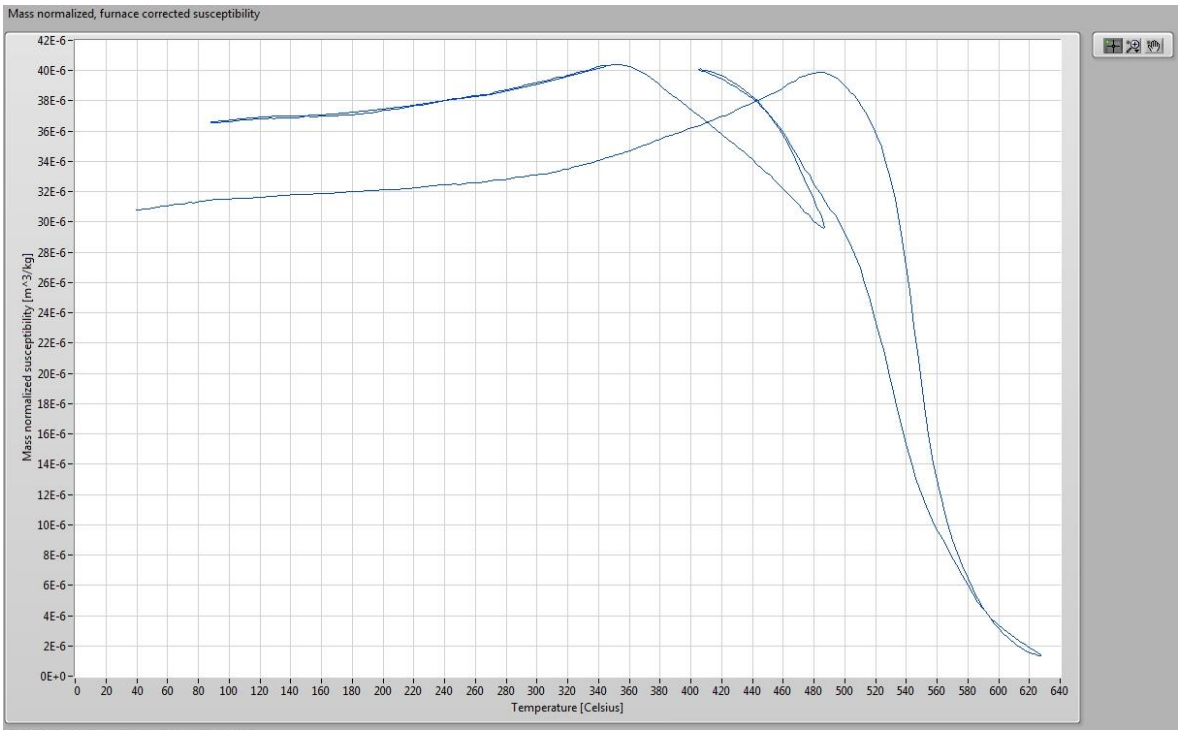

GR23-1

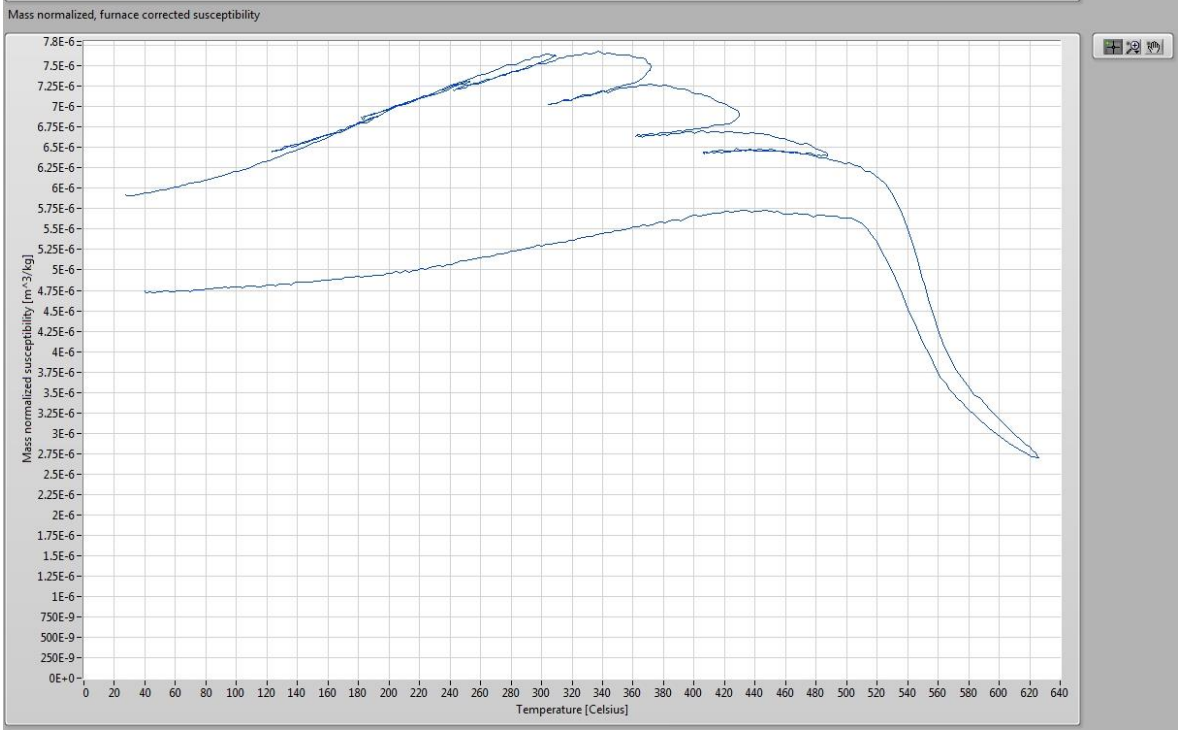

GR24-3

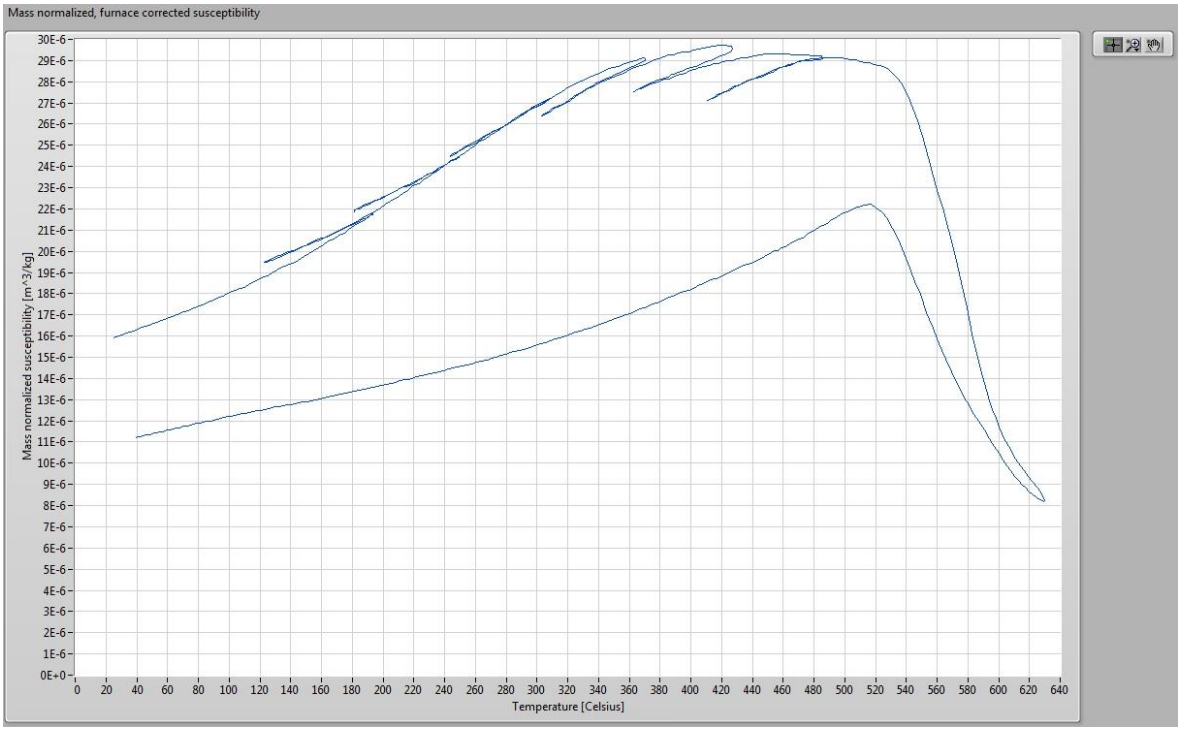

GR25-8

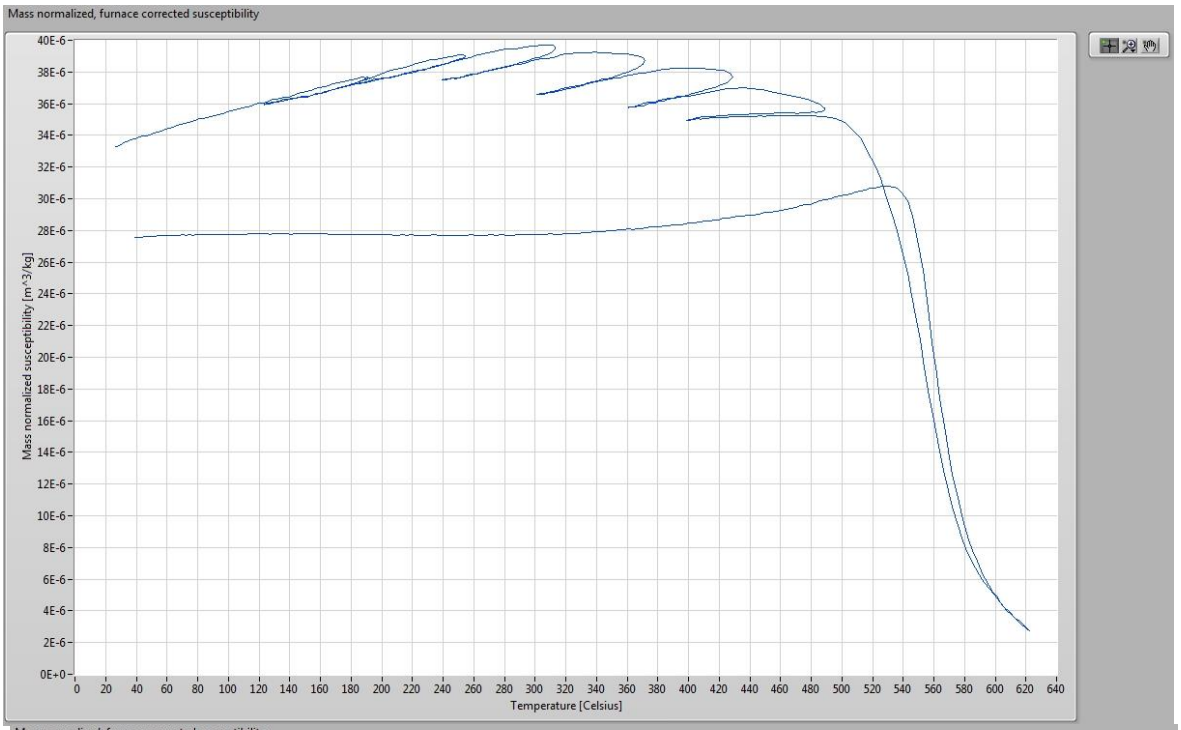

GR26-6

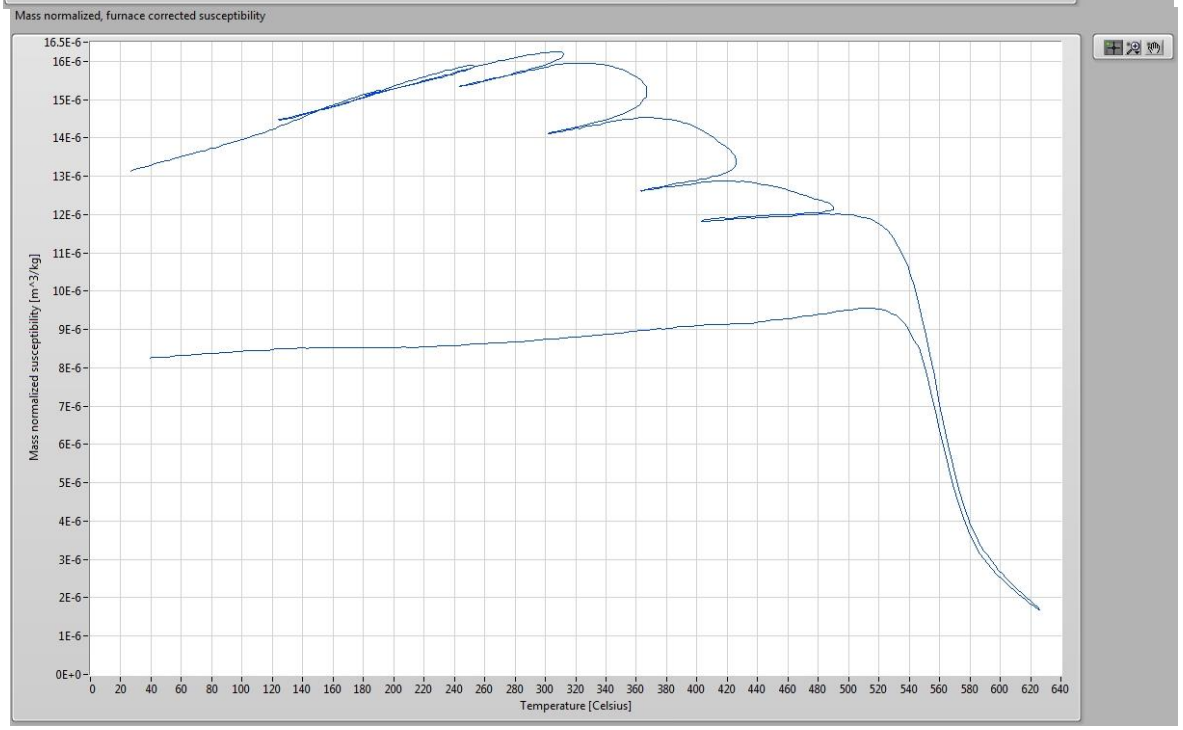

GR27-4

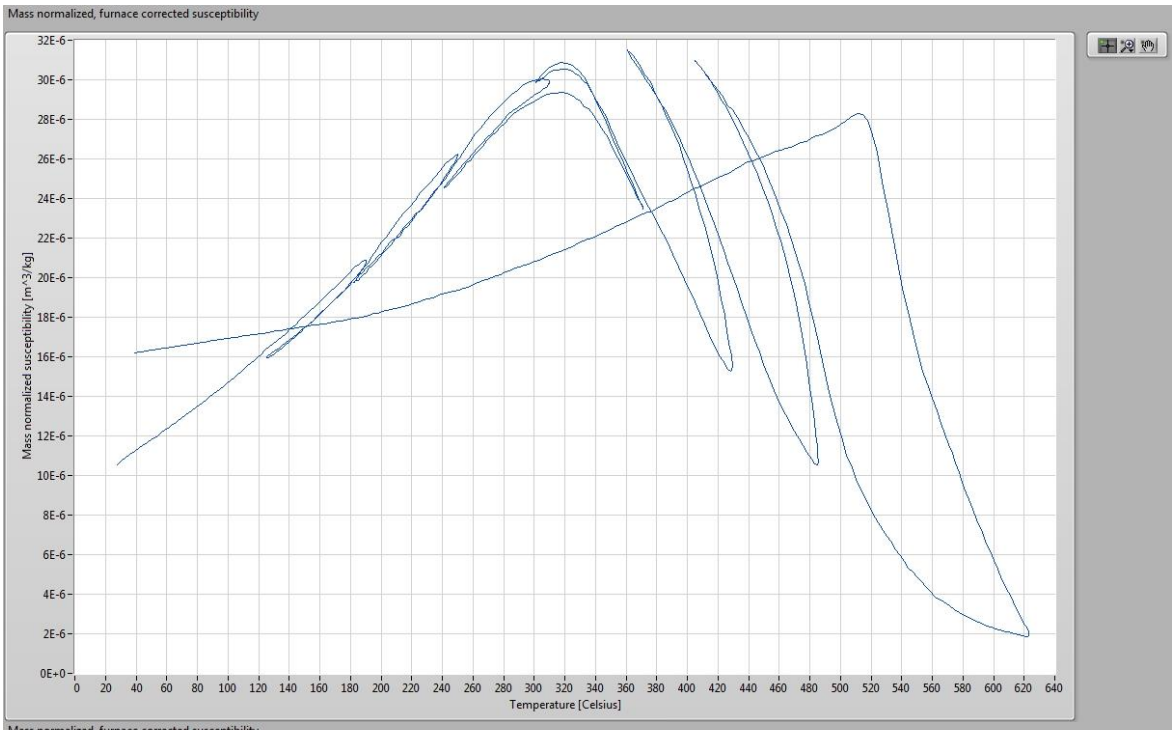

GR28-5

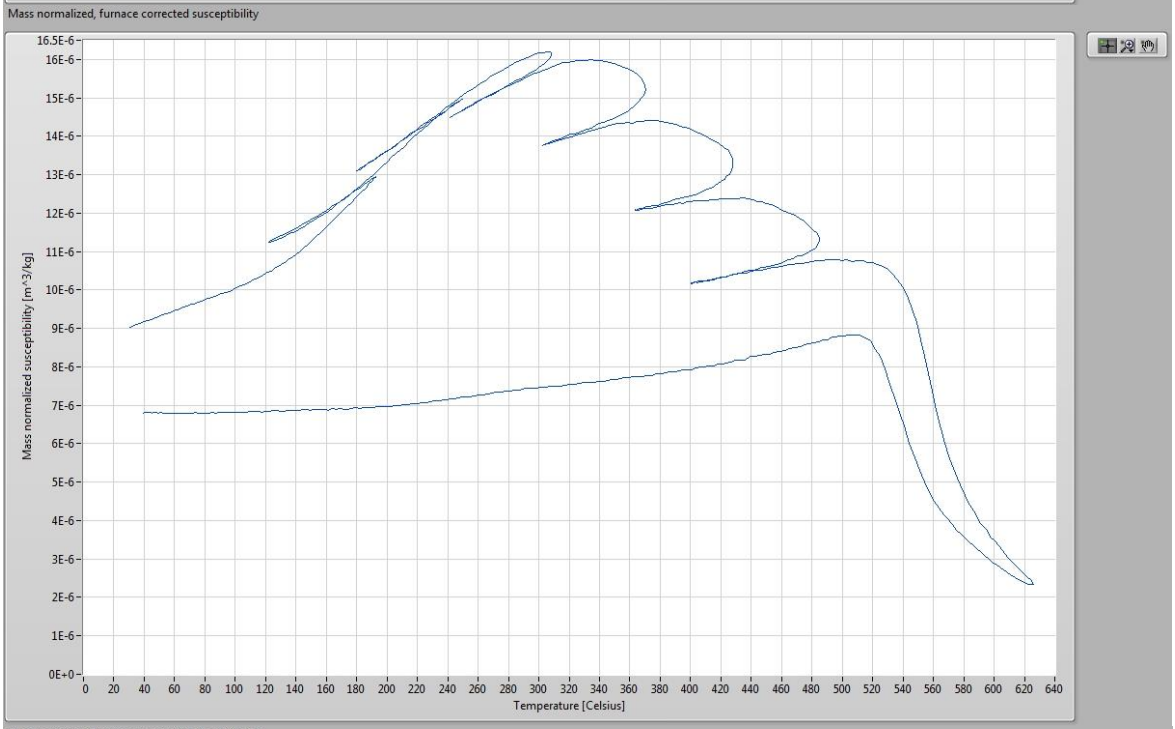

GR29-9

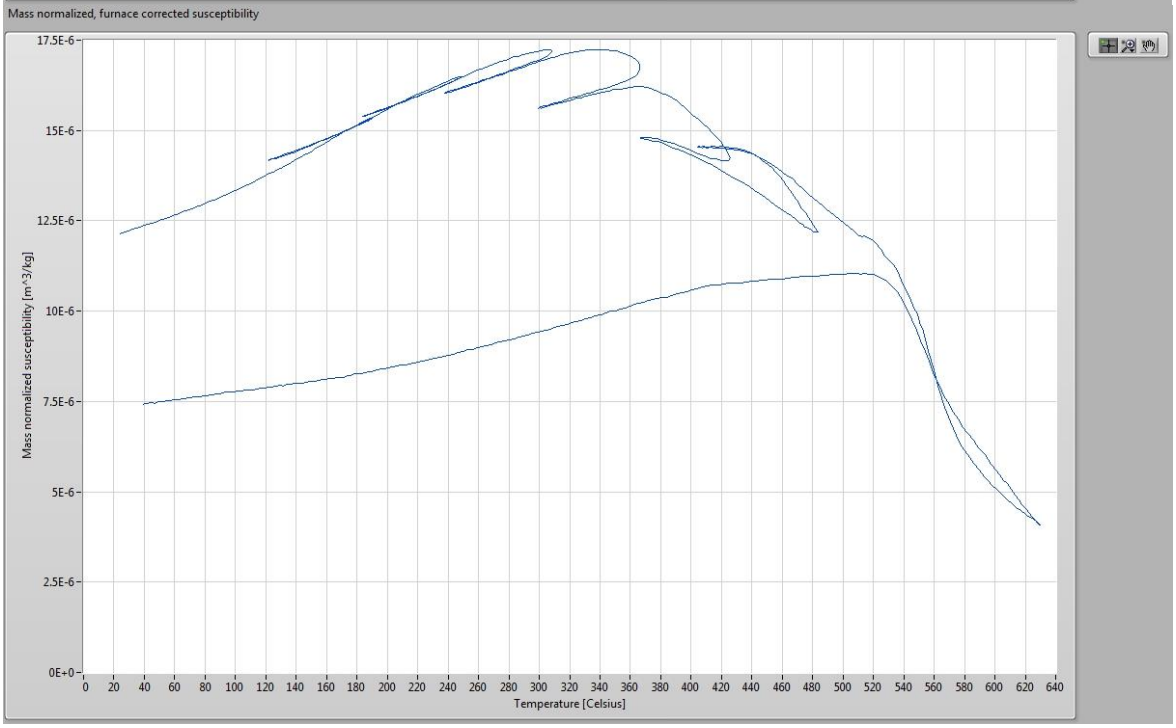

GR30-3

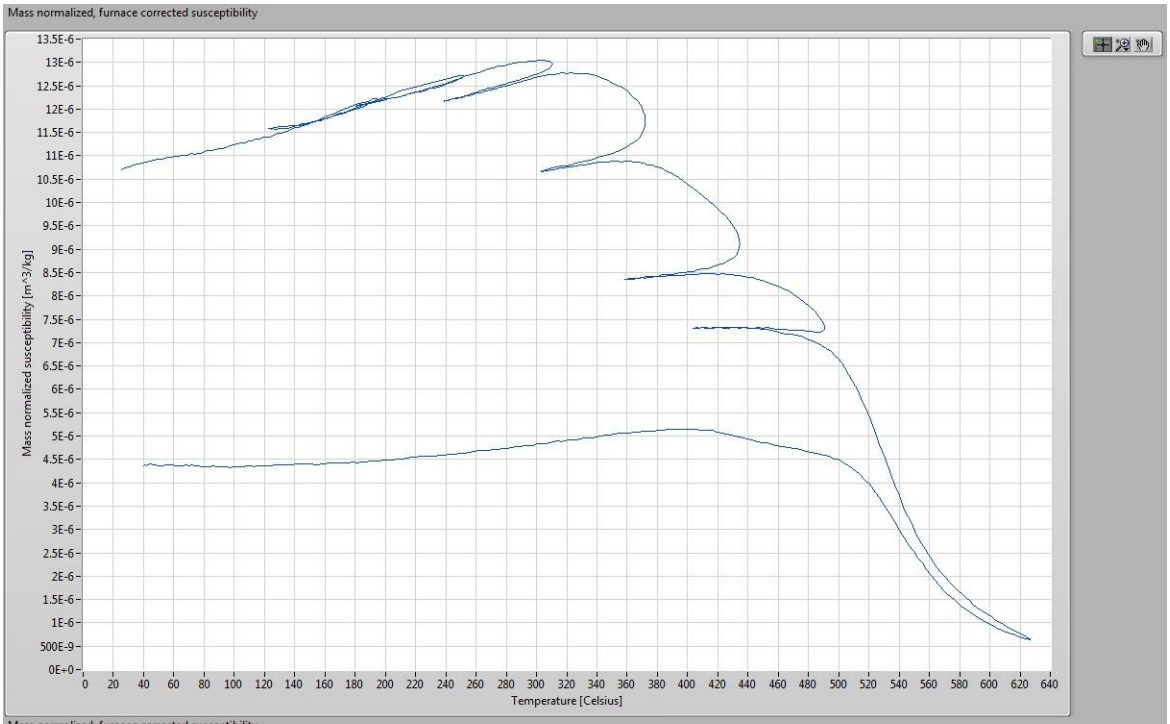

GR31-5

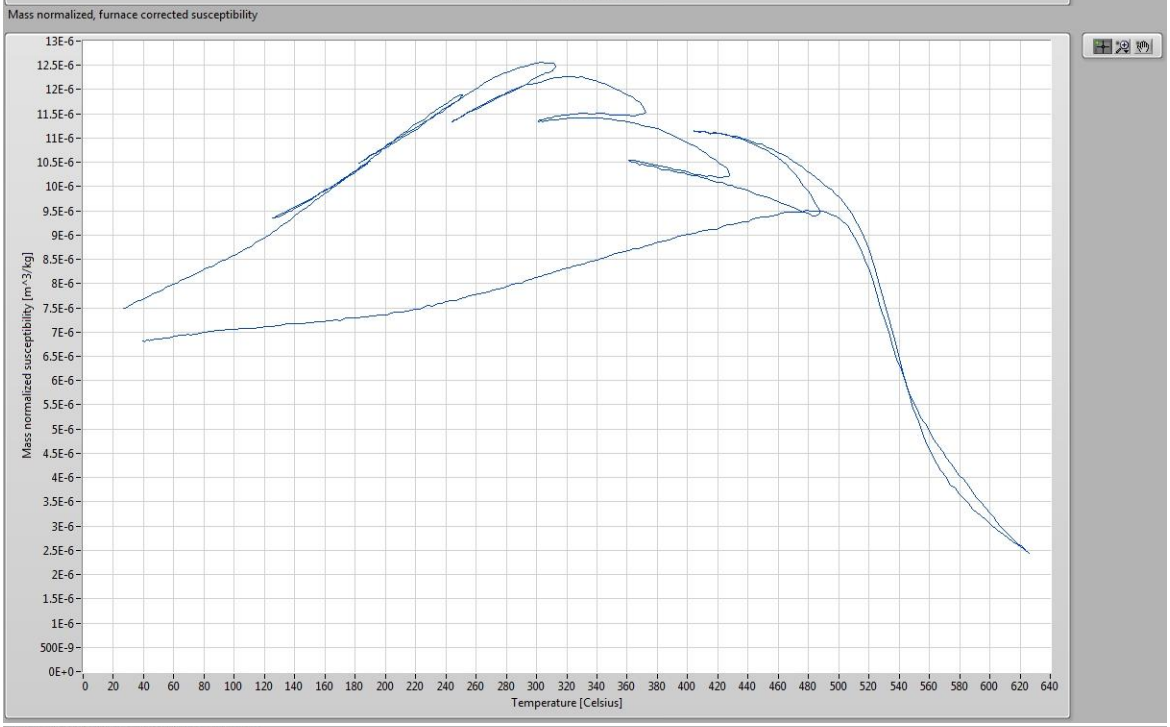

GR32-1

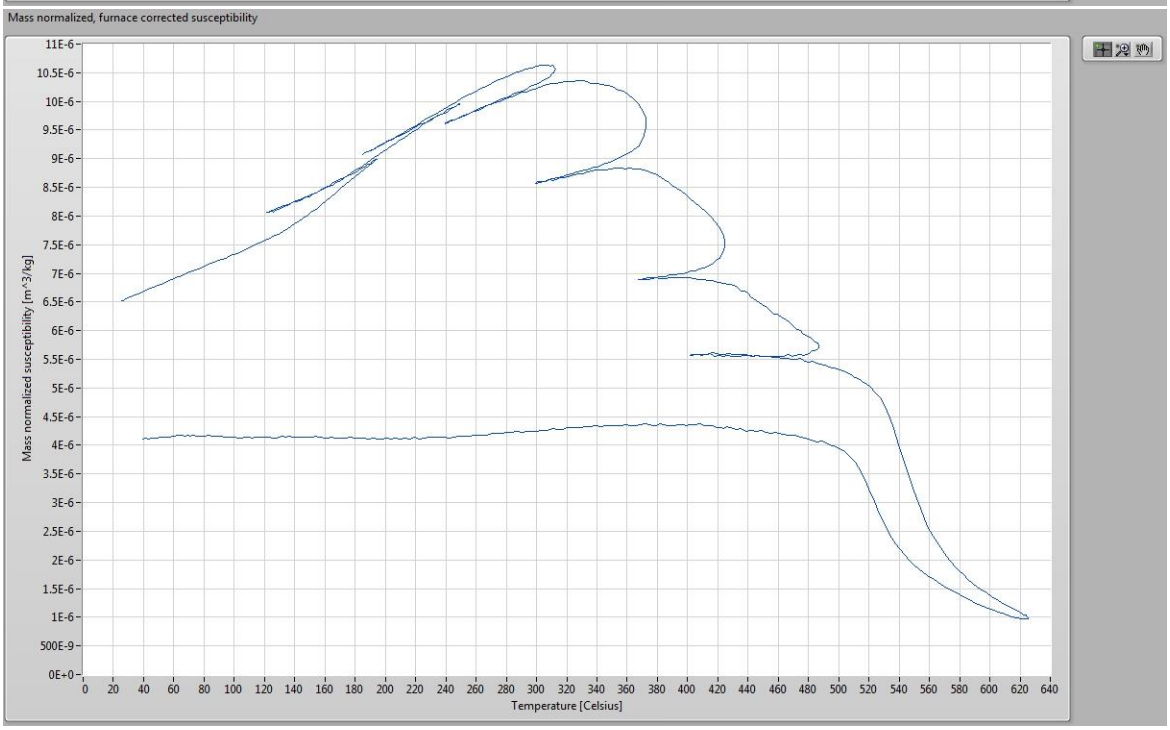

GR33-3

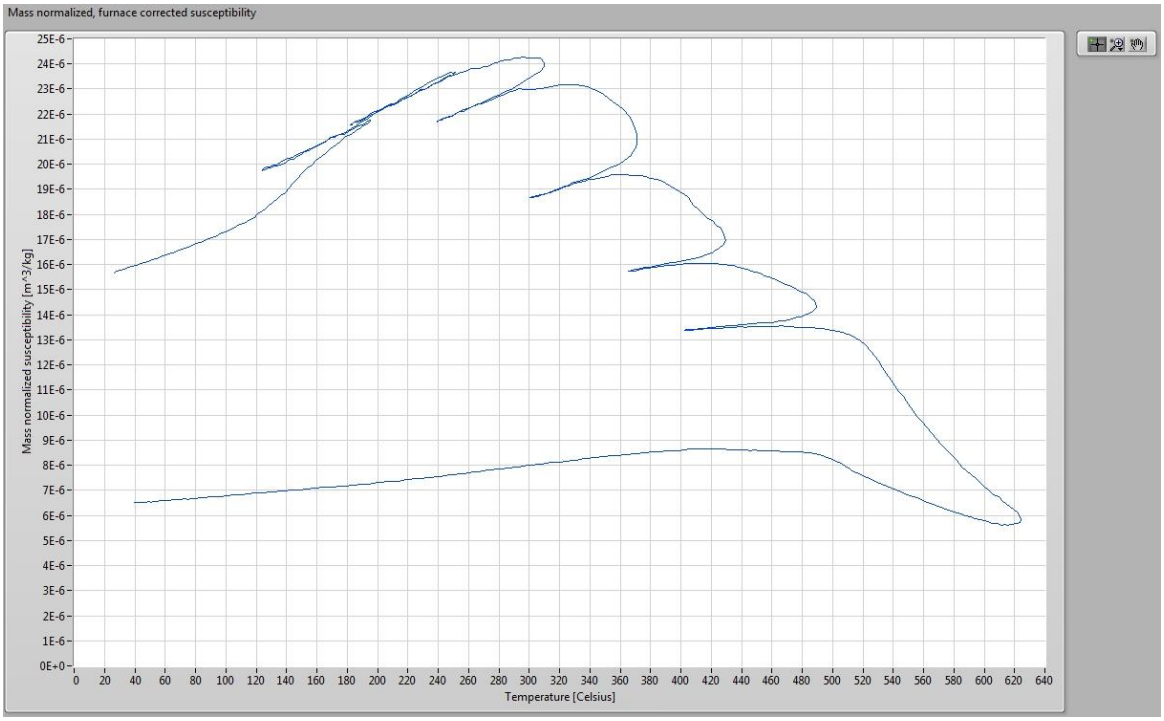

GR34-2

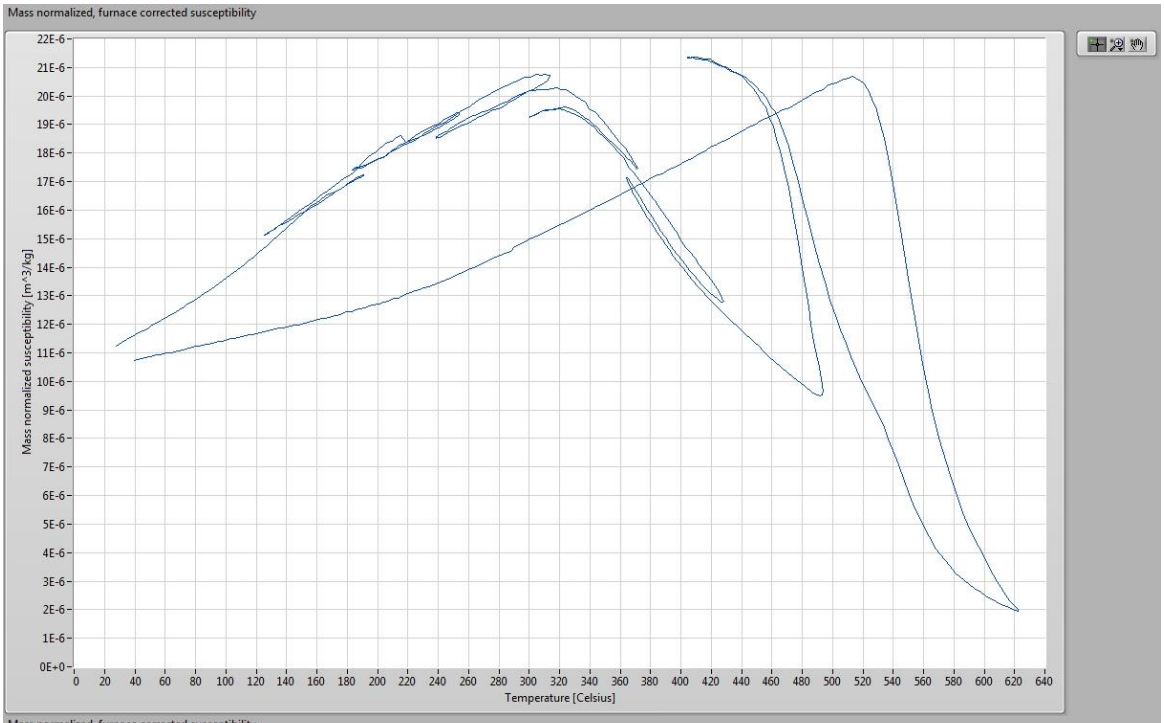

GR35-5

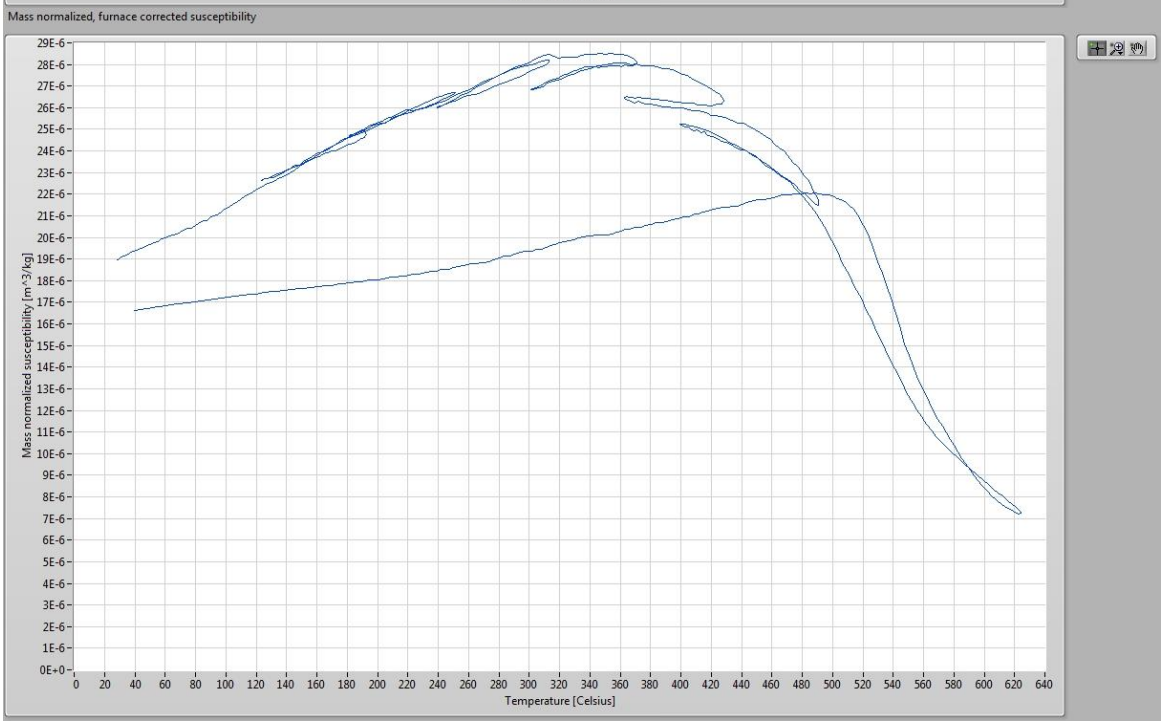

GR36-4

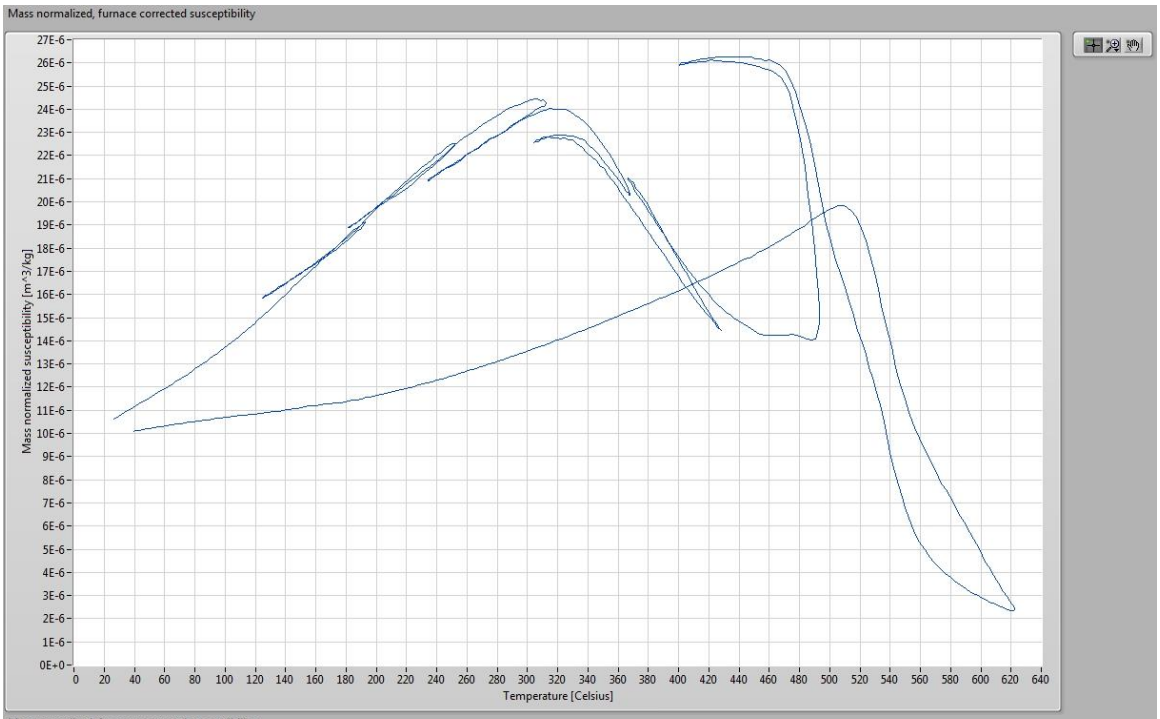

GR37-7

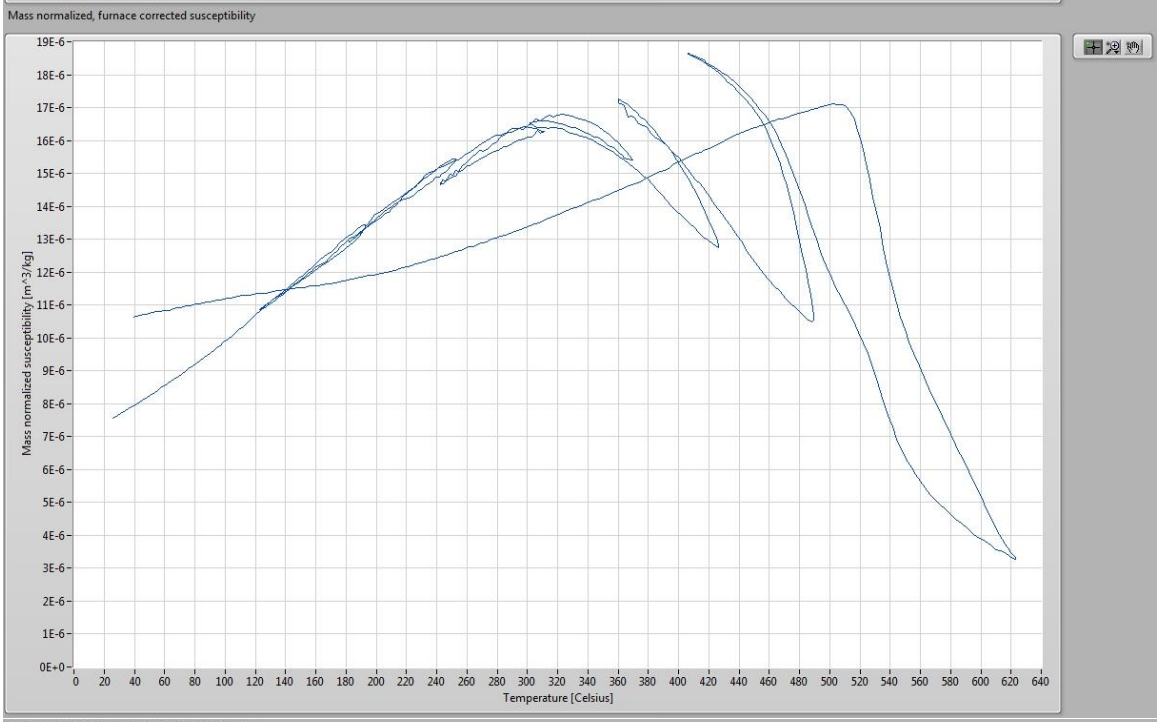

GR38-10

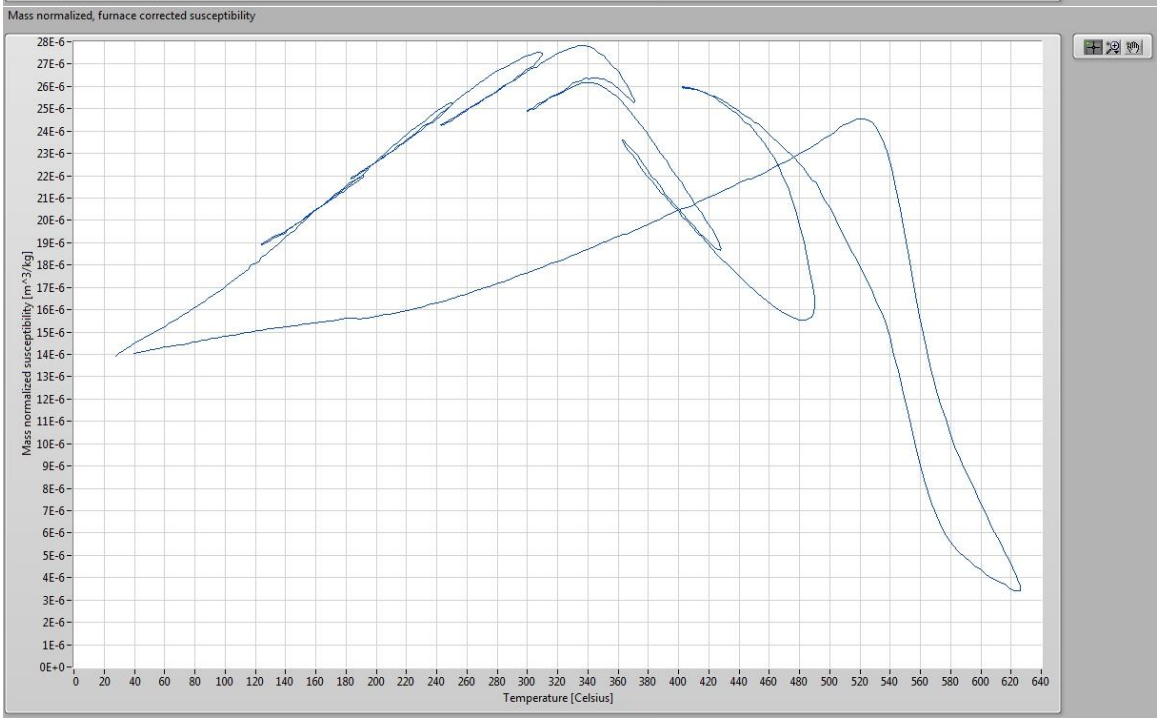

GR39-11

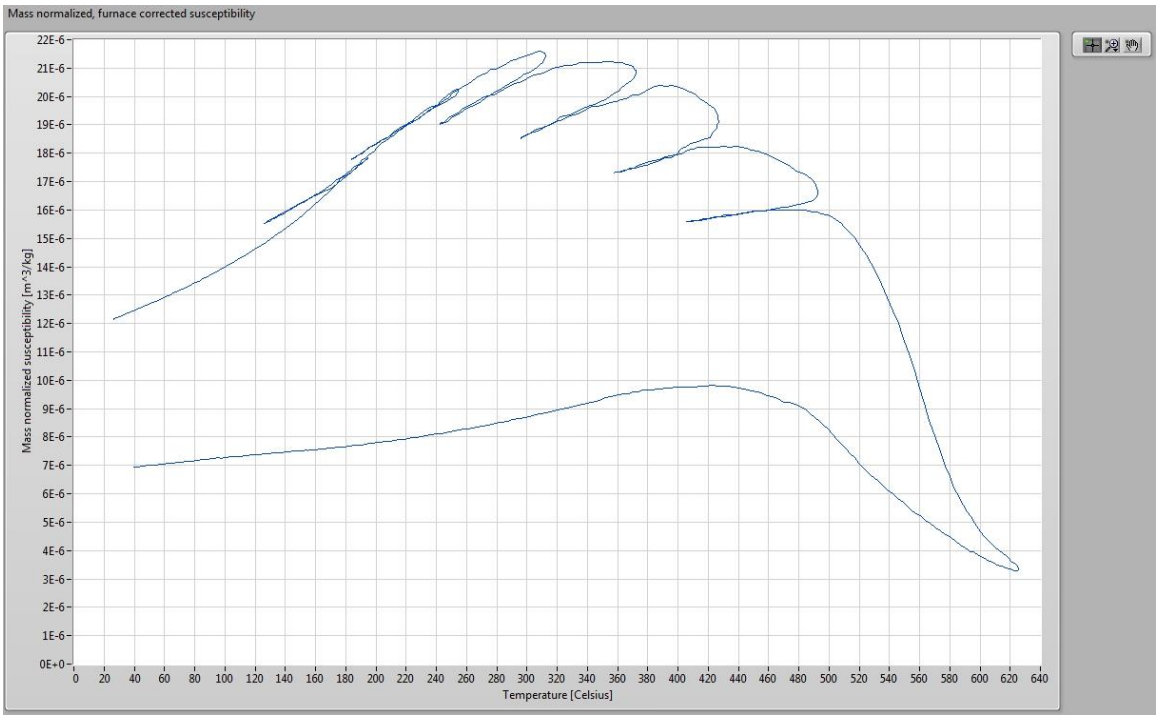

GR40-6

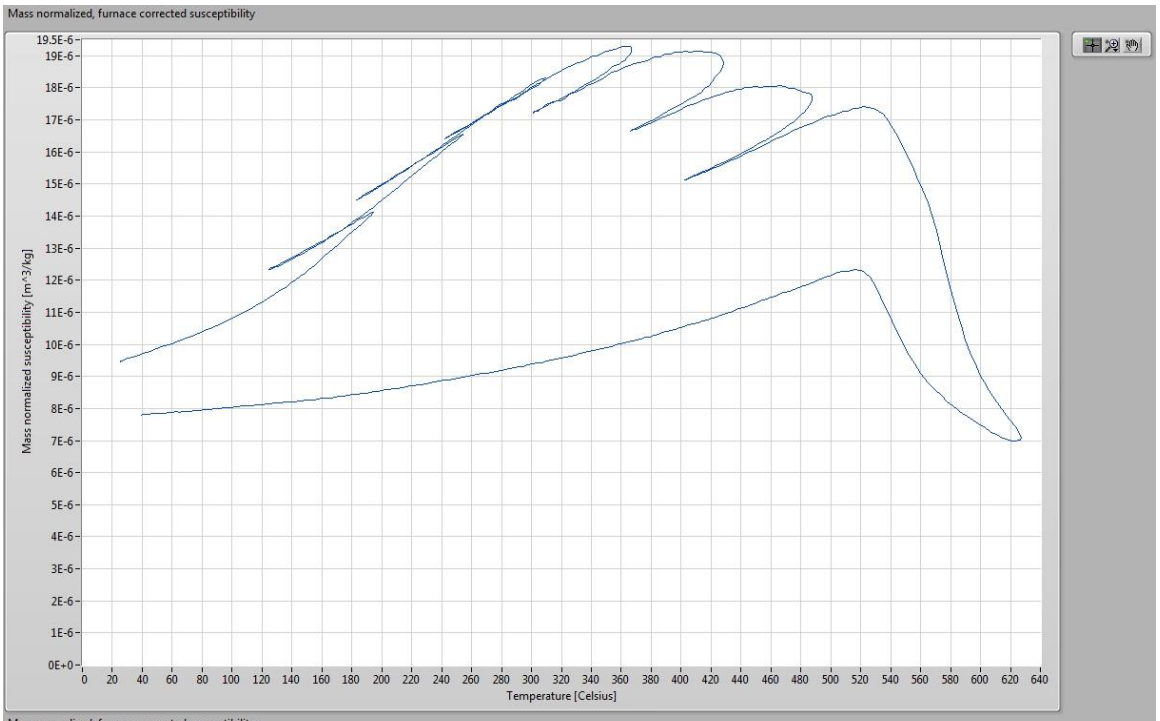

GR41-8

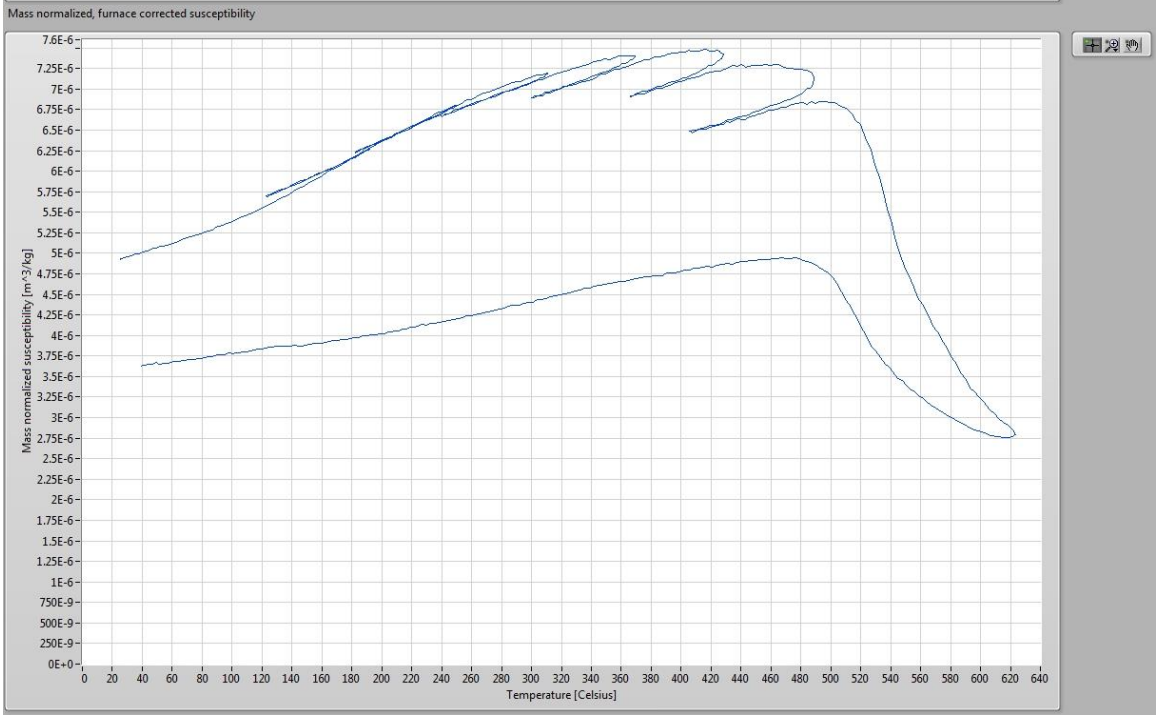

GR42-9

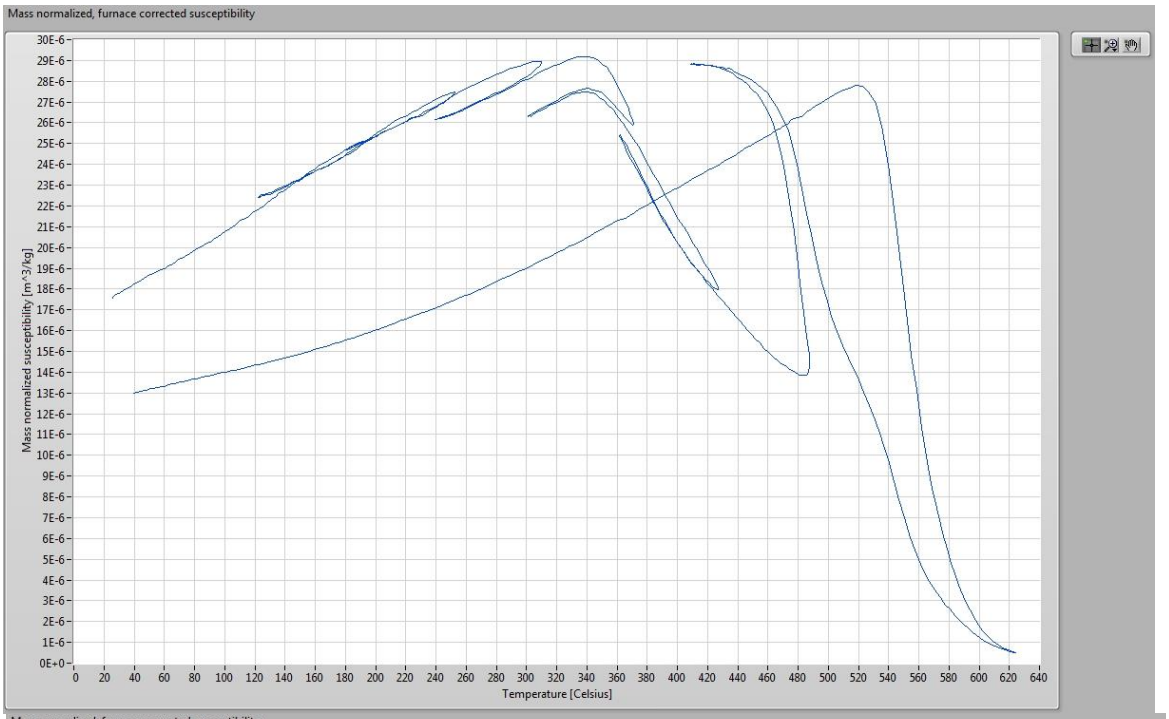

GR43-3

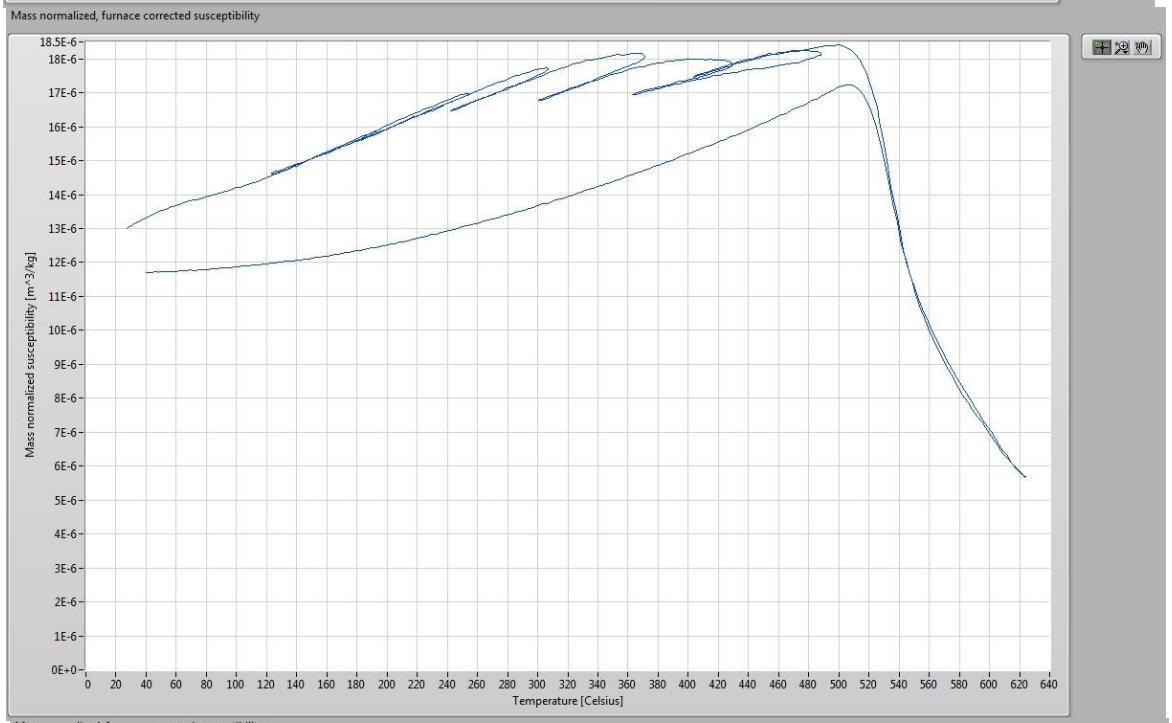

GR44-7B

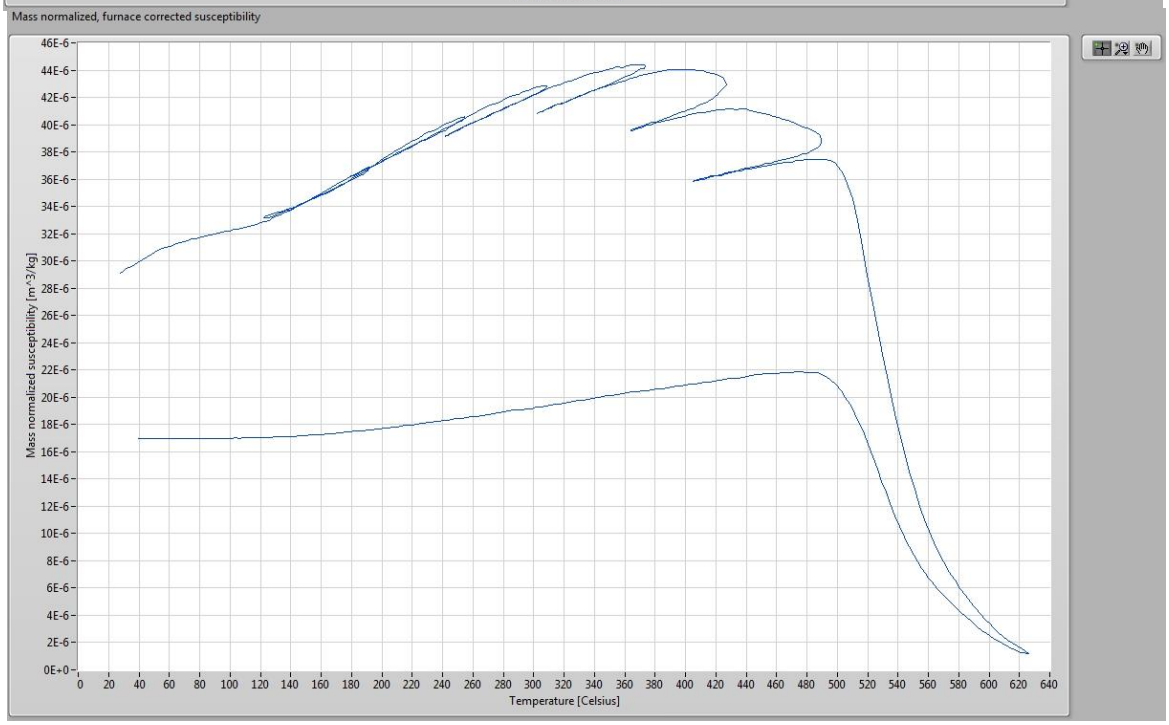

GR45-2

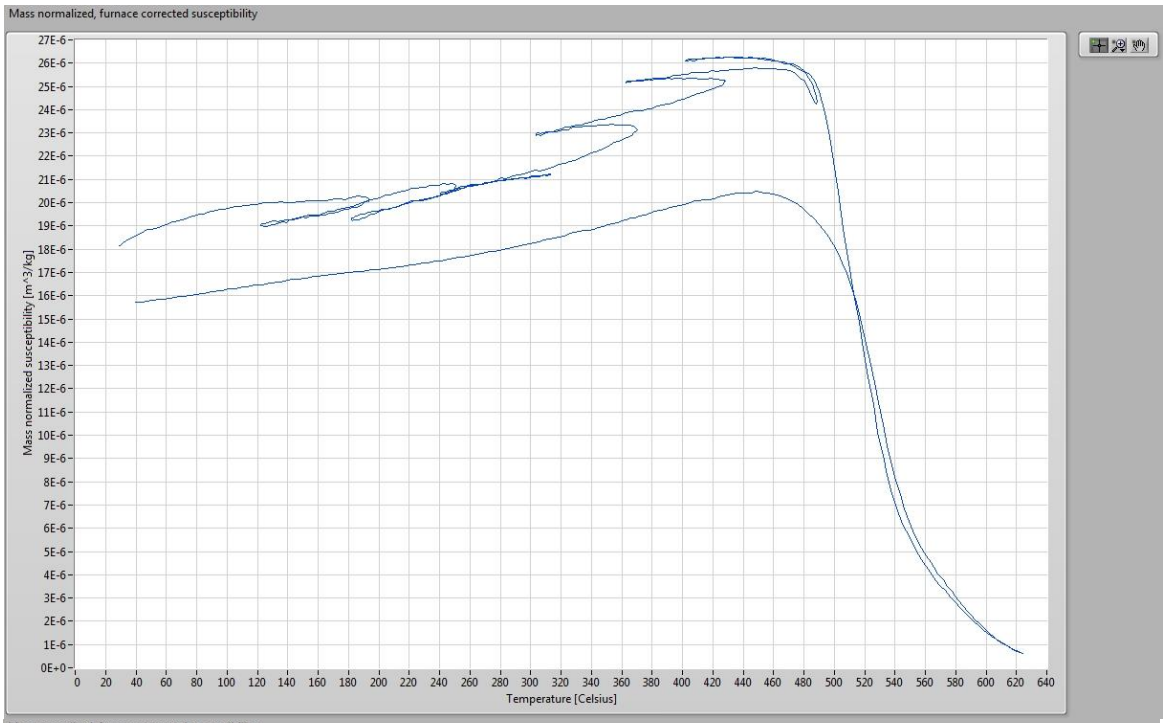

GR46-3

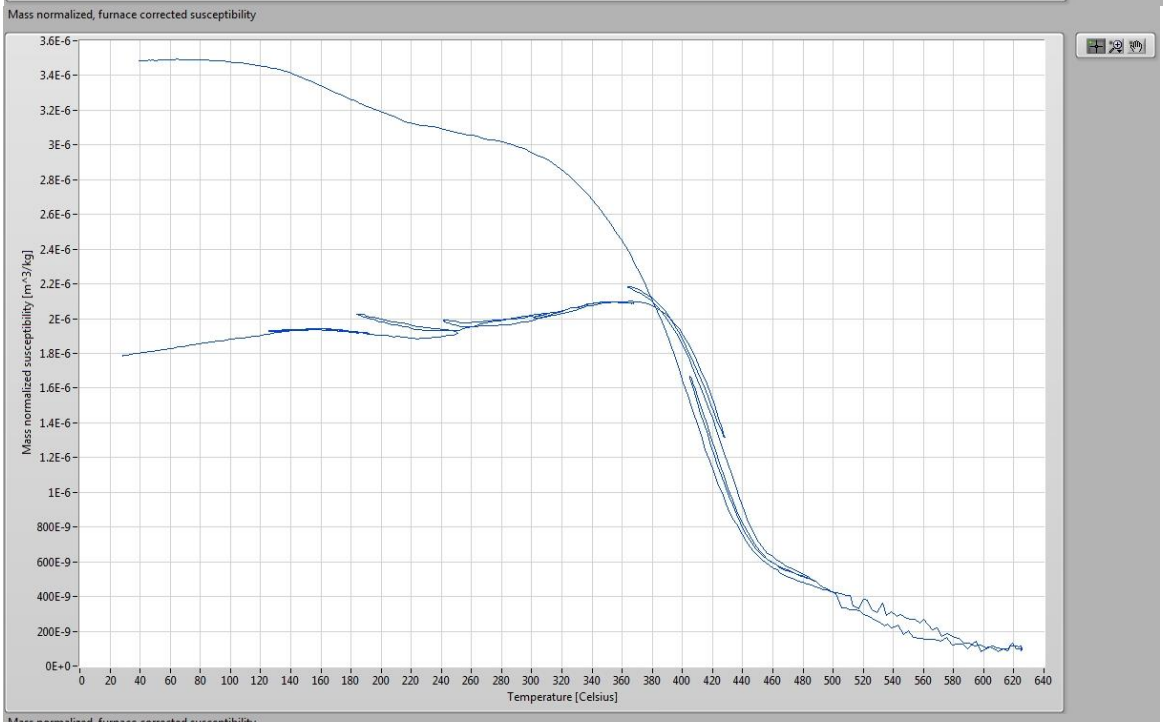

GR47-10

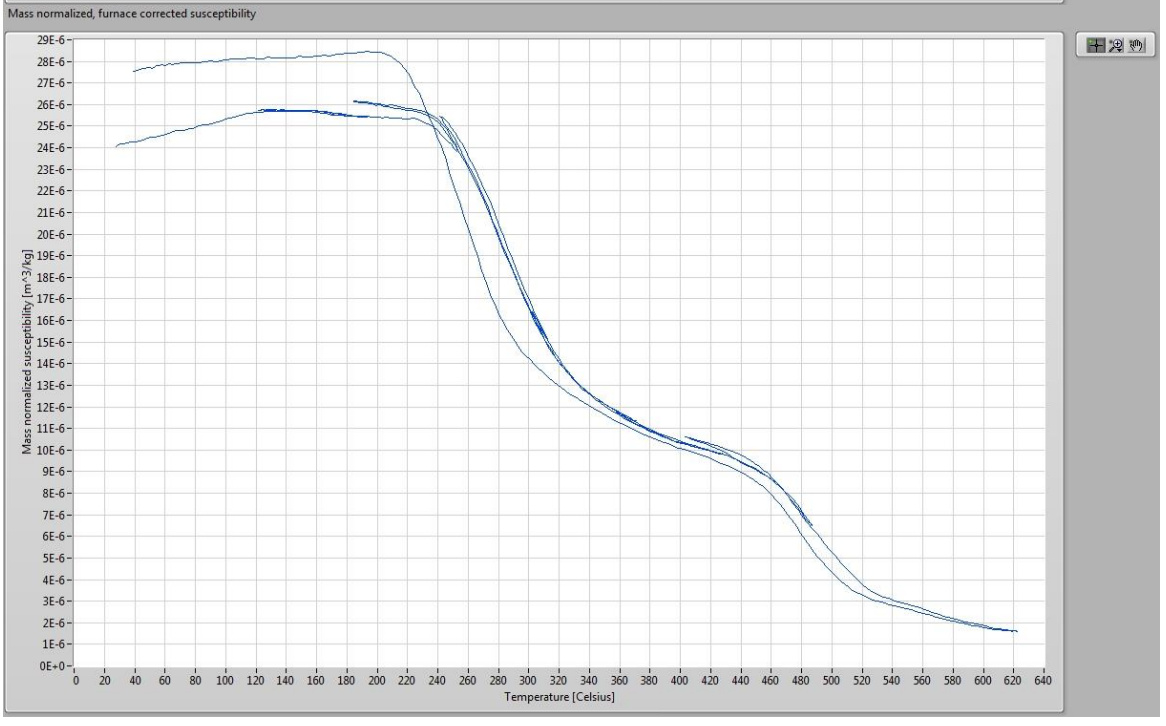

GR48-1

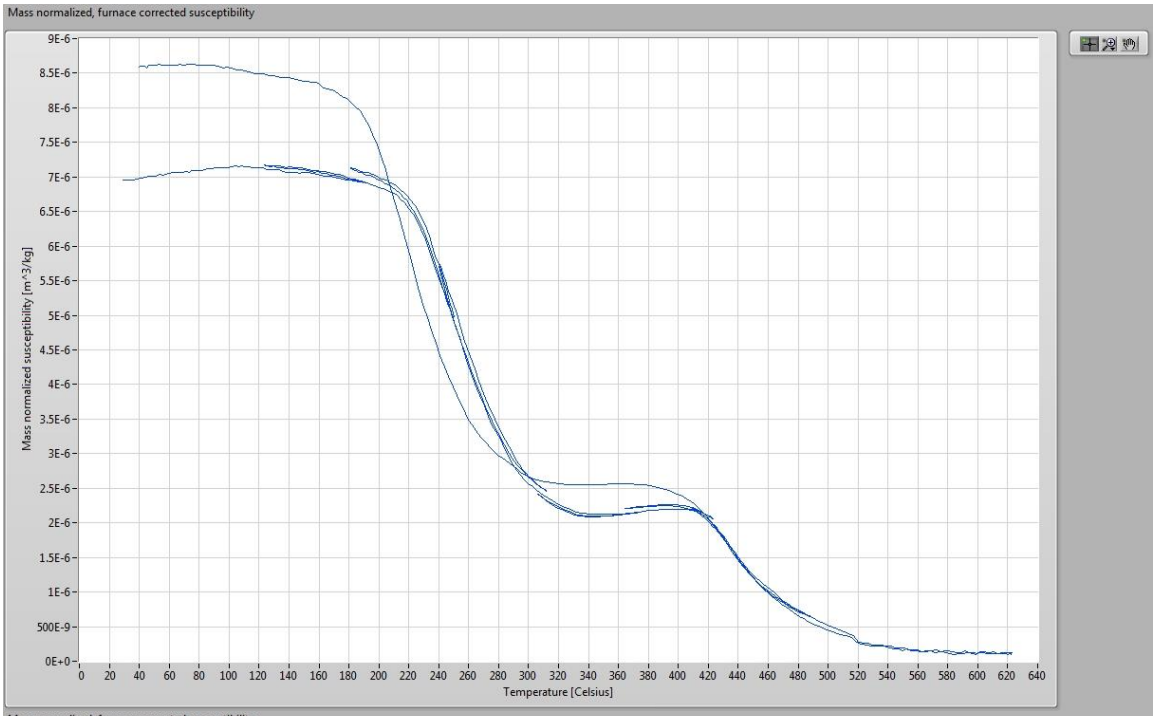

GR49-4

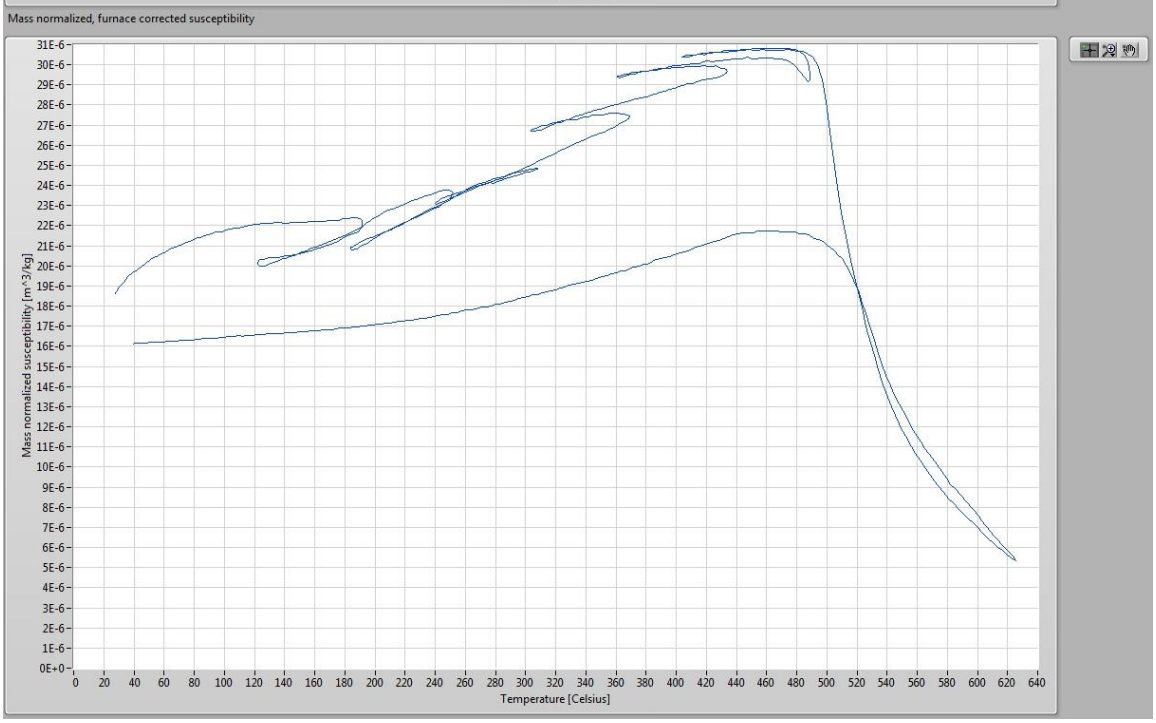

GR50-1

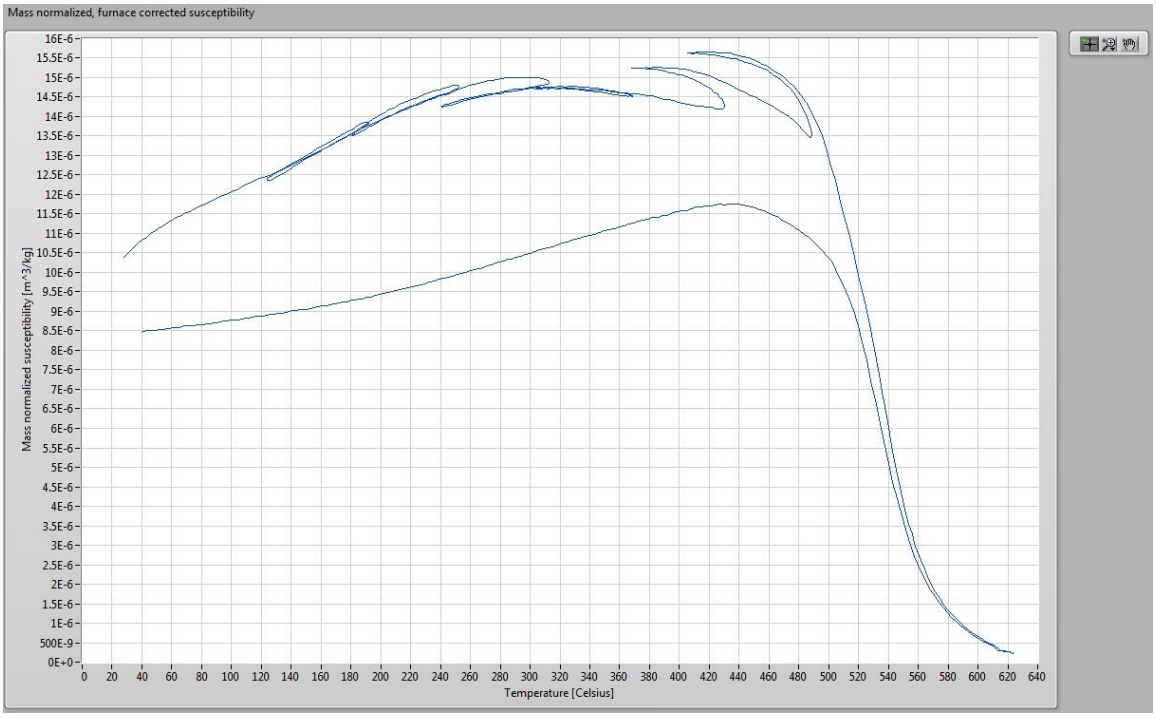

GR51-3

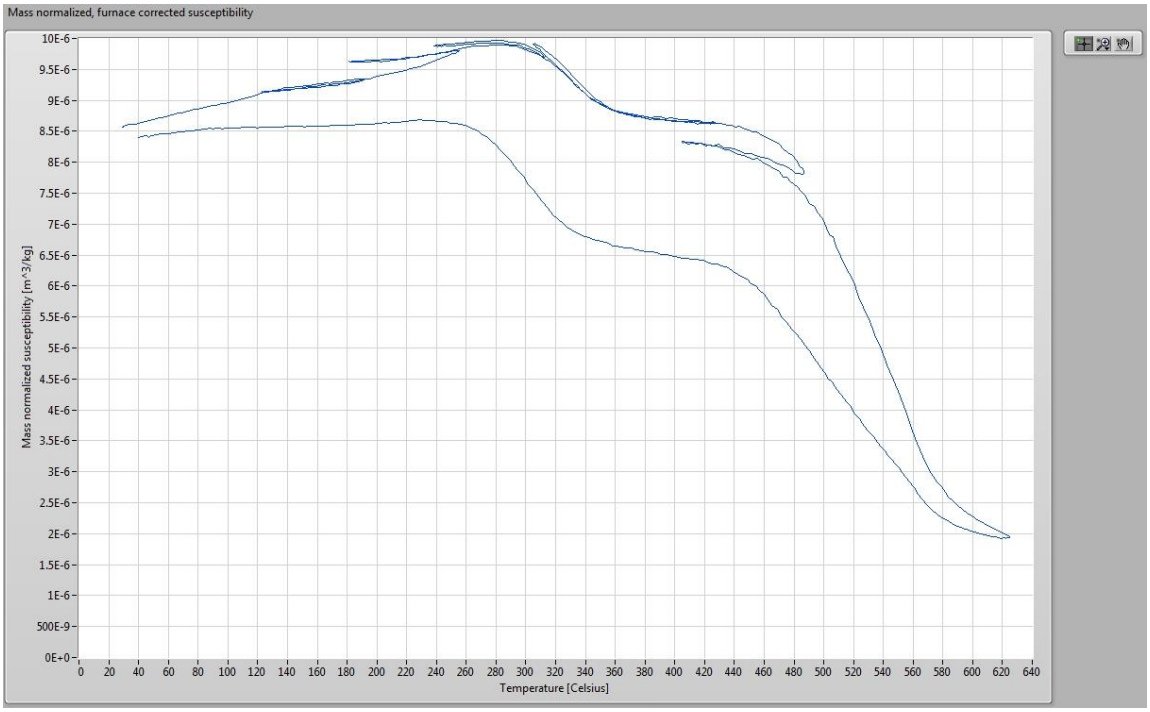

GR52-9

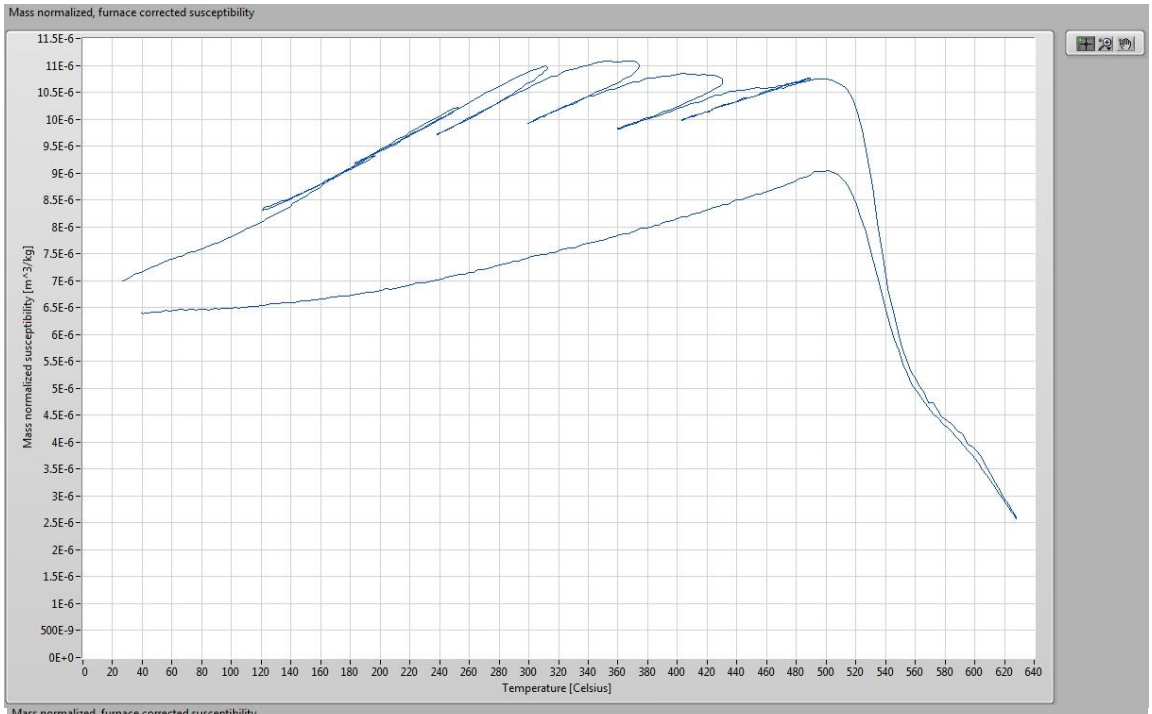

GR53-8

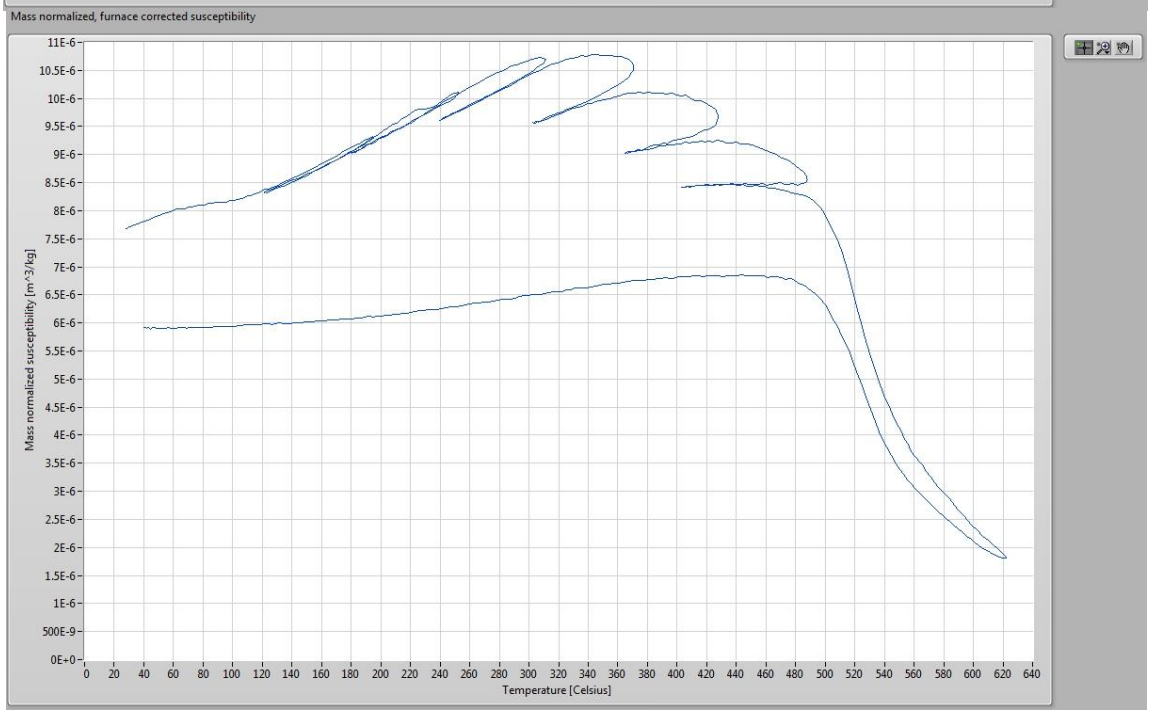

GR54-8

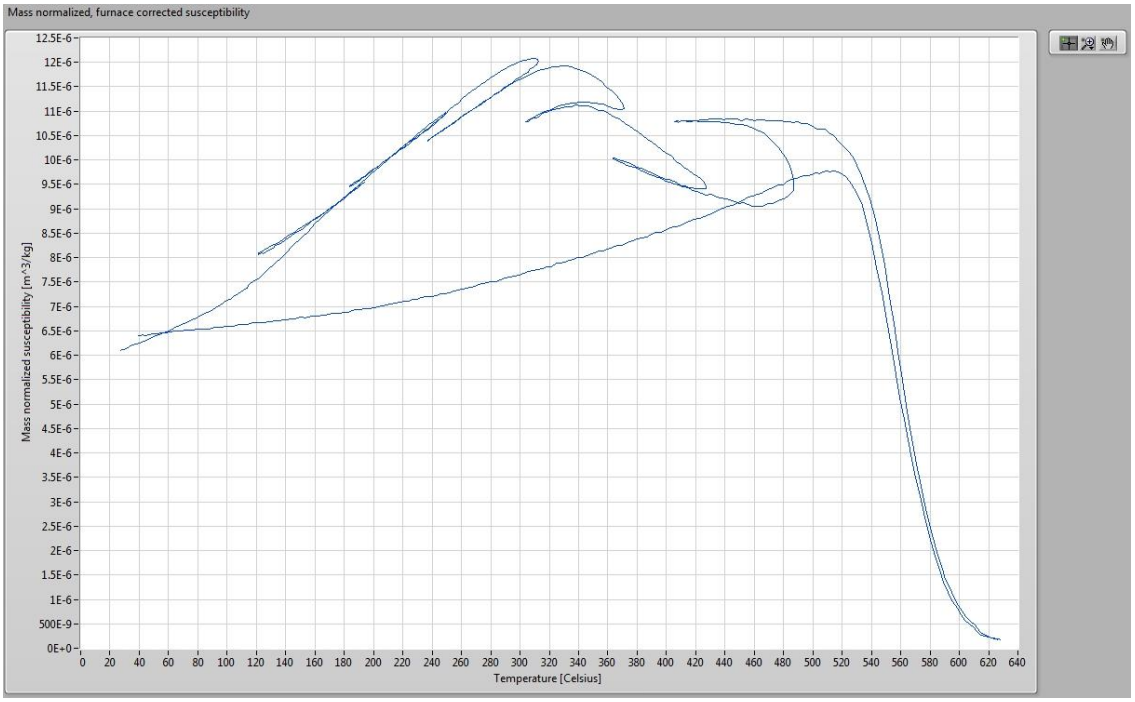

GR55-6

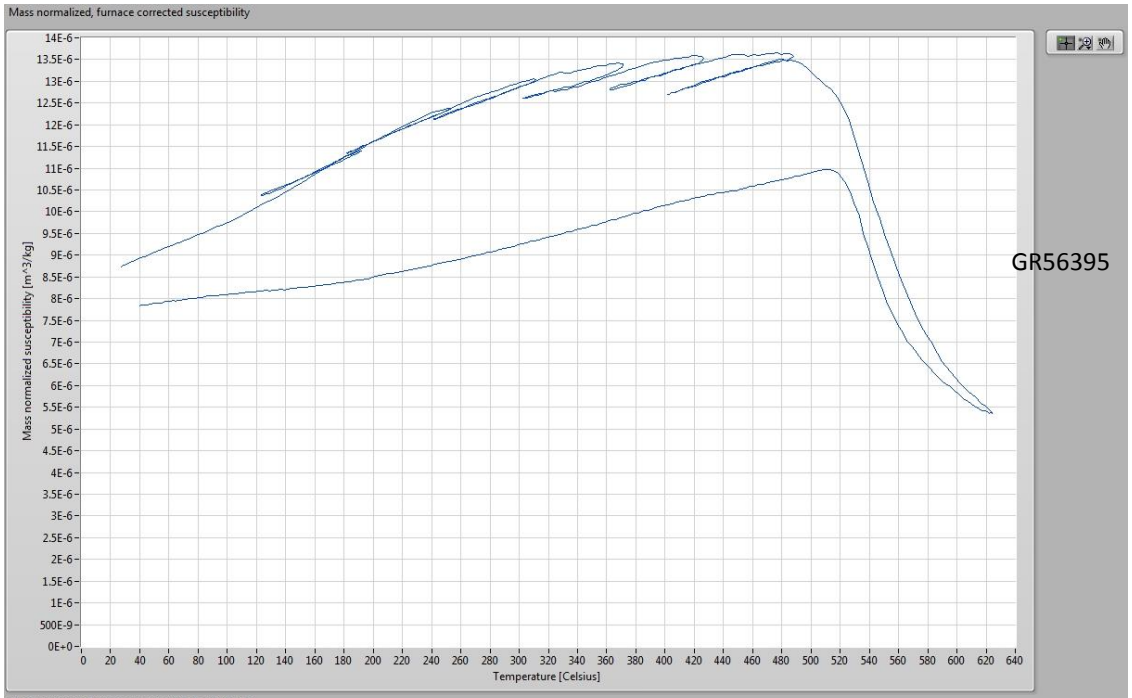

GR56395 40-6

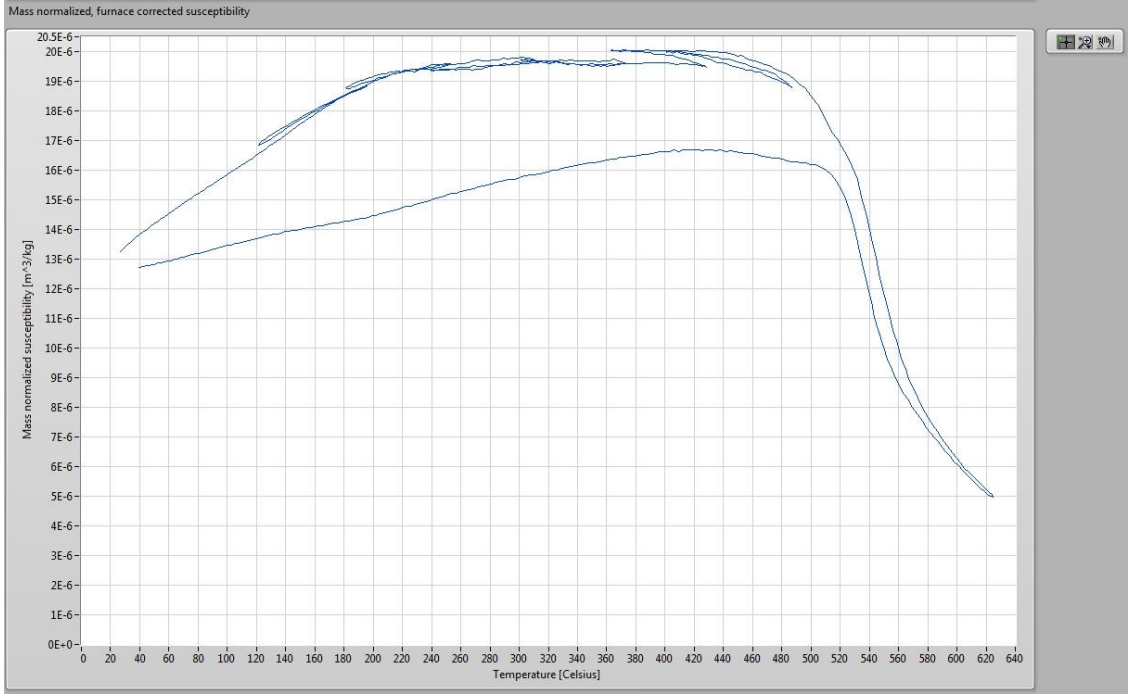

GR57-8

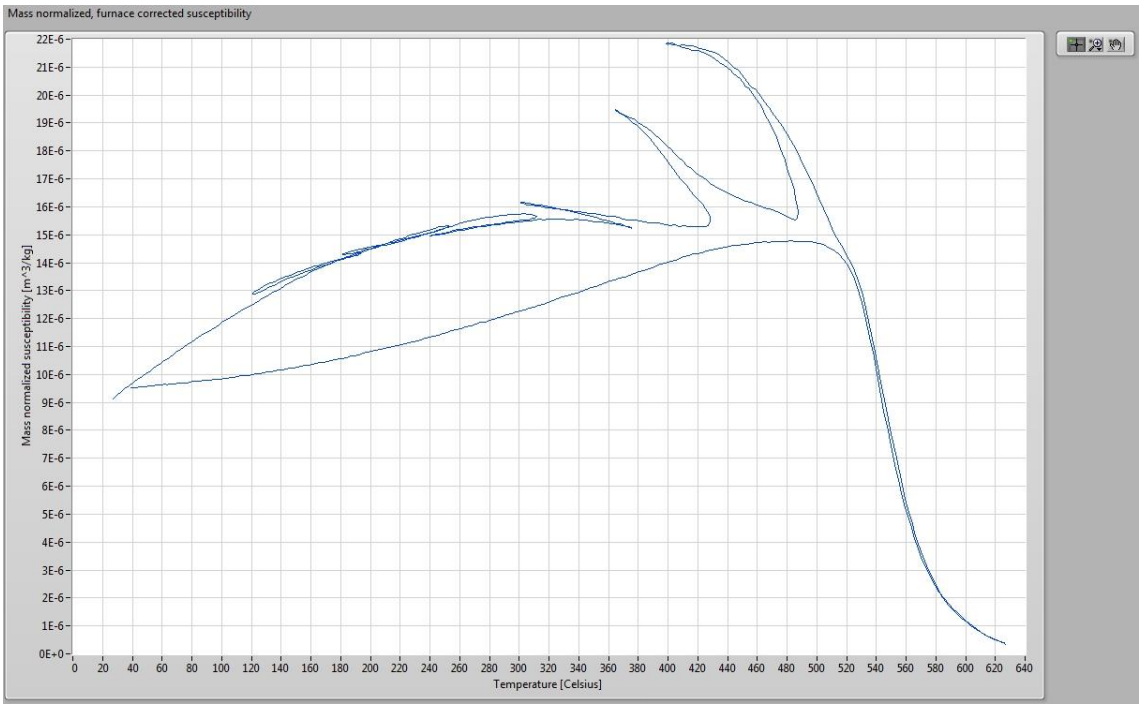

GR58-6

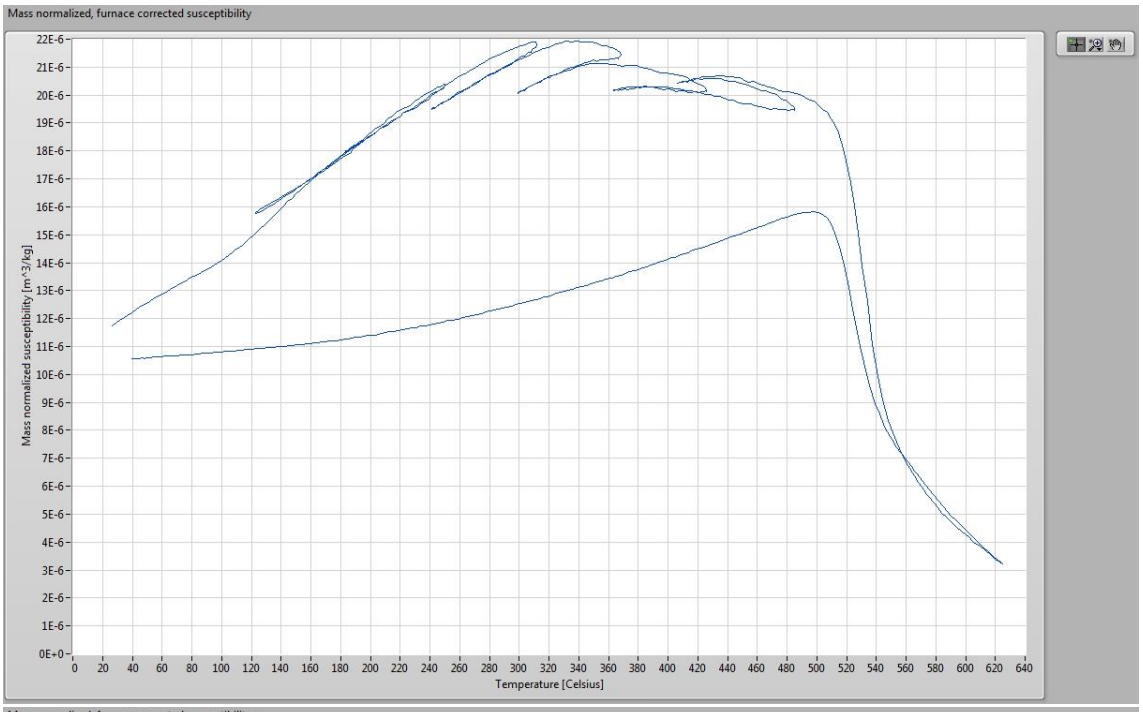

GR59-3

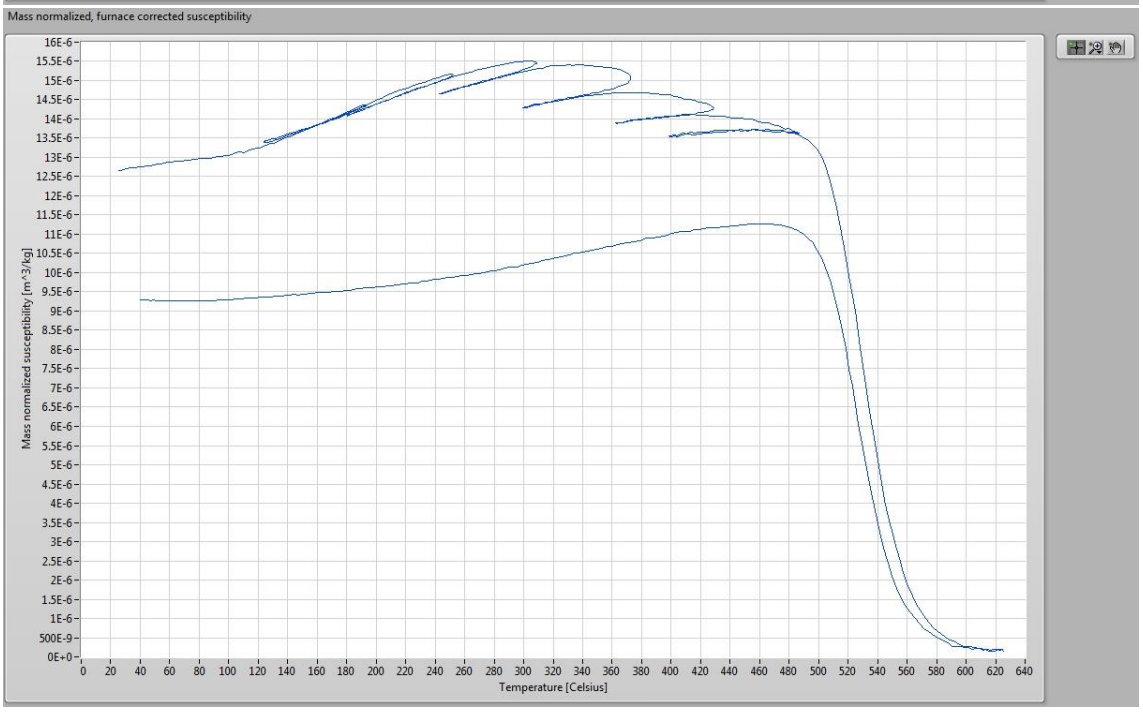

GR60-2

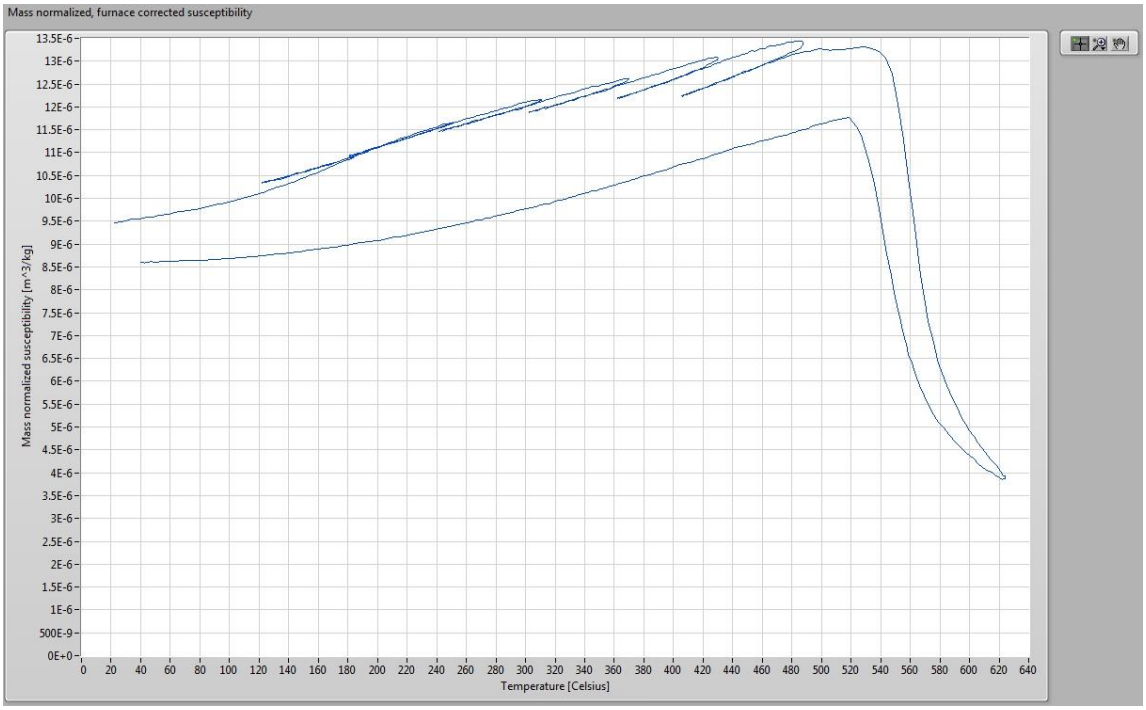

GR61-9

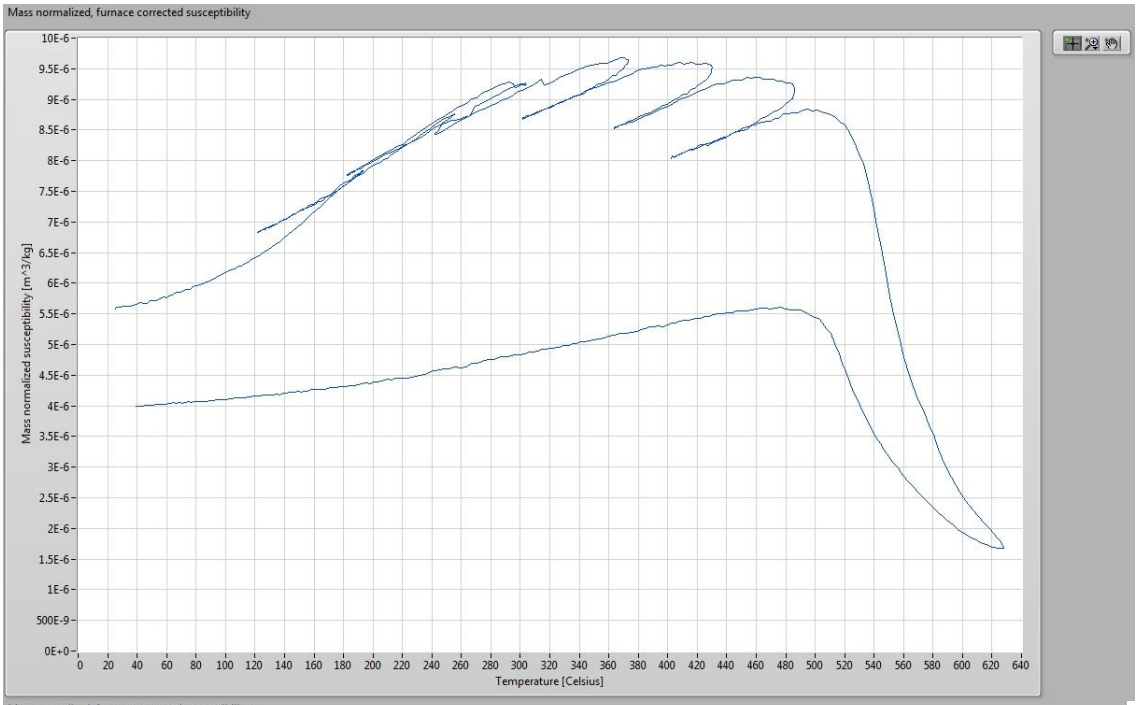

GR62-7

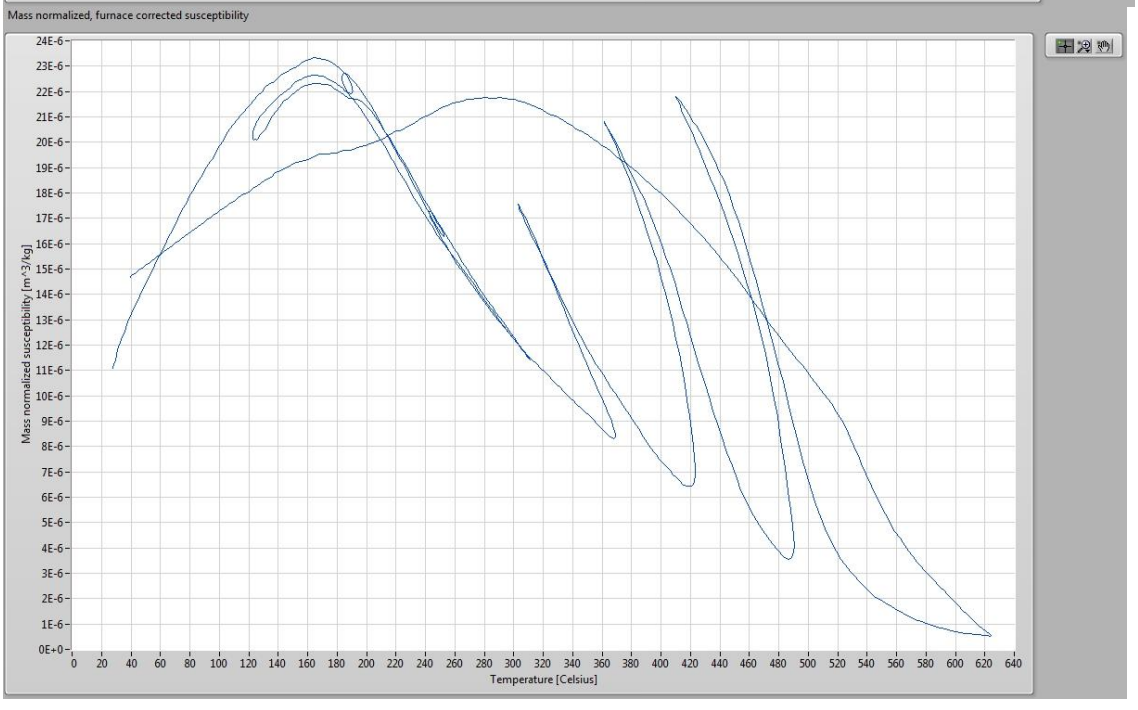

GR63-4

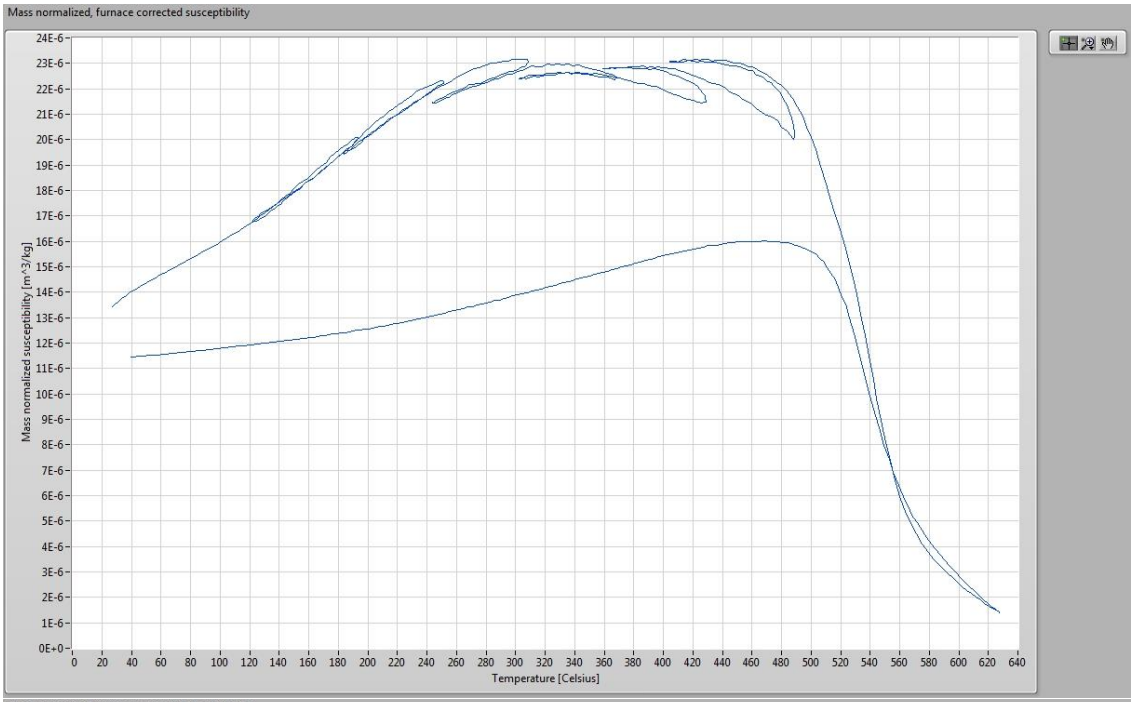

GR64-2

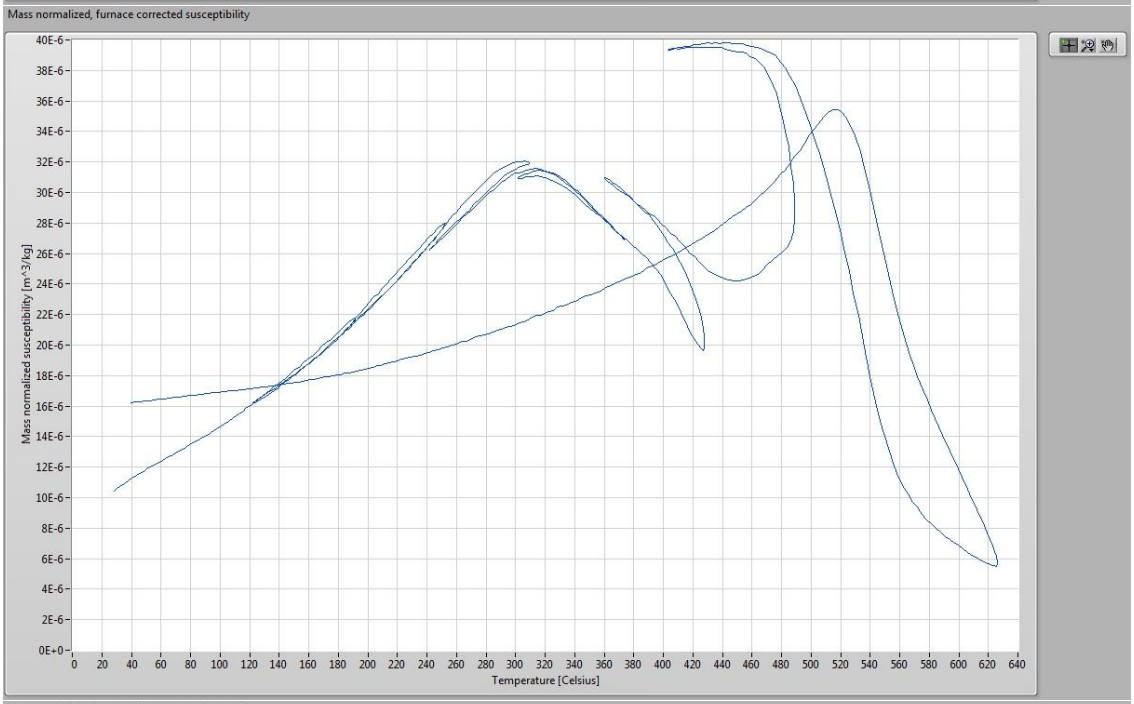

GR65-8

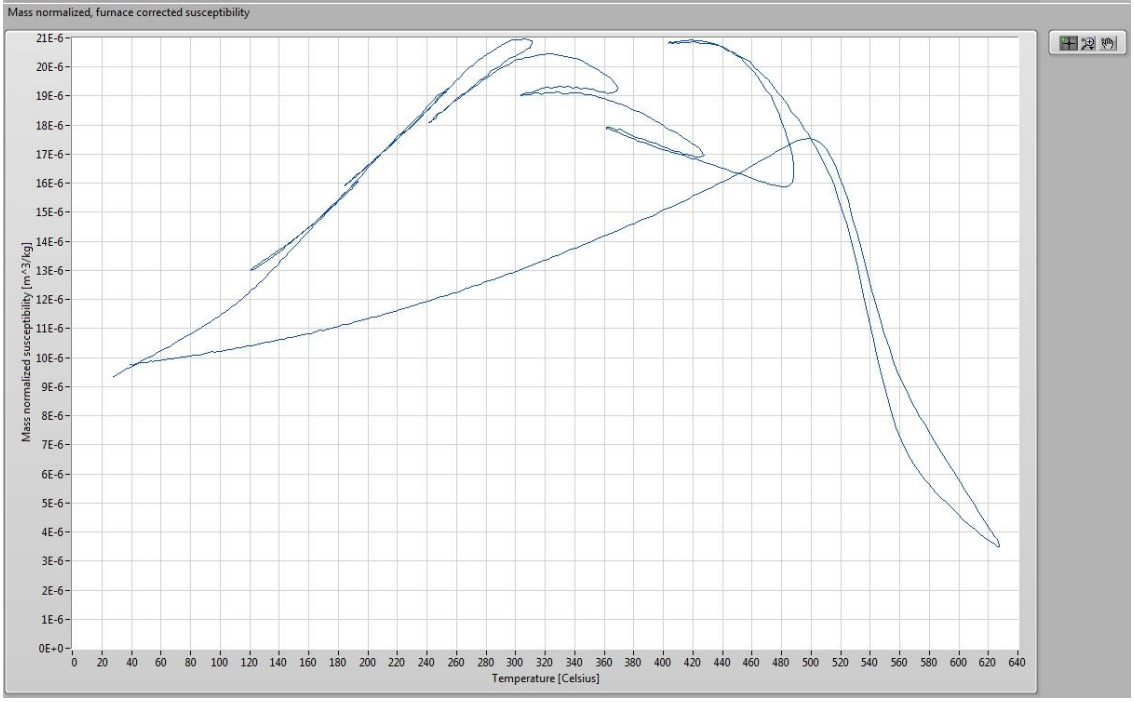

GR66-4

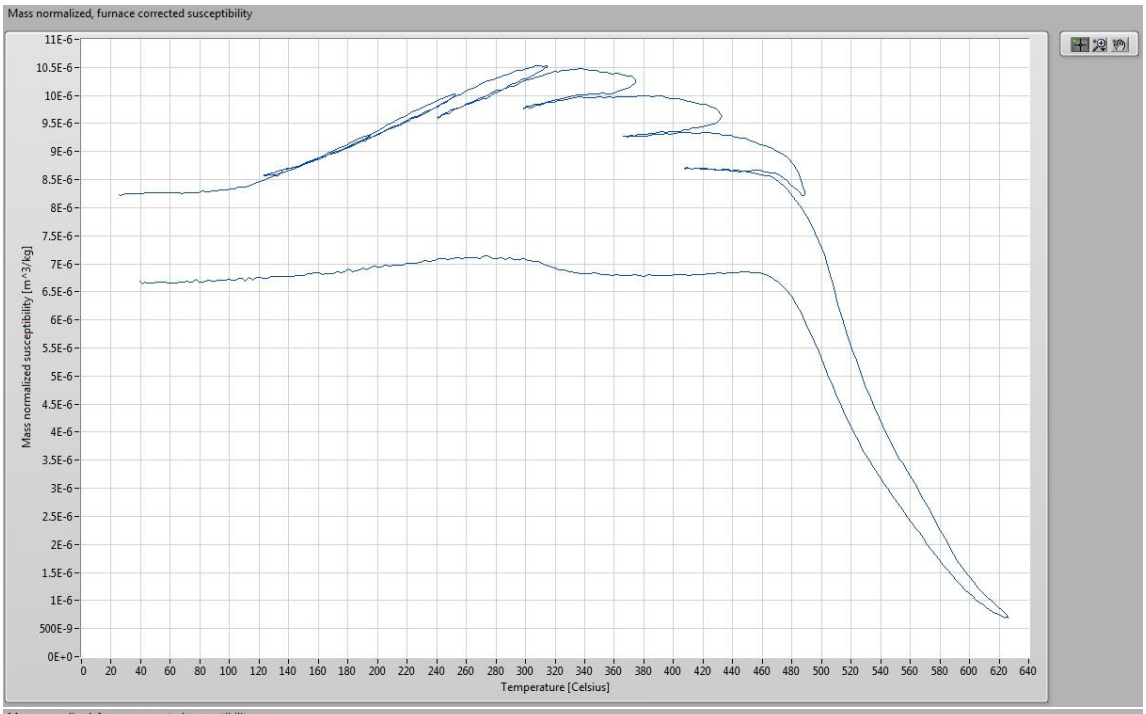

GR67-6

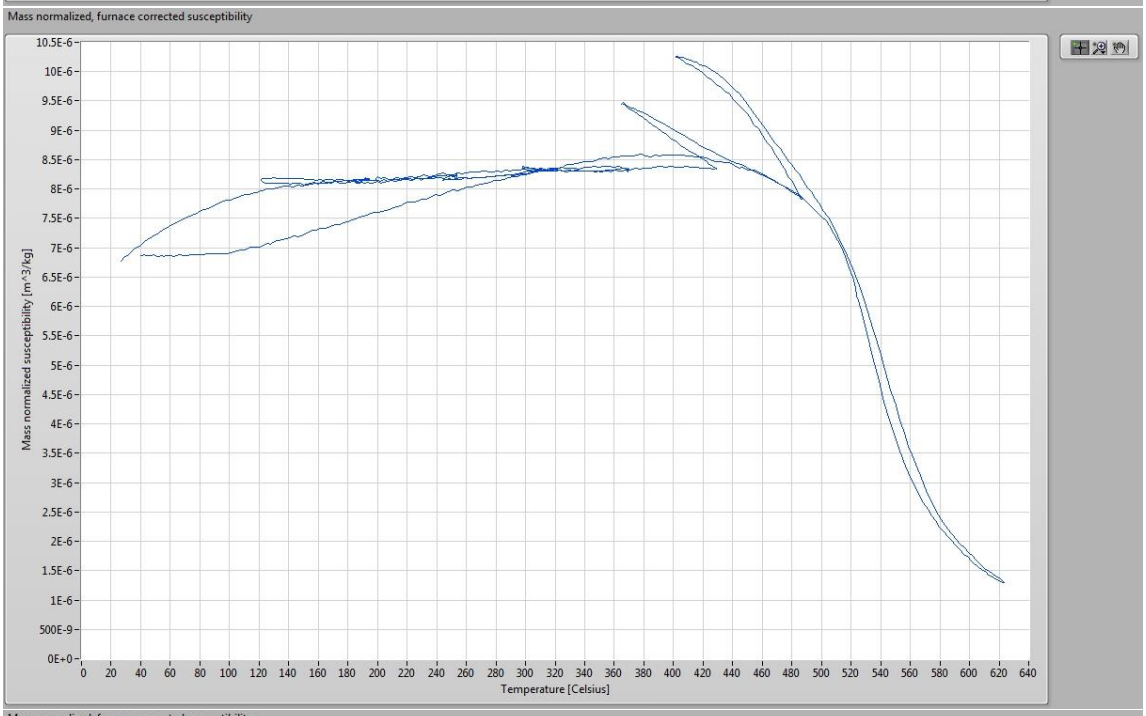

GR68-6

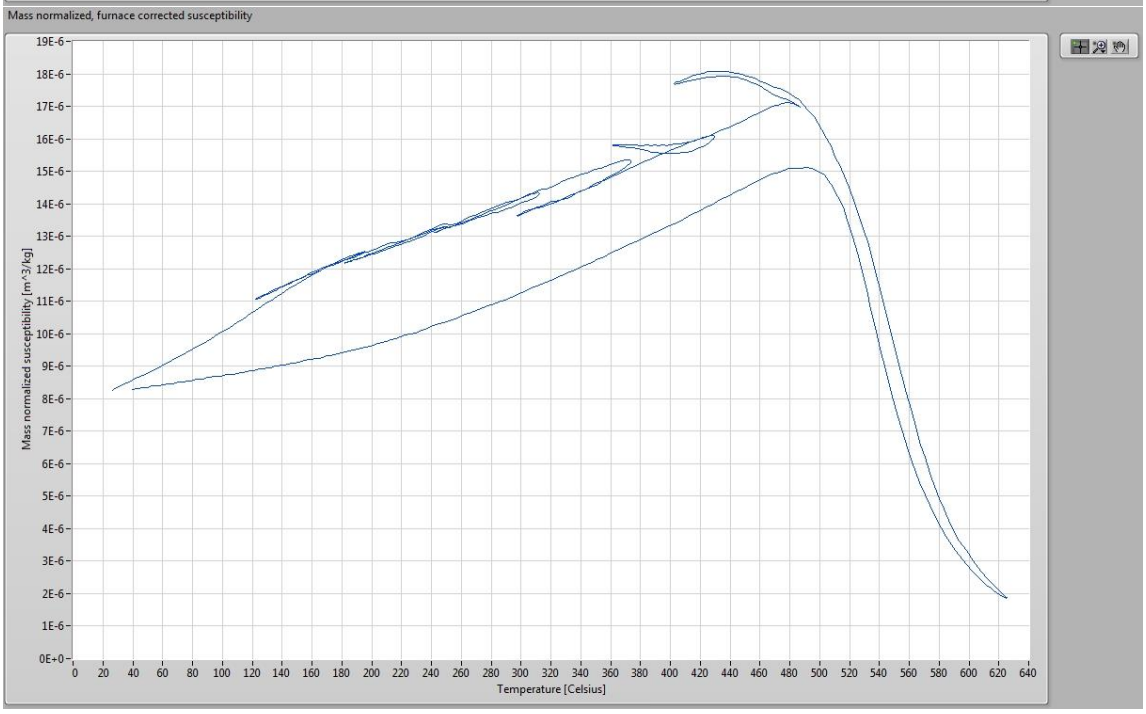

GR69-3

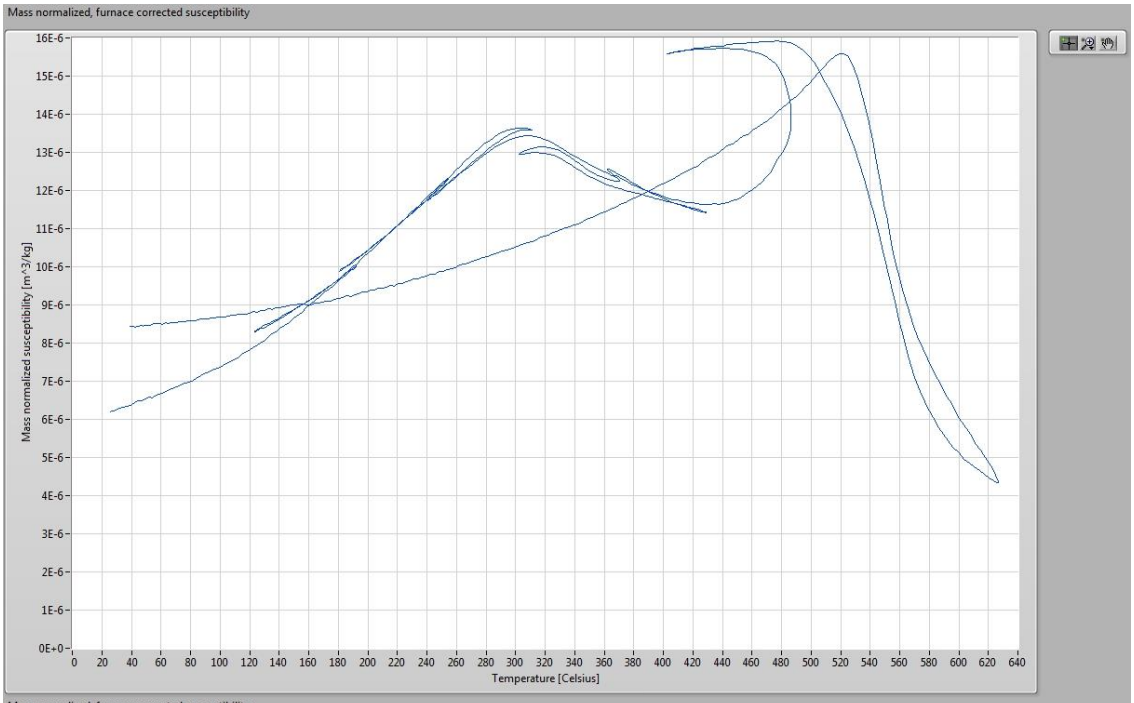

GR70-1

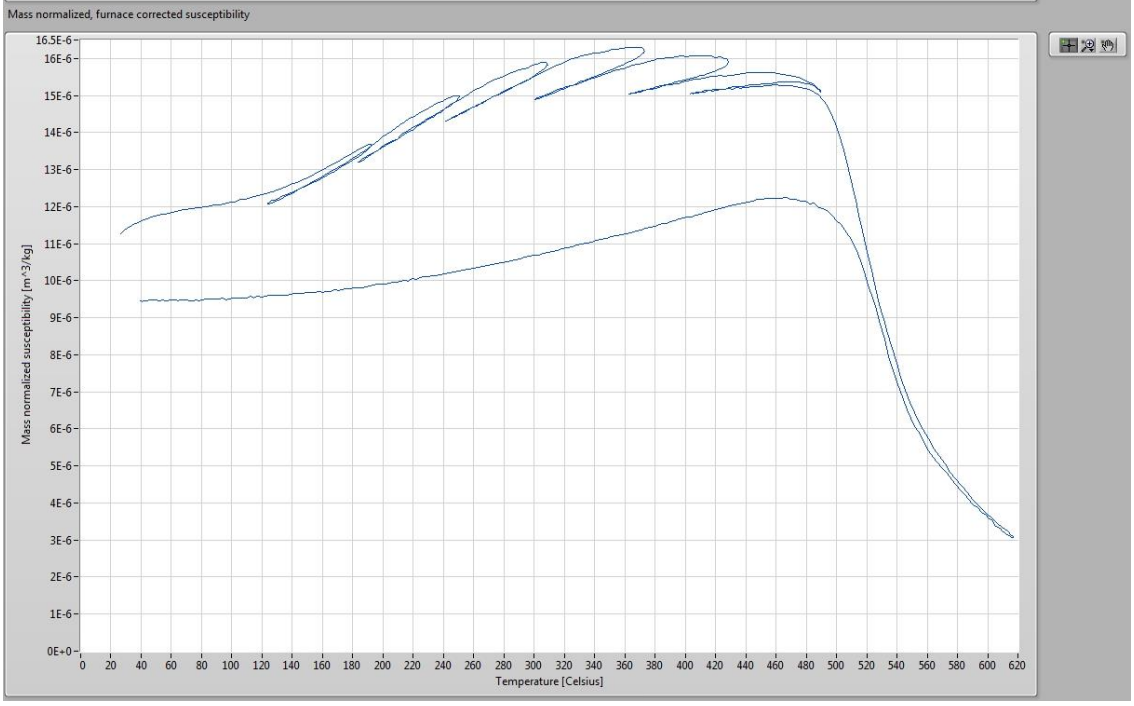

GR71-1

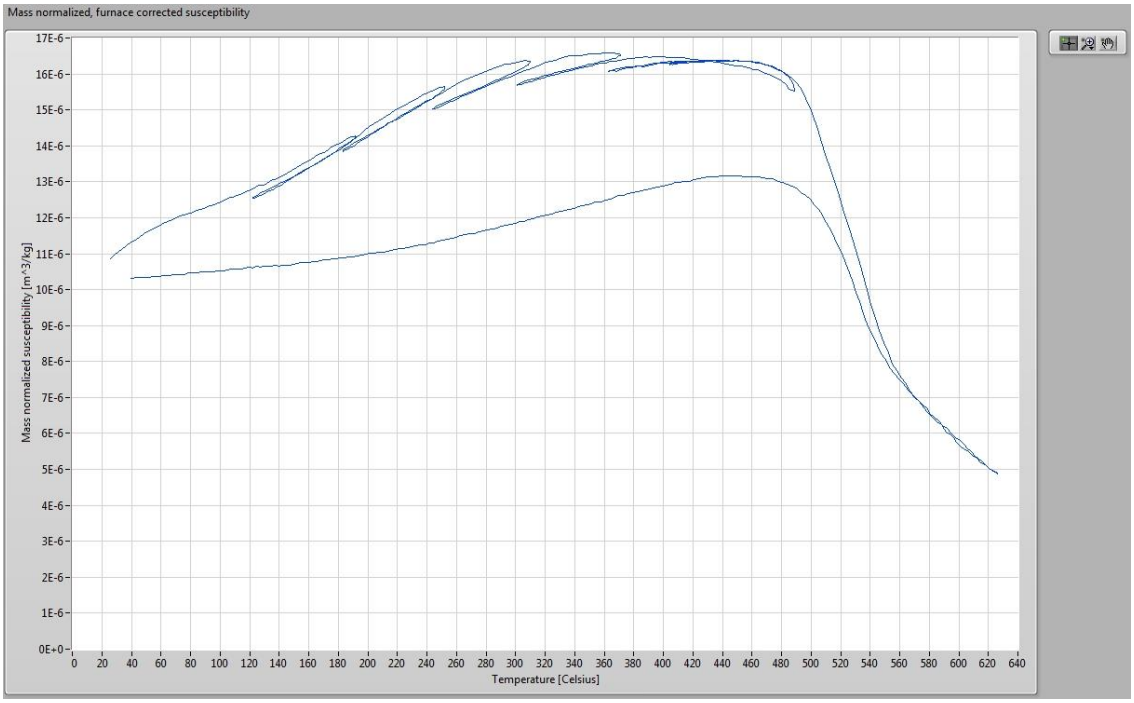

GR72-2

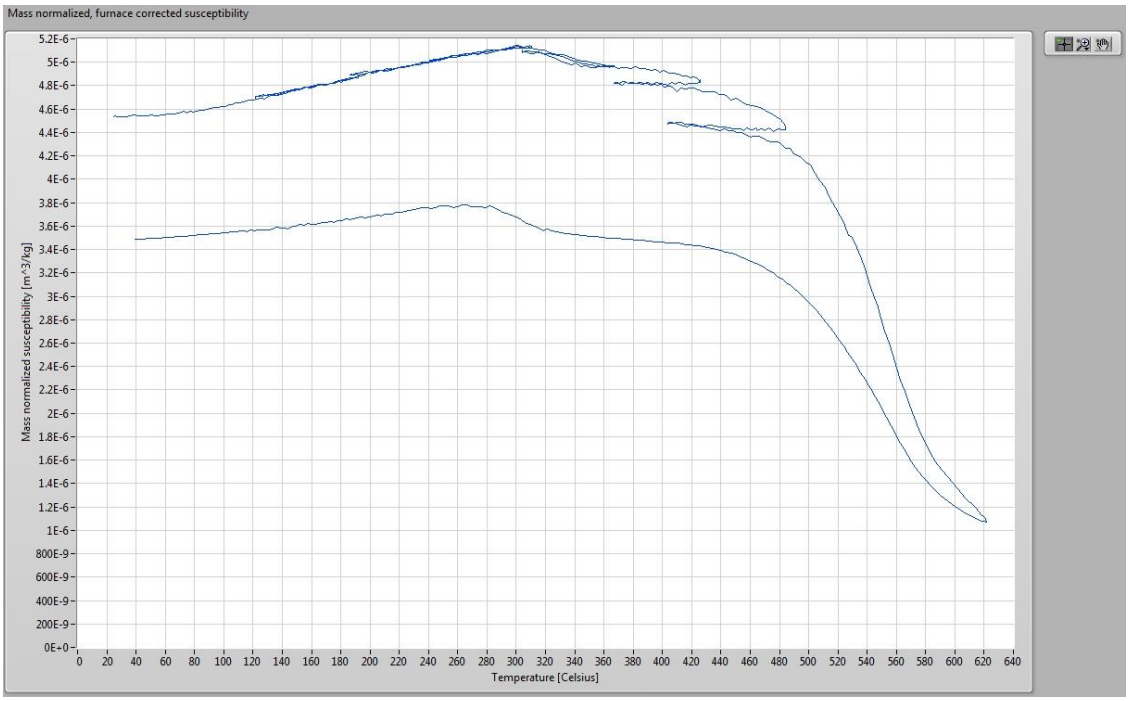

GR73-3

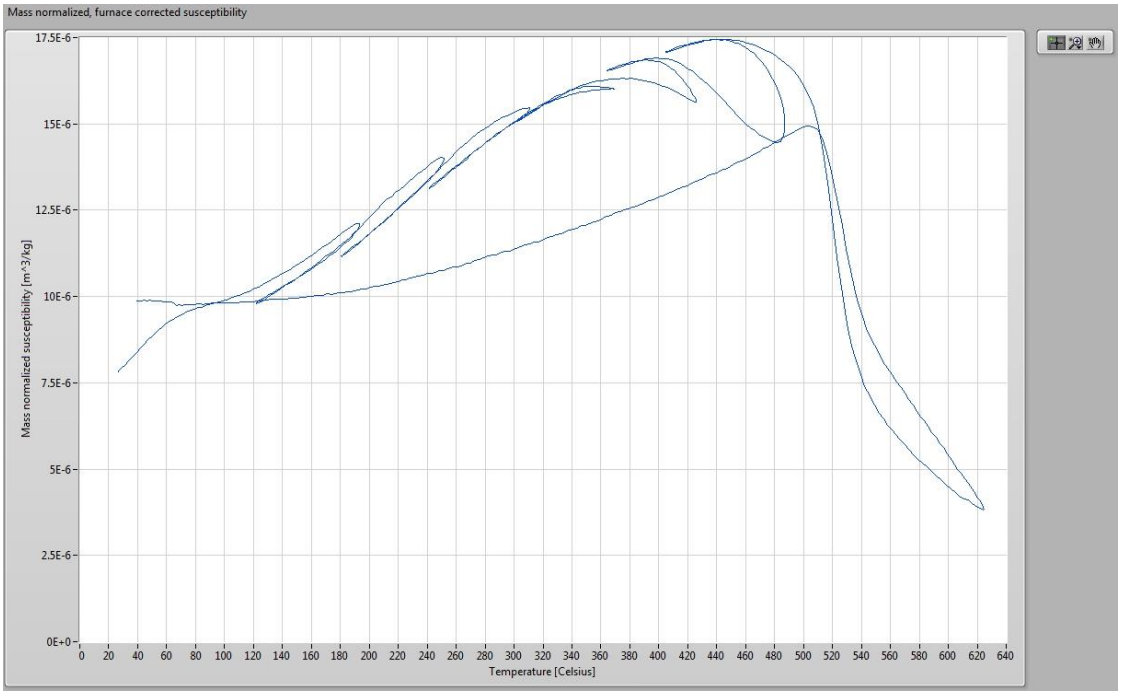

GR74-6

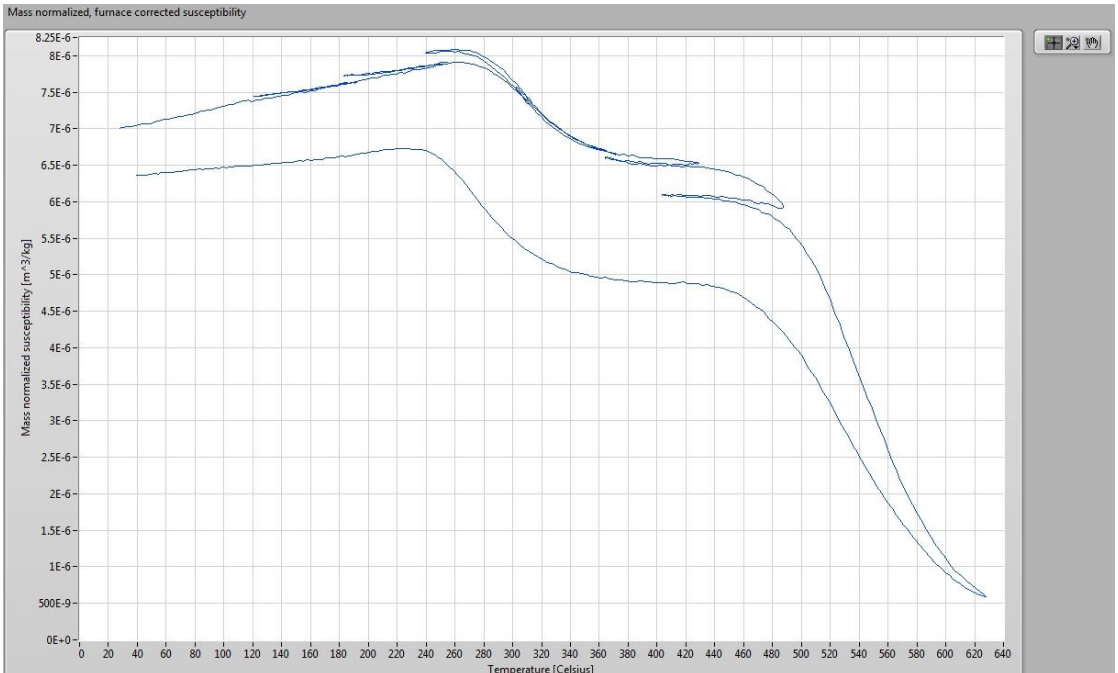

GR75-8

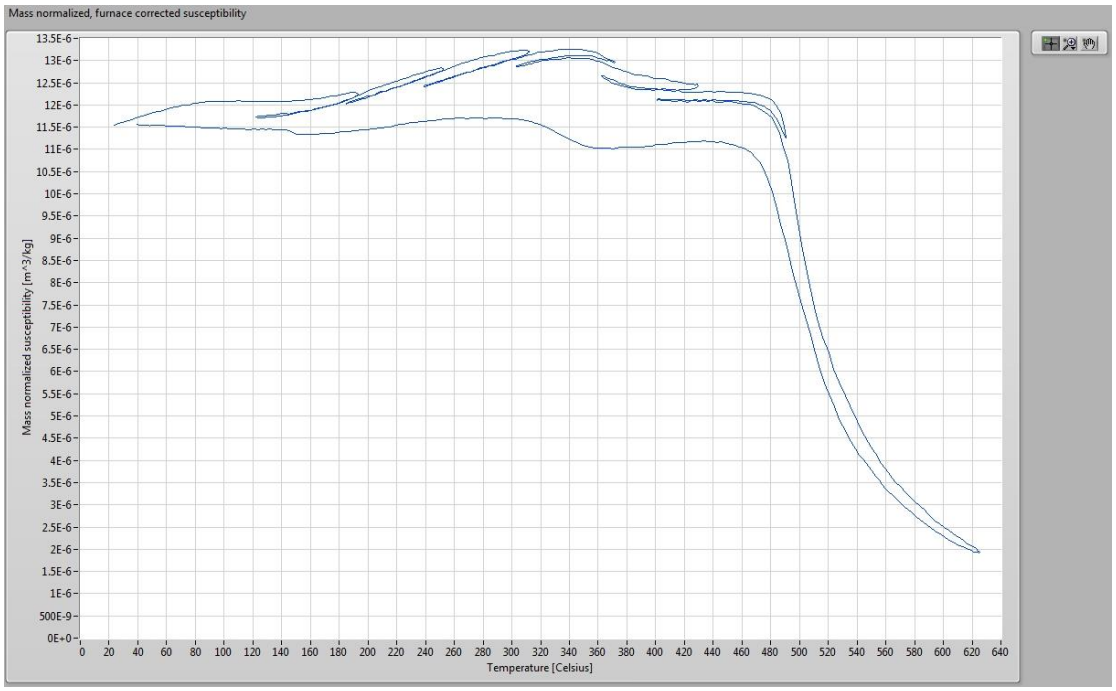

GR76-2

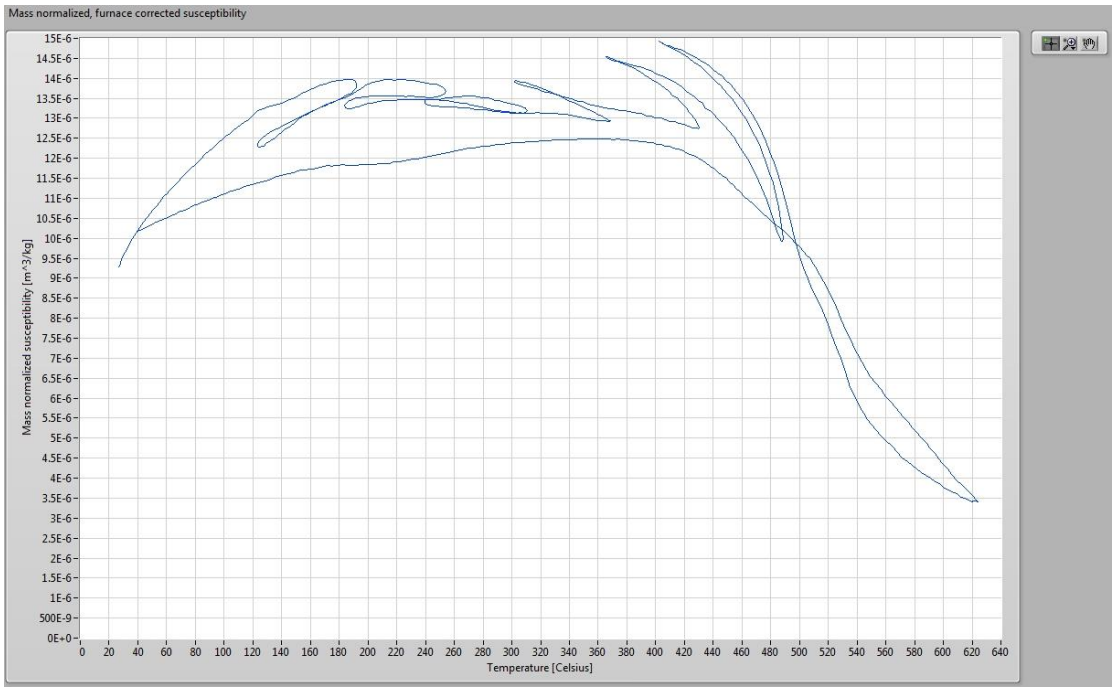

GR77-5

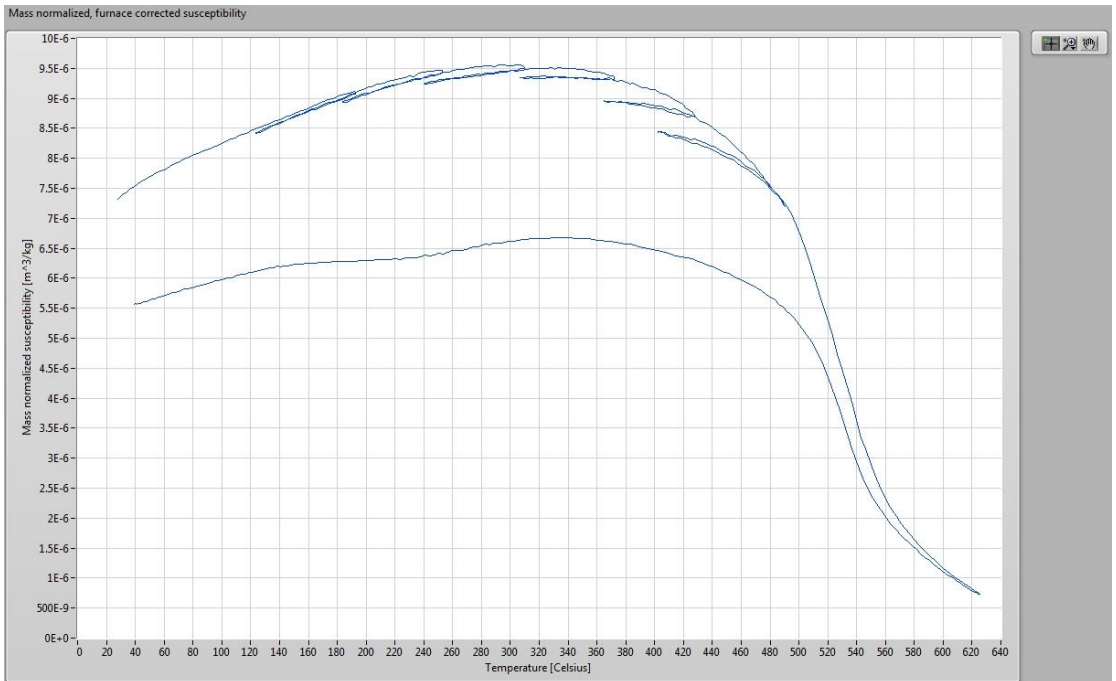

GR78-9

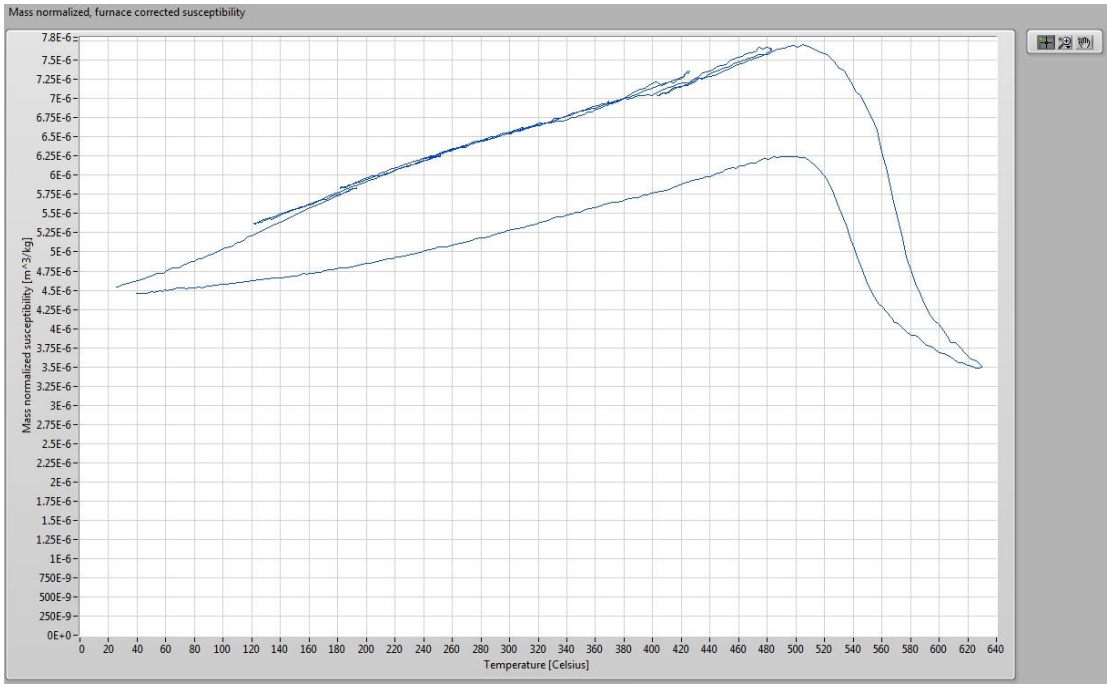

GR79-1

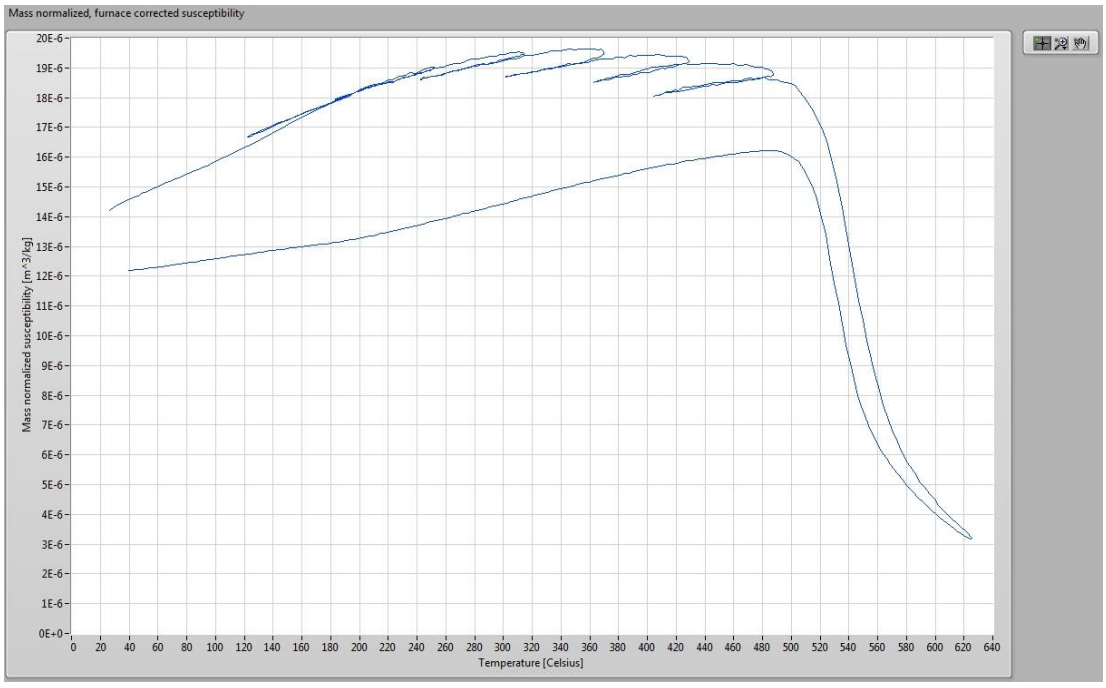

GR80-9

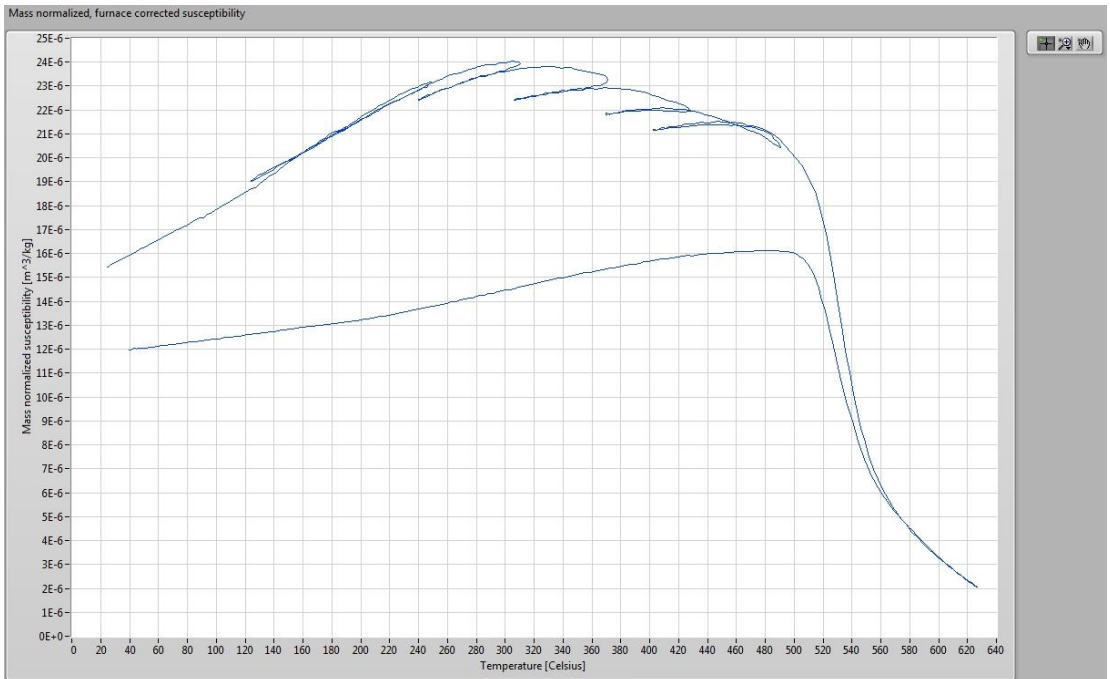

GR81-1

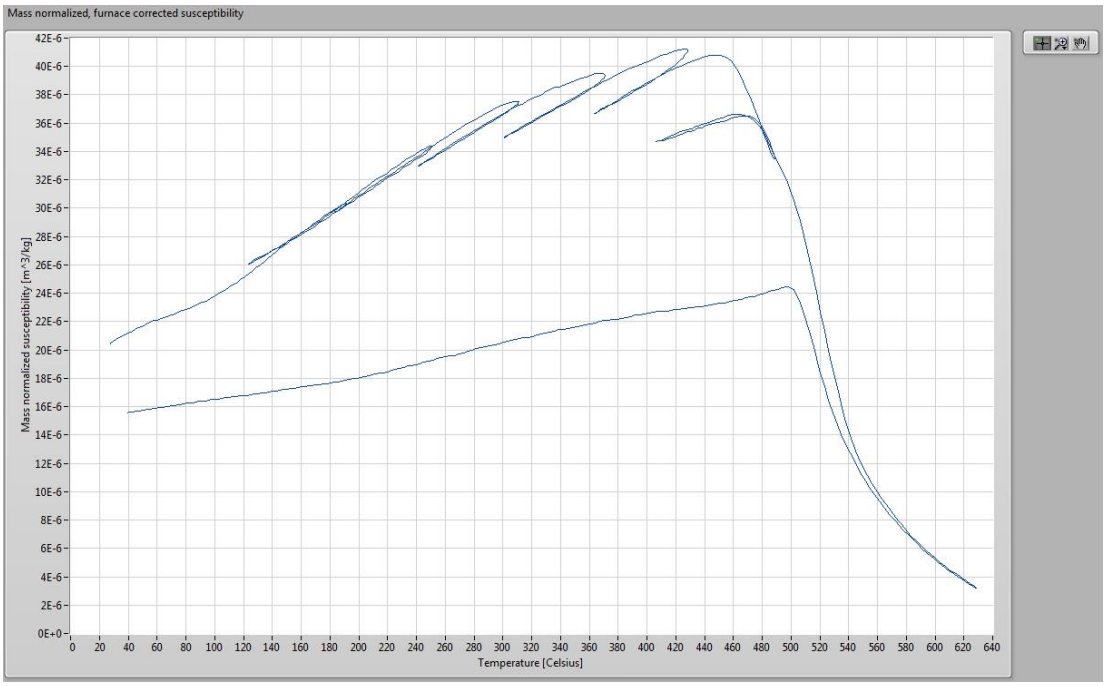

GR82-2

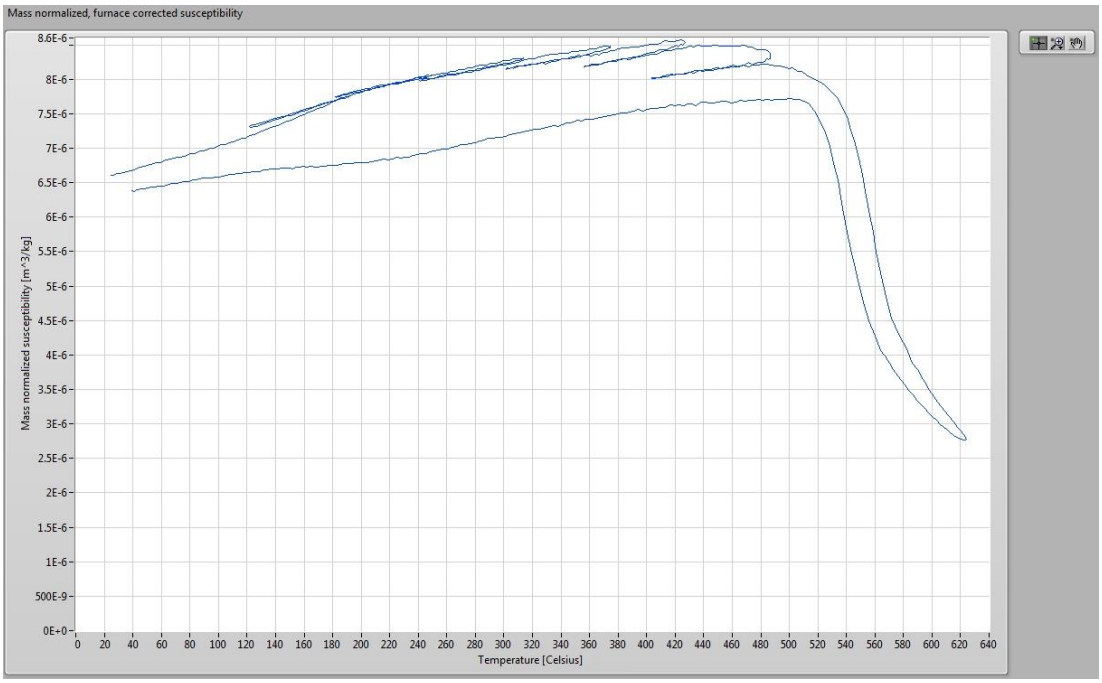

GR83-3

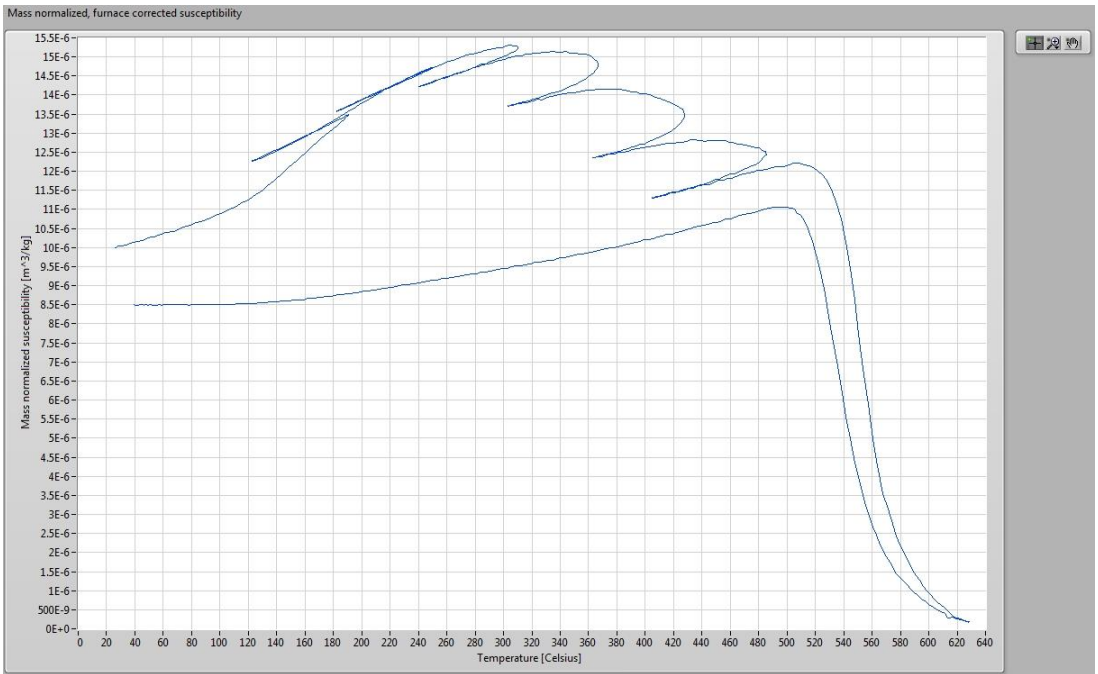

GR84-7

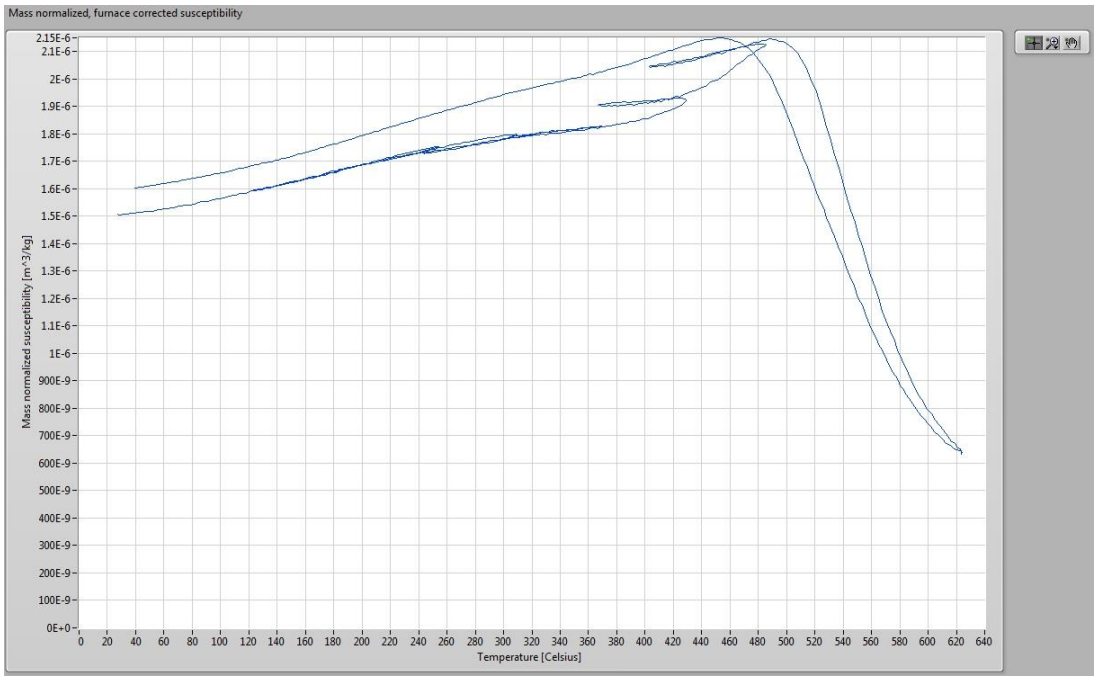

GR85-8

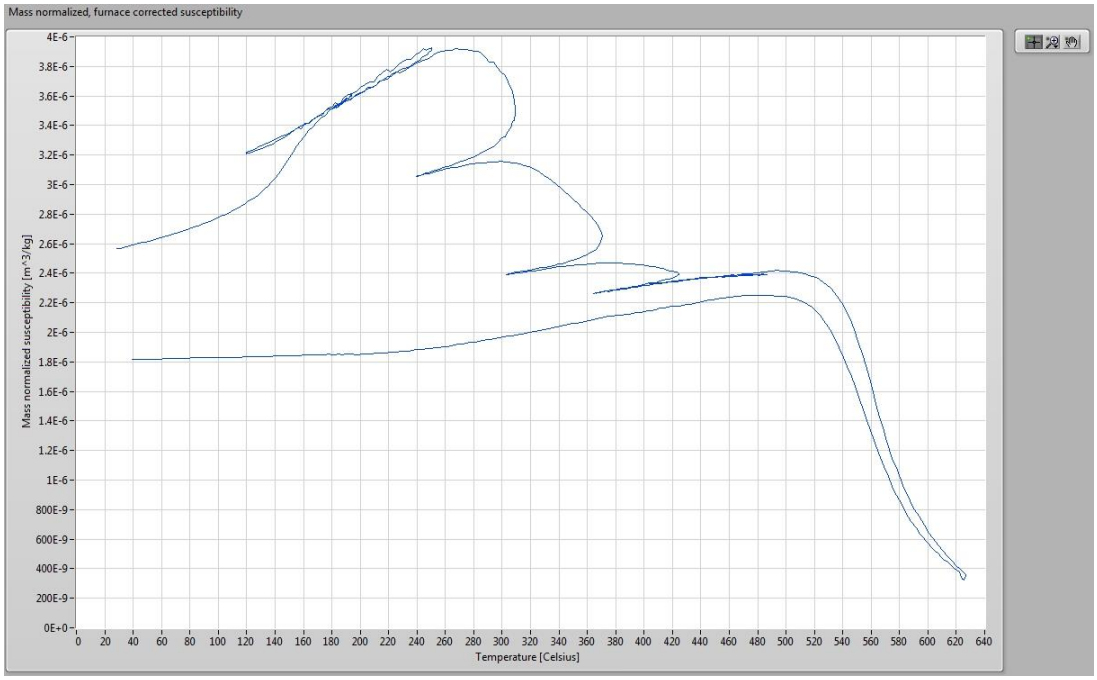

CK1-6

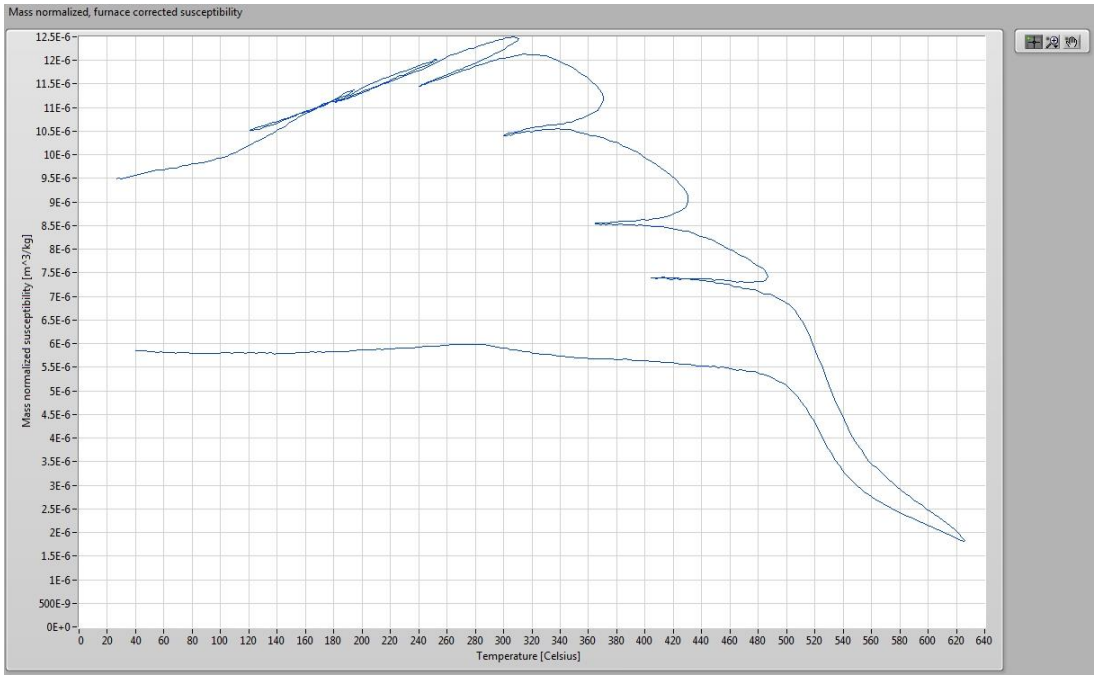

CK2-4

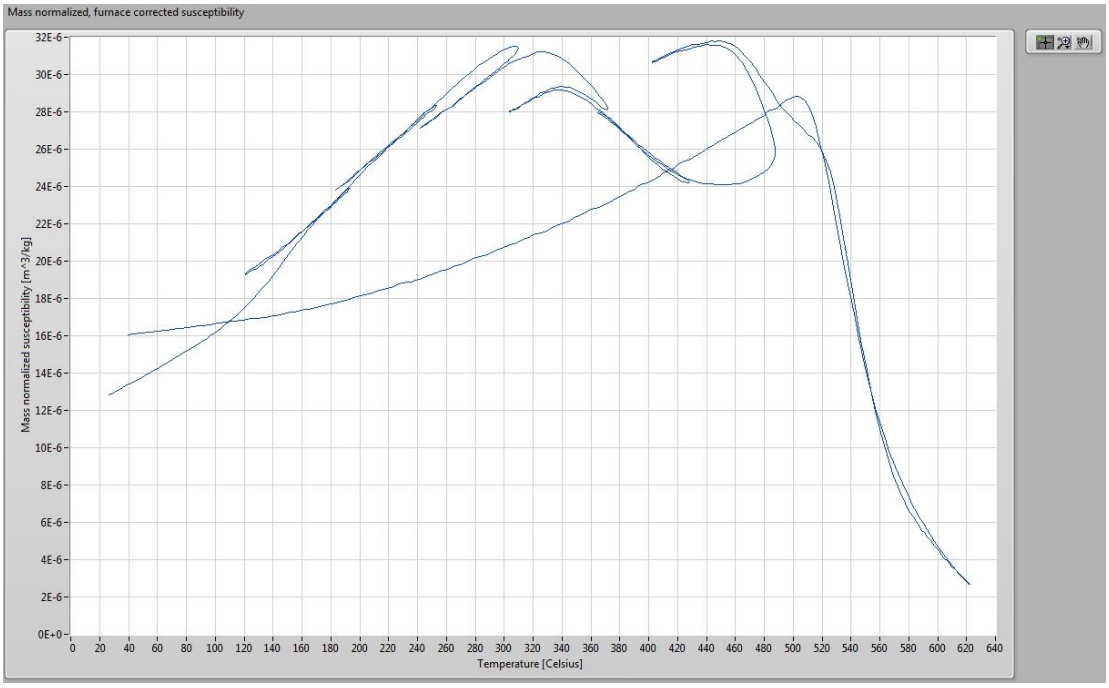

CK3-5

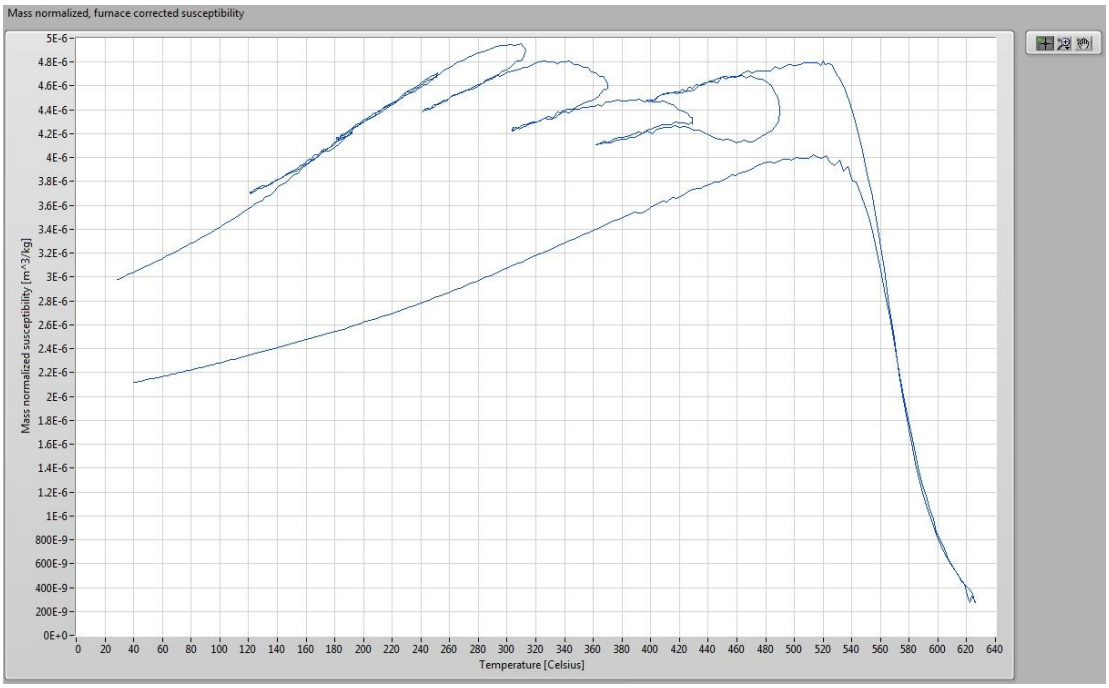

CK4-2

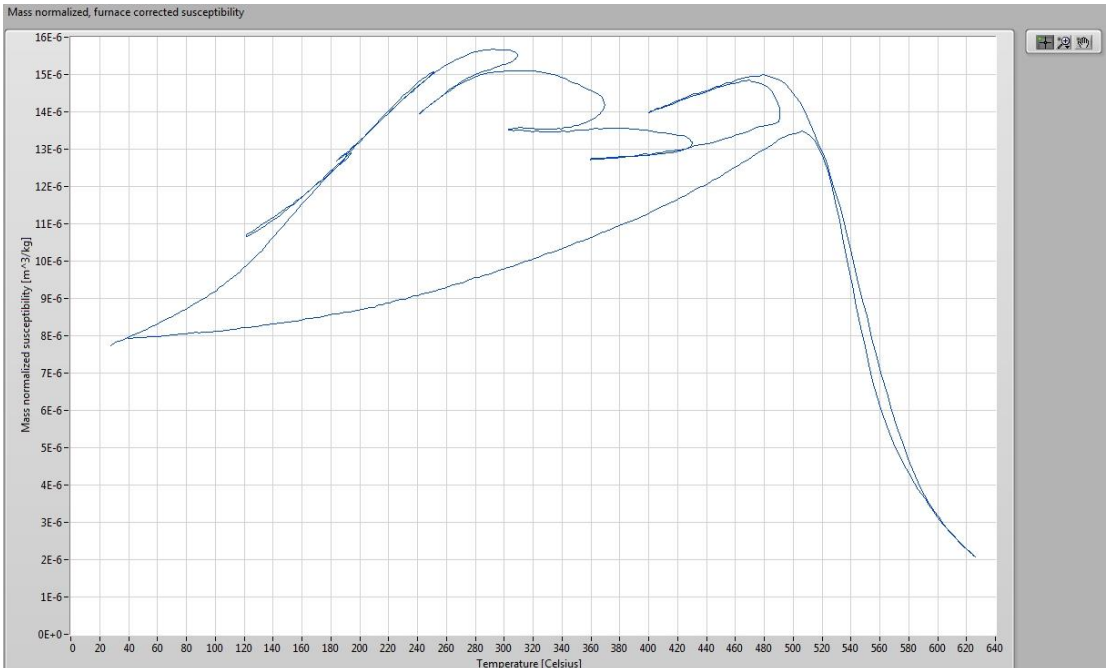

CK5-1

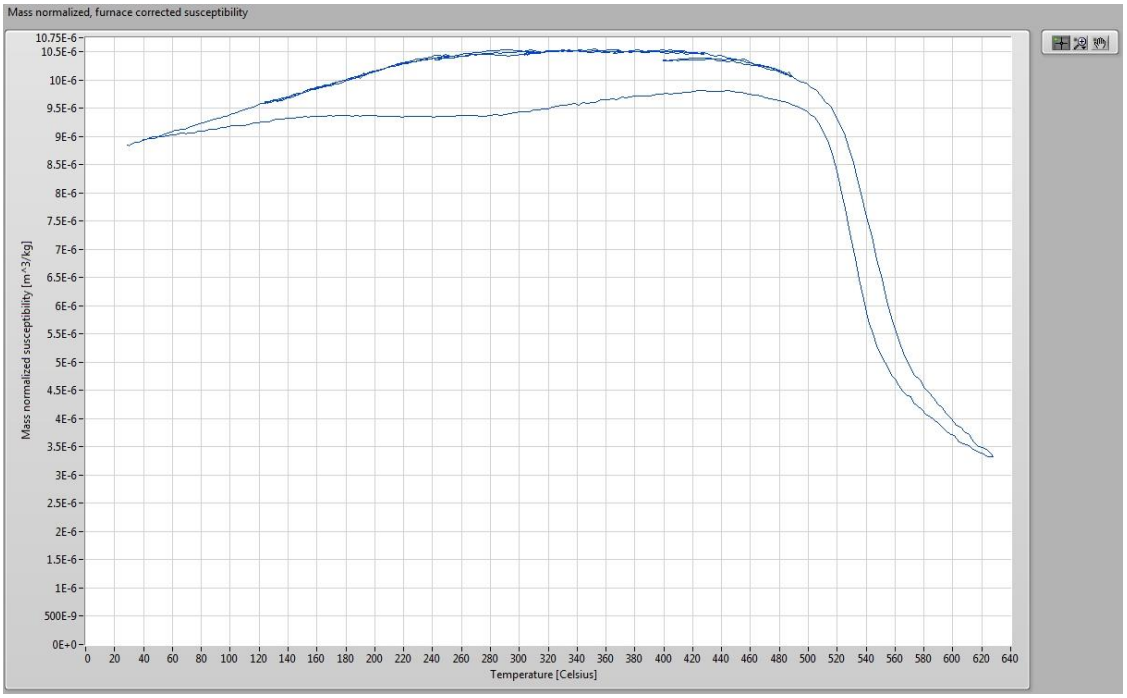

CK6-7

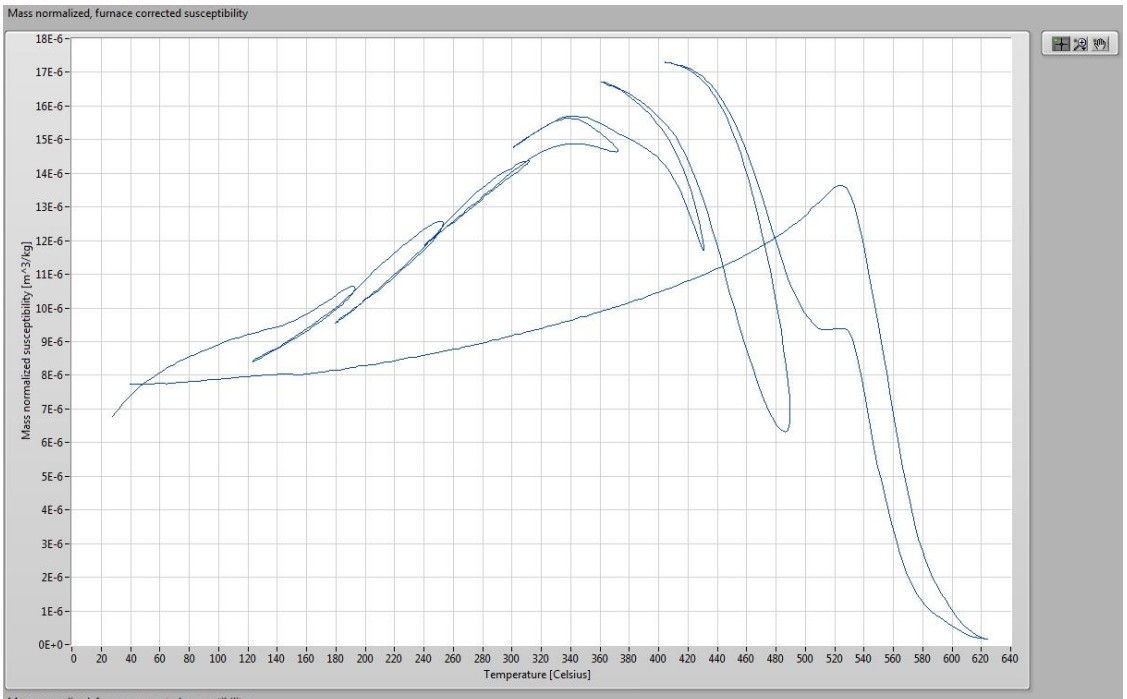

CK7-1

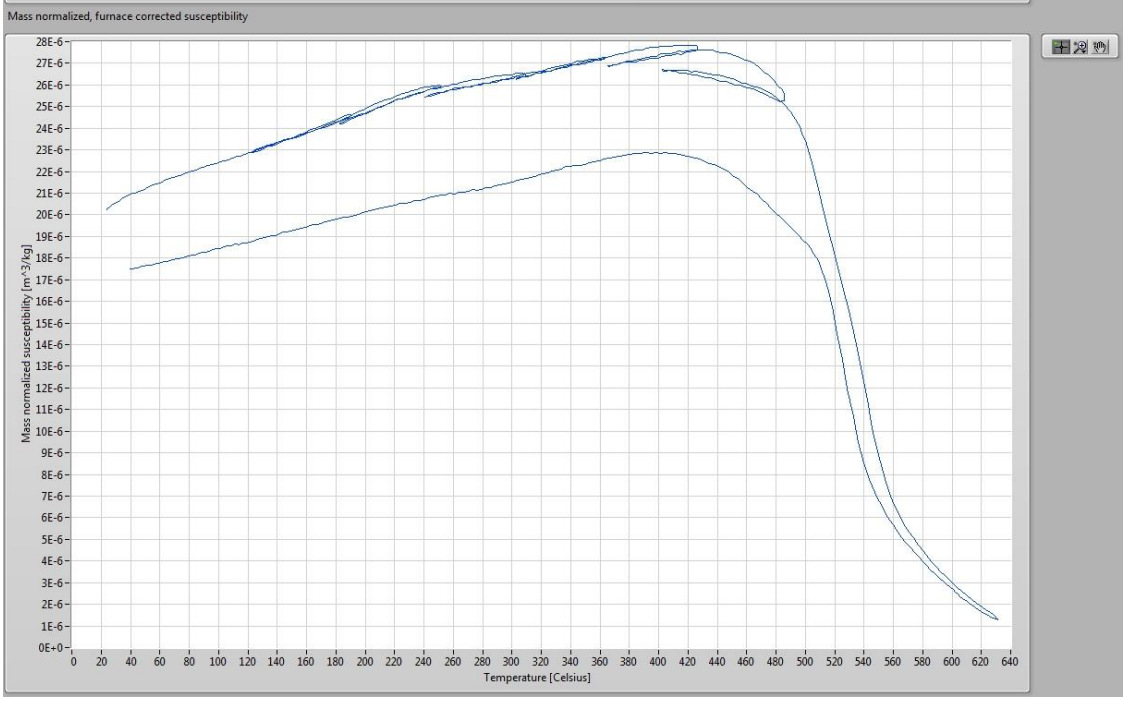

CK8-9

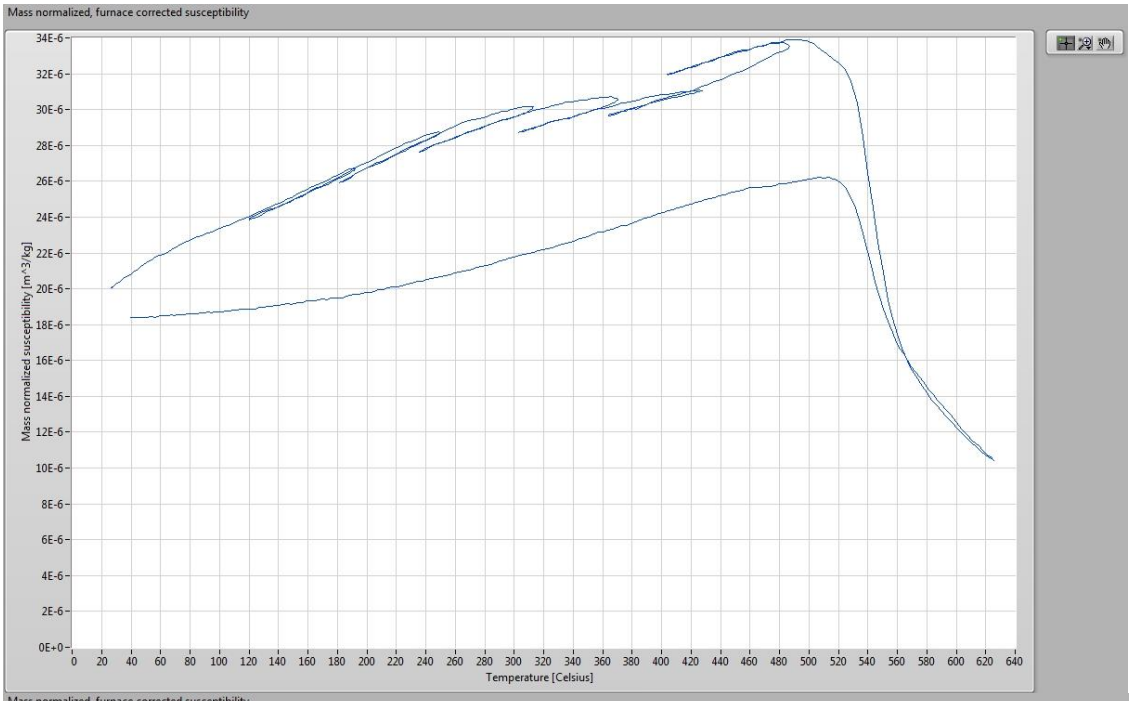

CK9-5

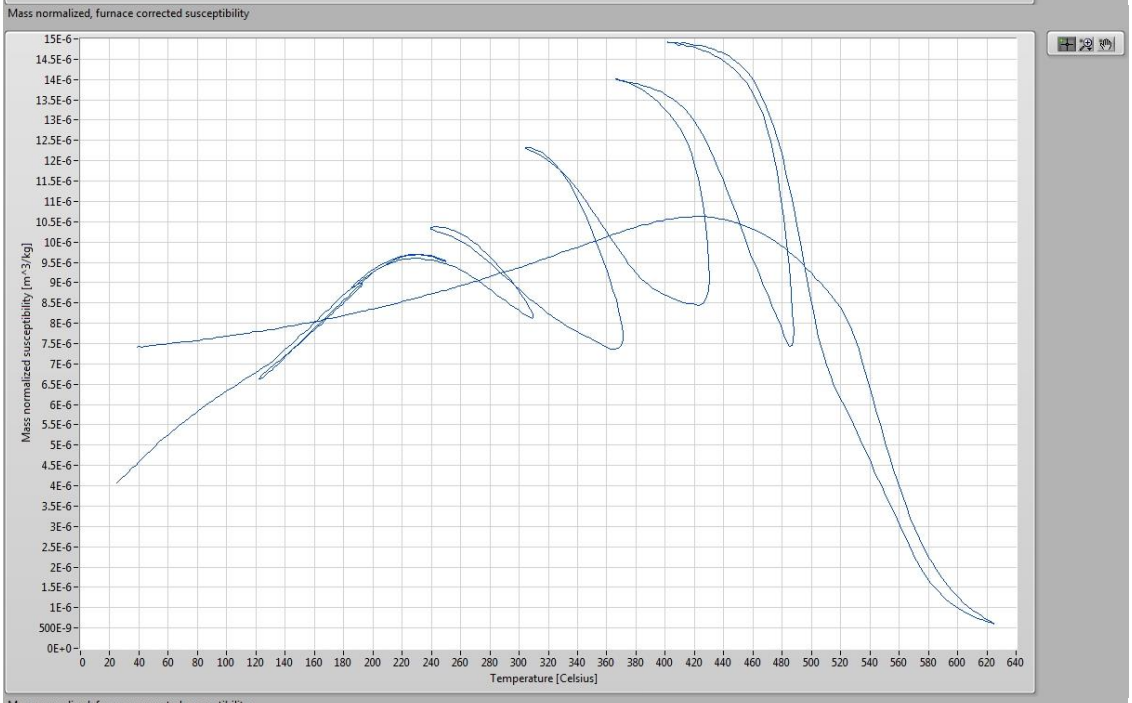

CK10-6

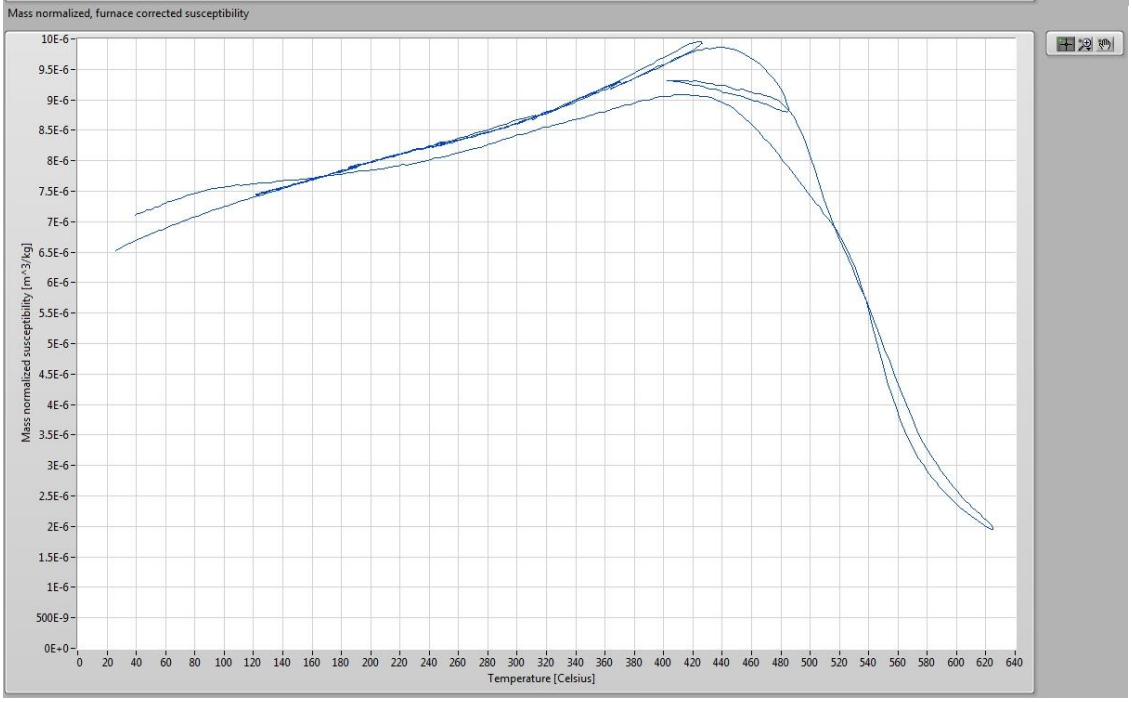

CK11-2

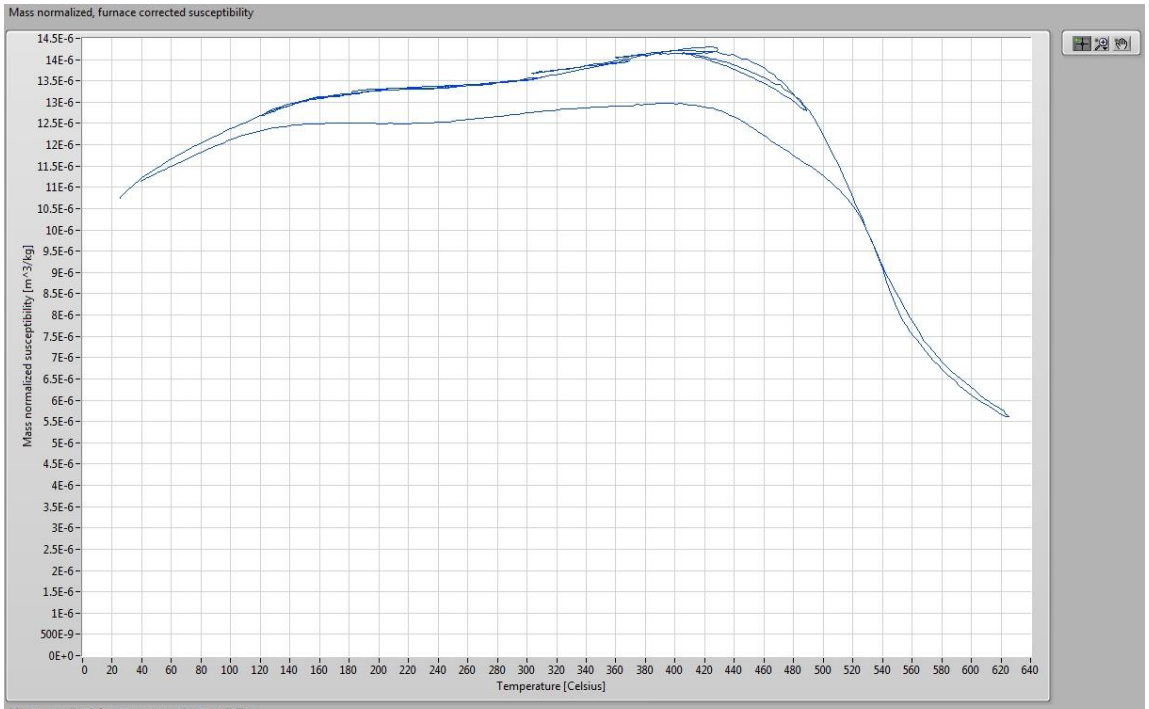

CK12-2

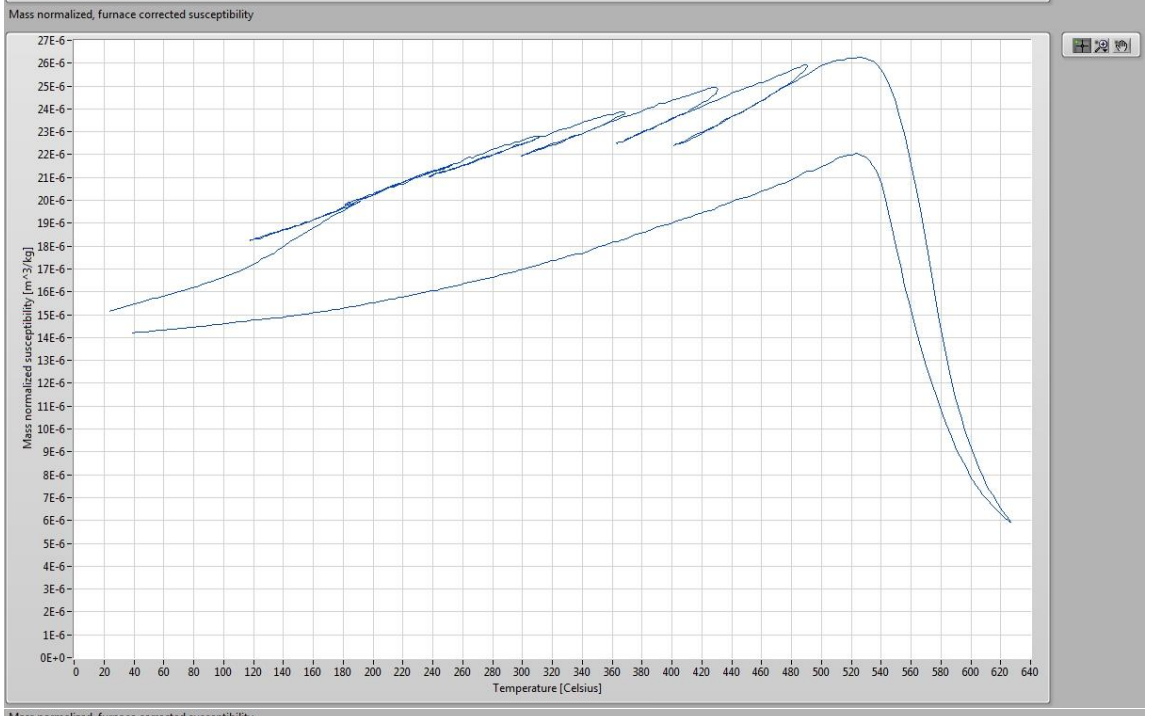

CK13-3

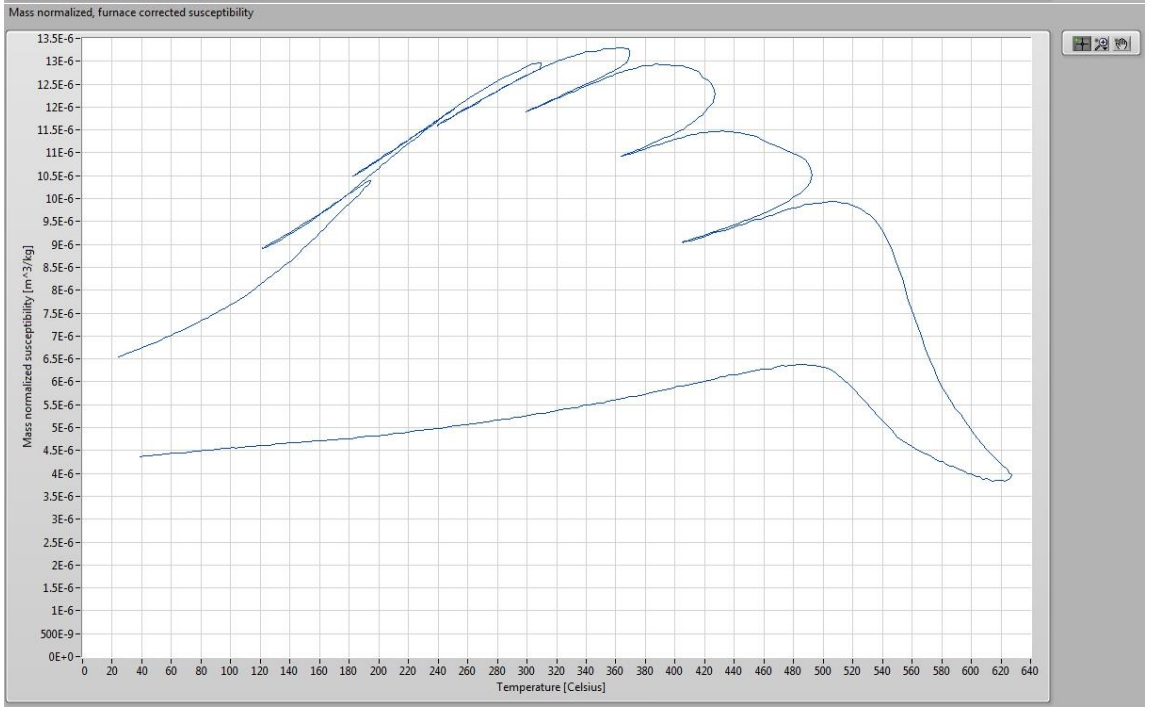

CK99-6

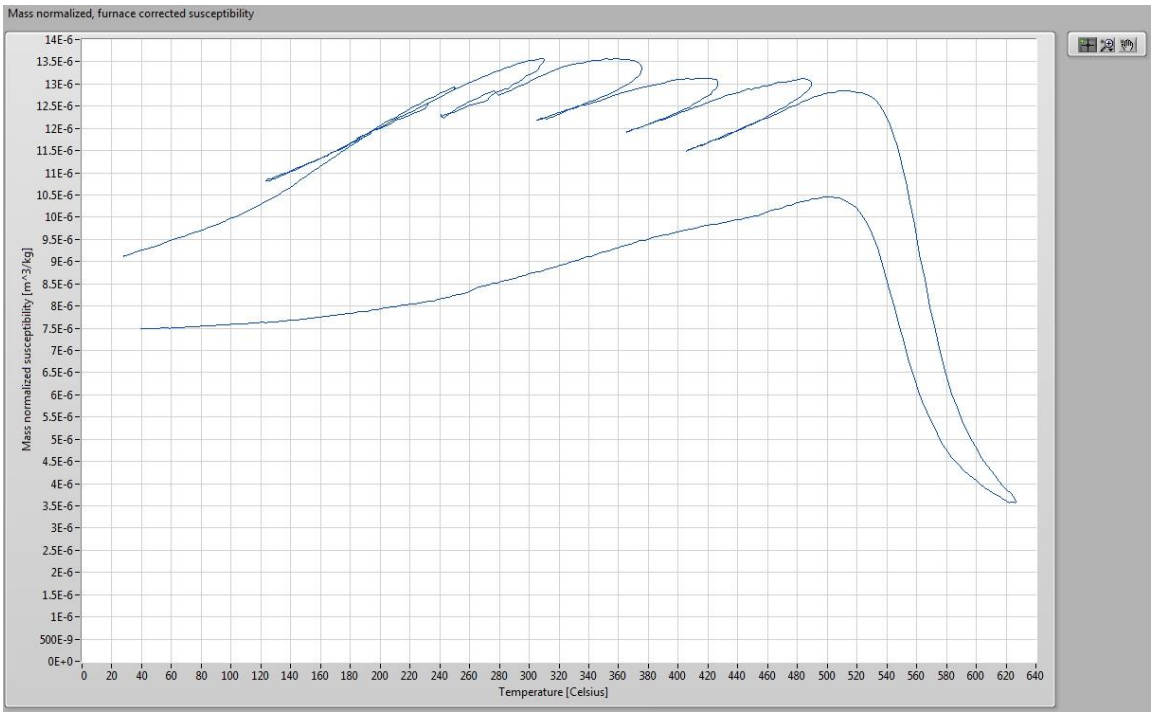
Mass normalized, furnace corrected susceptibility
Mass normalized susceptibility [m^3/kg]
14E-6
13.5E-6
13E-6
12.5E-6
12E-6
11.5E-6
11E-6
10.5E-6
10E-6
9.5E-6
9E-6
8.5E-6
8E-6
7.5E-6
7E-6
6.5E-6
6E-6
5.5E-6
5E-6
4.5E-6
4E-6
3.5E-6
3E-6
2.5E-6
2E-6
1.5E-6
1E-6
500E-9
0E+0
0 20 40 60 80 100 120 140 160 180 200 220 240 260 280 300 320 340 360 380 400 420 440 460 480 500 520 540 560 580 600 620 640
Temperature [Celsius]

CK100-4

APPENDIX D VSM DATA

Shaded red are the DCD measurements that did not show a intersection with the X-axis so the Hcr was manually calculated.

Sample	Hc	Hcr	Mr	Ms	Hcr/Hc	Mr/Ms	Group
GR1-10	171,058	394,015	7,36E-01	3,98E+00	2,3034	1,85E-01	Group D-2
GR2-8	104,761	450,947	5,22E-02	3,72E-01	4,3045313	1,40E-01	Group E
GR3-12	124,836	323,498	2,68E-01	1,72E+00	2,5913839	1,55E-01	Group D-1
GR4-7	517,966	888,471	8,40E-01	2,27E+00	1,7153076	3,70E-01	Group D-2
GR5-3	371,485	831,007	5,81E-01	1,81E+00	2,2369867	3,22E-01	Group D-2
GR6-11	49,38	213,91	1,77E-01	2,17E+00	4,3319158	8,18E-02	Group C-1
GR7-3	52,658	232,406	8,64E-02	1,10E+00	4,4134984	7,85E-02	Groep C-2
GR8-10	26,072	105,807	1,35E-01	2,33E+00	4,0582617	5,81E-02	Group C-1
GR9-3	24,772	84,146	1,30E-01	1,65E+00	3,396819	7,83E-02	Group C-1
GR10-8	126,485	405	2,40E-01	1,25E+00	3,2019607	1,92E-01	Group C-1
GR11-3	126,458	x	1,76E-01	9,75E-01	x	1,81E-01	Group A-2
GR12-5	61,858	290,763	9,19E-02	9,17E-01	4,7004914	1,00E-01	Group E
GR13-1	252,48	521,17	5,09E-01	2,25E+00	2,0642031	2,26E-01	Group D-2
GR14-2	106,837	313,54	1,63E-01	1,07E+00	2,9347511	1,52E-01	Group D-2
GR15-3	36,286	155,025	1,36E-01	2,89E+00	4,2723089	4,70E-02	Group C-1
GR16-10	35,428	182,76	1,56E-01	2,45E+00	5,1586316	6,38E-02	Group C-1
GR17-3	41,626	176,274	1,47E-01	2,04E+00	4,2347091	7,21E-02	Group A-1
GR18-1	83,692	602,952	5,02E-02	4,00E-01	7,2044162	1,25E-01	Group A-1
GR19-8	76,143	213	3,27E-02	2,65E-01	2,7973681	1,23E-01	Group D-1
GR20-2	60,002	234,778	1,08E-01	1,19E+00	3,9128362	9,12E-02	Group D-1
GR21-1	83,029	256,69	1,39E-01	1,40E+00	3,0915704	9,91E-02	Groep C-2
GR22	55,903	250,081	3,07E-01	3,39E+00	4,4734809	9,05E-02	Group C-1
GR23-2	102,044	347,5	7,28E-02	4,62E-01	3,4053938	1,58E-01	GroupA-1
GR24-4	61,937	257,944	8,16E-02	8,74E-01	4,1646189	9,34E-02	Group C-1
GR25-7	98,049	274,8	3,49E-01	2,88E+00	2,8026803	1,21E-01	Groep C-2
GR26-5C	46,105	224,51	4,58E-02	7,24E-01	4,8695369	6,32E-02	Group C-1
GR27-9	42,909	160,858	2,19E-01	3,95E+00	3,7488173	5,54E-02	Group D-1
GR28-5	88,351	144,082	4,06E-01	1,69E+00	1,6307908	2,41E-01	Group A-2
GR29-4	83,684	198,378	2,70E-01	1,86E+00	2,3705607	1,45E-01	Group D-2
GR30-6	137,82	289,157	3,70E-01	1,96E+00	2,0980772	1,88E-01	Group A-1
GR31-1	42,343	182,125	7,73E-02	1,05E+00	4,3011832	7,38E-02	Group D-1
GR32-5	97,841	293,95	1,08E-01	7,23E-01	3,0043642	1,49E-01	Group A-1
GR33-8	421,604	748,084	1,17E+00	3,61E+00	1,774376	3,24E-01	Group D-2
GR34-9	225,426	441,997	8,63E-01	3,23E+00	1,9607188	2,67E-01	Group D-2
GR35-4	79,131	196,939	1,51E-01	1,18E+00	2,4887718	1,29E-01	Group A-1
GR36-3	66,411	257,9	6,41E-02	5,58E-01	3,8833928	1,15E-01	Group C-1
GR37-1	152,581	285,199	3,00E-01	1,47E+00	1,8691646	2,04E-01	Group A-2
GR38-11	157,109	241,707	2,68E-01	9,03E-01	1,5384669	2,97E-01	Group A-1
GR39-7	77,866	213,193	6,83E-02	5,25E-01	2,7379472	1,30E-01	Group A-1
GR40-4	559,799	979,707	1,03E+00	2,54E+00	1,7501049	4,06E-01	Group D-2
GR41-6	437,187	685,194	7,27E-01	2,03E+00	1,567279	3,59E-01	Group C-2
GR42-2	284,705	527,3	5,34E-01	2,11E+00	1,8520925	2,53E-01	Group C-1

Sample	Hc	Hcr	Mr	Ms	Hcr/Hc	Mr/Ms	Group
GR43-10	132,001	302,3	1,30E-01	7,33E-01	2,2901342	1,77E-01	Group A-1
GR44-2	140,599	335,493	2,57E-01	1,84E+00	2,3861692	1,39E-01	Group E
GR45-4	45,578	180,966	2,74E-01	5,42E+00	3,9704682	5,05E-02	Group C-1
GR46-8	43,813	170,802	1,71E-01	3,63E+00	3,898432	4,70E-02	Group A-2
GR47-5	127,236	315,869	3,55E-02	1,03E-01	2,4825442	3,46E-01	Group B-1
GR48-6	60,962	329,369	1,79E-02	7,60E-02	5,4028575	2,36E-01	Group B-1
GR49-3	129,392	240,741	3,35E-02	9,58E-02	1,8605555	3,50E-01	Group B-1
GR50-3	46,695	138,604	1,46E-01	2,06E+00	2,9682835	7,09E-02	Group A-2
GR51-3	107,001	255,876	1,85E-01	1,32E+00	2,3913421	1,40E-01	Group A-1
GR52-8	69,257	219,158	2,62E-02	1,70E-01	3,1644166	1,54E-01	Group B-2
GR53-8	79,291	250	9,61E-02	8,37E-01	3,152943	1,15E-01	Group E
GR54-1	94,443	237,902	2,84E-01	2,26E+00	2,5190009	1,25E-01	Group C-1
GR55-3	97,968	274,848	2,59E-01	2,28E+00	2,8054875	1,14E-01	Group A-2
GR56-3B	100,892	276,233	2,87E-01	2,48E+00	2,7379079	1,16E-01	Group E
GR57-1	27,011	113,384	4,54E-02	9,27E-01	4,1976972	4,89E-02	Group E
GR58-2	72,552	135,55	2,44E-01	1,58E+00	1,8683151	1,54E-01	Group A-1
GR59-4	217,175	410,498	4,98E-01	2,21E+00	1,8901715	2,25E-01	GroupA-1
GR60-5	135,85	277,714	4,94E-01	2,38E+00	2,0442694	2,07E-01	Group C-1
GR61-7	354,888	556,372	9,42E-01	3,04E+00	1,5677397	3,10E-01	Group E
GR62-1	440,097	708,1	6,18E-01	1,72E+00	1,6089635	3,61E-01	Group C-2
GR63-2	82,306	132,845	3,21E-01	1,21E+00	1,6140379	2,65E-01	Group A-2
GR64-2	95,483	211,705	3,17E-01	2,25E+00	2,217201	1,41E-01	Group A-1
GR65-8	115,901	195,859	2,68E-01	1,03E+00	1,6898819	2,60E-01	Group A-1
GR66-5	108,731	226,783	1,53E-01	9,84E-01	2,0857253	1,56E-01	Group A-2
GR67-7	101,63	232,828	6,99E-02	4,27E-01	2,2909377	1,64E-01	Group C-1
GR68-8	229,262	416,79	3,40E-01	1,21E+00	1,8179637	2,82E-01	Group A-1
GR69-9	293,665	493,425	5,03E-01	1,48E+00	1,6802309	3,39E-01	Group A-1
GR70-2	119,07	197,31	1,14E-01	4,81E-01	1,6570925	2,37E-01	Group A-1
GR71-5	77,245	193,679	1,07E-01	9,62E-01	2,5073338	1,11E-01	Group C-2
GR72-2	79,605	225,93	9,00E-02	7,02E-01	2,8381383	1,28E-01	Group E
GR73-2	119,276	325,725	5,80E-02	3,00E-01	2,7308511	1,94E-01	Group E
GR74-2	55,433	115,816	1,00E-01	8,37E-01	2,089297	1,20E-01	Group A-2
GR75-8	87,434	212,37	7,27E-02	4,39E-01	2,4289178	1,66E-01	Group B-2
GR76-9	77,066	257,121	1,00E-01	1,20E+00	3,336374	8,34E-02	Group C-2
GR77-L	54,936	121,717	6,28E-02	5,44E-01	2,2156145	1,15E-01	Group A-2
GR78-4	89,668	227,287	6,04E-02	5,08E-01	2,5347616	1,19E-01	Group E
GR79-4	318,477	558,009	1,84E-01	5,86E-01	1,7521171	3,14E-01	Group E
GR80-4B	x	255,734	x	x	x	x	Group E
GR81-3	x	284,022	x	x	x	x	Groep C-1
GR82-5	185,636	414,881	3,40E-01	2,02E+00	2,2349167	1,68E-01	Group E
GR83-2B	285,03	524,389	4,58E-01	1,84E+00	1,8397677	2,49E-01	Group E
GR84-6B	270,008	476,278	4,24E-02	1,33E-01	1,7639403	3,19E-01	Group C-2
GR85-1B	346,941	1076,9	1,26E-02	3,60E-02	3,103986	3,50E-01	Group E
CK1-1	110,707	297,041	1,08E-01	6,03E-01	2,6831275	1,79E-01	Group D-2
CK2-8B	61,343	122,06	1,15E-01	8,17E-01	1,9897951	1,41E-01	Group D-1
CK3-7B	224,18	538,975	1,04E-01	6,24E-01	2,4042064	1,66E-01	Group A-2
CK4-7	203,255	406,651	9,03E-02	3,65E-01	2,0006937	2,47E-01	Group D-1

Sample	Hc	Hcr	Mr	Ms	Hcr/Hc	Mr/Ms	Group
CK5-L	380,047	655,02	3,14E-01	1,01E+00	1,7235237	3,13E-01	Group A-2
CK6-1C	179,917	434,981	2,23E-01	1,68E+00	2,4176759	1,33E-01	Group E
CK7-3B	59,144	125,961	7,81E-02	7,07E-01	2,1297342	1,11E-01	Group A-2
CK8-9B	87,963	254,683	1,30E-01	1,35E+00	2,8953424	9,60E-02	Group E
CK9-7	58,475	141,926	1,29E-01	1,52E+00	2,4271227	8,51E-02	Group E
CK10-10	237,477	379,146	8,57E-02	2,97E-01	1,5965588	2,89E-01	Group A-1
CK11-8	203,669	408,504	3,38E-01	1,77E+00	2,005725	1,91E-01	Group E
CK12-1	141,516	323,445	3,12E-01	1,89E+00	2,2855719	1,65E-01	Group E
CK13-8	361,797	598,998	6,67E-01	2,34E+00	1,655619	2,85E-01	Group C-2
CK99-3	481,526	759,213	6,35E-01	1,69E+00	1,5766812	3,76E-01	Group D-2
CK100-8	471,577	765,542	4,06E-01	1,06E+00	1,6233659	3,84E-01	Group C-2